NASA CR-135065
PWA-5434

NASA

STUDY OF UNCONVENTIONAL AIRCRAFT ENGINES DESIGNED FOR LOW ENERGY CONSUMPTION

FINAL REPORT

by

D. E. Gray

PRATT & WHITNEY AIRCRAFT DIVISION
UNITED TECHNOLOGIES CORPORATION

Prepared for

NATIONAL AERONAUTICS AND SPACE ADMINISTRATION

NASA Lewis Research Center
Contract NAS3-19465

1. Report No.	2 Government Accession No.	3. Recipient's Catalog No
NASA CR-135065		

4. Title and Subtitle	5 Report Date
STUDY OF UNCONVENTIONAL AIRCRAFT ENGINES DESIGNED FOR LOW ENERGY CONSUMPTION	June 1976
	6 Performing Organization Code

7. Author(s)	8. Performing Organization Report No.
D. E. Gray	PWA-5434
	10. Work Unit No.

9. Performing Organization Name and Address	11 Contract or Grant No
Pratt & Whitney Aircraft Division of United Technologies Corporation East Hartford, Conn. 06108	NAS3-19465
	13 Type of Report and Period Covered
12. Sponsoring Agency Name and Address	Contractor Report
National Aeronautics and Space Administration Washington, D. C. 20546	14 Sponsoring Agency Code

15. Supplementary Notes

Project Manager, William C. Strack, Wind Tunnel and Flight Division, NASA-Lewis Research Center, Cleveland, Ohio

16. Abstract

Declining U. S. oil reserves and escalating energy costs underline the need for reducing fuel consumption in aircraft engines. This report identifies the most promising unconventional aircraft engines based on their potential for fuel savings and improved economics. The study includes evaluation of the engines installed in both a long-range and medium-range aircraft. Projected technology advances are identified and evaluated for their state-of-readiness for application to a commercial transport. Programs are recommended for developing the necessary technology.

17. Key Words (Suggested by Author(s))	18 Distribution Statement
Fuel Consumption Direct Operating Costs Low Energy Consumption Fuel Conserving Unconventional Engines	

19 Security Classif (of this report)	20 Security Classif (of this page)	21 No of Pages	22 Price*
Unclassified	Unclassified	147	

* For sale by the National Technical Information Service Springfield, Virginia 22151

FOREWORD

The work described herein, which was conducted by Pratt & Whitney Aircraft Division of United Technologies Corporation, was performed under NASA Project Managers, Mr. James Dugan and Mr. William Strack, of NASA-Lewis Research Center. The report was prepared by D. E. Gray, the Pratt & Whitney Aircraft Program Manager, assisted by F. D. Havens, W. J. Kropp, Jr., and R. A. Lewis, Jr.

TABLE OF CONTENTS

TABLE OF CONTENTS (Cont'd)

LIST OF ILLUSTRATIONS

LIST OF ILLUSTRATIONS (Cont'd)

LIST OF ILLUSTRATIONS (Cont'd)

LIST OF ILLUSTRATIONS (Cont'd)

LIST OF ILLUSTRATIONS (Cont'd)

LIST OF TABLES

LIST OF TABLES (Cont'd)

1.0 SUMMARY

The intent of this study program was to explore the potential applications of more unconventional engine cycle concepts that may offer significantly lower energy consumption in future advanced air transports. This program supplements the prior advanced technology studies (contract NAS3-19132) which emphasized the application of advanced fuel conservative technology to the conventional turbofan engine cycle.

The most promising unconventional engine concept studied was an advanced turboprop which indicated approximately a 20 percent potential fuel savings relative to an advanced conventional turbofan. The regenerative turboprop, the second-best choice, showed approximately a 15 percent potential fuel saving relative to the turbofan. These improvements were based on engine technology that could potentially be available for a 1985 engine development start date. The practical realization of the indicated fuel savings potential with these powerplants is dependent upon achieving a projected, new technology propeller cruise efficiency approaching 80 percent at Mach 0.8 and 9.14 km (30000 ft) altitude. This is consistent with the cruise condition operating characteristics of current turbofan-powered aircraft. To be accepted by a major segment of the flying public, the turboprop must meet the standards set by the turbofan in terms of cabin noise and vibration. Additionaliy, the airline operators must be assured of truly competitive economics of operation. Maintenance requirements and engine-to-airframe aerodynamic, structural, and acoustical interactions need to be fully assessed to establish the practicality of the turboprop. Hamilton Standard Division provided technical propeller data and they strongly support the view that such requirements as passenger comfort and operating economics can be met by the application of advanced technology to turboprop systems.

The initial effort in the program was a survey and analytical screening of unconventional concepts. These concepts included variations in the primary cycle, unconventional propulsors, and unconventional engine installations. Based on this screening and further refined analysis, two unconventional propulsion systems, the turboprop and the regenerative turboprop, were selected for conceptual design and engine/aircraft evaluation. Regenerator technical information was provided by AiResearch Manufacturing Company of California for this study. Results of this evaluation clearly indicated the turboprop to be superior to the regenerative turboprop in both fuel savings potential and economics. The work under this contract was concluded with the formulation of various programs designed to acquire the technology necessary to achieve improvements found possible in the study.

Fuel consumption and airline direct operating cost (DOC) were used as figures-of merit in the evaluation to define critical technology requirements and to quantify the associated benefits. Fuel consumption calculations were based on representative flight stage lengths and aircraft utilization. The DOC includes the effects of investment, maintenance, and fuel costs associated with the engine design improvements. These costs, directly incurred by the airlines' operation, are an important measure of the economic benefits associated with energy savings. DOC improvements ranging from 3 to 9 percent were estimated for the turboprop relative to the turbofan.

In the long term, fuel consumption savings will almost certainly have to be achieved with increasingly more stringent pollution control requirements. Determining the effect of advanced fuel conservative technology on engine noise and exhaust emissions was an integral part of the work conducted during this program.

LOWERING FUEL CONSUMPTION

The advanced turboprop engine showed a potential for a 20 percent fuel savings relative to the advanced turbofan with comparable technology. This translates into a 28 to 35 percent fuel savings compared with a current turbofan technology. The cruise thrust specific fuel consumption improvement attendant with an advanced Mach 0.8 cruise speed propeller is the predominant factor in the resultant turboprop fuel savings. The turboprop is more effective in saving fuel at shorter flight lengths where a large portion of the fuel is consumed during climb. The inherently greater takeoff-to-cruise thrust capability of the propeller provides both fast and efficient climb operation to significantly increase the fuel savings differential over that indicated during cruise. Medium and long range, four-engine, advanced turboprop aircraft were assumed in the evaluation.

IMPROVING AIRLINE ECONOMICS

Direct operating costs were estimated for the turboprop and turbofan installations in medium range and long range aircraft. In the medium range aircraft, 3 to 5 percent reductions in direct operating cost (DOC) relative to the advanced turbofan were indicated for an advanced turboprop system. In the long range aircraft these reductions were 7 to 9 percent. These benefits were based on a domestic fuel price of 8 cents per liter (30 ¢ /gal), an international fuel price of 12 cents per liter (45 ¢ /gal), and a 1974 economy.

IMPACT OF FUEL CONSERVATION TECHNOLOGY ON THE ENVIRONMENT

With projected acoustic technology for the 1985 time period, the advanced turbofan and advanced turboprop far field noise characteristics are similar. A FAR-36 minus 10 EPNdB level is possible for either system with source noise and/or treatment advances which provide a 4 to 5 EPNdB lower total noise compared with existing high bypass ratio turbofans.

Near field noise characteristics indicate a small takeoff gross weight penalty for the turboprop in order to meet the interior noise levels of the turbofan-powered airplane. Propeller acoustic characteristics need to be a primary consideration in future technology programs.

Emission levels are for the turboprop relative to the turbofan to reflect its lower fuel consumption. In either system, the achievement of EPA 1981 proposed regulations in NO_x emissions would require substantially more technology relative to that being demonstrated in present experimental burners.

RECOMMENDED TECHNOLOGY PROGRAMS

A broad range of technology advances is required to bring the turboprop to a state-of-readiness. The gas generator (primary cycle) technology requirements are the same as those for the advanced turbofan gas generator (described in reference NASA report CR-135002, Study of

Turbofan Engines Designed for Low Energy Consumption). The technology program for the propeller/gearbox system must address high efficiency cruise operation with structural adequacy. Supercritical propeller blading sections, a contoured nacelle shape, and swept blade tips all need to be investigated for improved high speed performance. Composites and other advanced materials will be needed to meet the efficiency, weight, and reliability goals which have been established for the propeller and gear system. In order to obtain public acceptance of the turboprop in the future, the technology program must address goals of reduced propeller source noise and vibration. The overall technology plan for the turboprop would culminate with flight tests of an available, possibly modified, turboshaft engine and an advanced technology propeller/gearbox system.

2.0 INTRODUCTION

The growing concern over diminishing fossil fuel supplies, compounded by escalating costs of oil-based energy, has stimulated the research and development of effective fuel conservation measures on a nationwide basis. As part of this effort, the National Aeronautics and Space Administration (NASA) has extended the scope of a continuing series of Advanced Transport Technology studies to include investigations directed towards minimizing fuel consumption in America's commercial aircraft fleet. These propulsion studies have encompassed the minimization of performance loss in current operational turbofan engines, as well as the study of fuel conserving turbofan and unconventional propulsion concepts which could be operational fifteen years in the future.

The objective of this study was to explore the potential for unconventional engine cycle concepts to significantly lower energy consumption requirements of commercial transport aircraft, as compared with such aircraft powered by conventional turbofan engines. The study considered concepts for improving cycle efficiency, for improving propulsive efficiency, and for generally reducing fuel consumption by, for example, reducing installation penalties. Unconventional engine installations such as multiple gas generators or multiple propulsors were also considered. Propeller and gearbox information included in the study were provided by the Hamilton Standard Division of United Technologies Corporation. AiResearch Manufacturing Company of California conducted a significant portion of the heat exchanger analysis required for the study of regenerative engine cycles. The program was closely related to the NASA-sponsored Study of Turbofan Engines Designed for Low Energy Consumption and drew upon the baseline engine data and the definition of technology levels from that program.

The study described in this report was divided into three principal tasks:

- Task I studies identified and parametrically analyzed alternate engine concepts that potentially offered reduced energy consumption for commercial subsonic transports. The study included regenerative cycles, reheat cycles, intermittent flow processes, propulsor concepts, and unconventional engine installations. The thermodynamic and/or propulsion benefits associated with each of the engine concepts were assessed. General cycle requirements, engine performance, weight, cost, noise, emissions, and basic and applied research requirements were considered in screening the candidate concepts. A comparison was made between these results and those using a reference conventional turbofan engine. The studies incorporated component technologies that are appropriate for engines starting development in approximately 1985.

- Under Task II, two of the most promising engine concepts from Task I were further analyzed which included engine layouts, weights, dimensions, center of gravity, and preliminary aerodynamic and mechanical design definition of components. The fuel savings potential and economic benefits of these engine cycles in advanced subsonic transport aircraft were estimated and compared with a modern turbofan engine.

- Task III evaluated the state-of-readiness for application to a commercial transport of each advanced propulsion technology item incorporated into the two concepts refined in Task II. Where deficiencies, weaknesses, or opportunities were evident, actions were recommended to accelerate the development of selected technologies.

The engine concepts studied in the proposed program were defined toward the goal of compliance with the emission standards established by the Environmental Protection Agency and with the noise limitations established by 10 EPNdB below FAR 36.

3.0 RESULTS OF STUDY

The most promising unconventional engine concept resulting from this program is the advanced turboprop engine. This engine features an advanced technology turboshaft and an advanced small diameter propeller which is projected to maintain high efficiency levels up to a Mach 0.8 cruise speed.

3.1 FUEL SAVINGS AND ECONOMIC BENEFITS

When compared to an advanced turbofan engine, which was defined using technology improvements forecast for 1985, the unconventional turboprop engine showed additional gains in fuel savings and economic benefits. Table 3.1-I presents the fuel savings and indicates the unique technology requirements needed to achieve these savings. The turboprop fuel savings result primarily from better cruise thrust specific fuel consumption (TSFC) and, secondarily, from the fast and efficient climb potential of the advanced propeller. To a lesser extent, as shown in Table 3.1-I, the regenerative turboprop and shrouded, variable-pitch fan concepts also indicated fuel savings potential.

TABLE 3.1-I

UNCONVENTIONAL PROPULSION SYSTEMS WITH FUEL SAVINGS POTENTIAL

Propulsion System	Fuel Savings Relative to 1985 Turbofan Technology	Fuel Savings Relative to 1975 Turbofan Technology	Areas of Unique Technology Development*
Turboprop	20%	30%	Prop-fan and gearbox.
Regenerative Turboprop	15%	25%	Prop-fan, Gearbox and recuperator.
Shrouded, Variable-Pitch fan	12%	22%	Shrouded, variable-pitch fan

*This technology is in addition to the advanced turbofan technology identified in the LEC turbofan final report. (ref. 1)

A comparison of the direct operating costs (DOC) are presented in Figure 3.1-1. The turboprop costs are lower than the advanced turbofan reflecting the 20 percent fuel savings of the turboprop. The higher acquisition and maintenance costs for the regenerative turboprop completely offset its fuel savings resulting in a significantly higher DOC. The DOC bands shown in the figure reflect the range in the performance, acquisition cost, and maintenance costs being forecast for future powerplants.

The selection of these unconventional propulsion systems was the result of screening many concepts. These included variations of the primary cycle with heat exchange, unconventional thermodynamic processes, different types of propulsors, and unconventional engine installation arrangements.

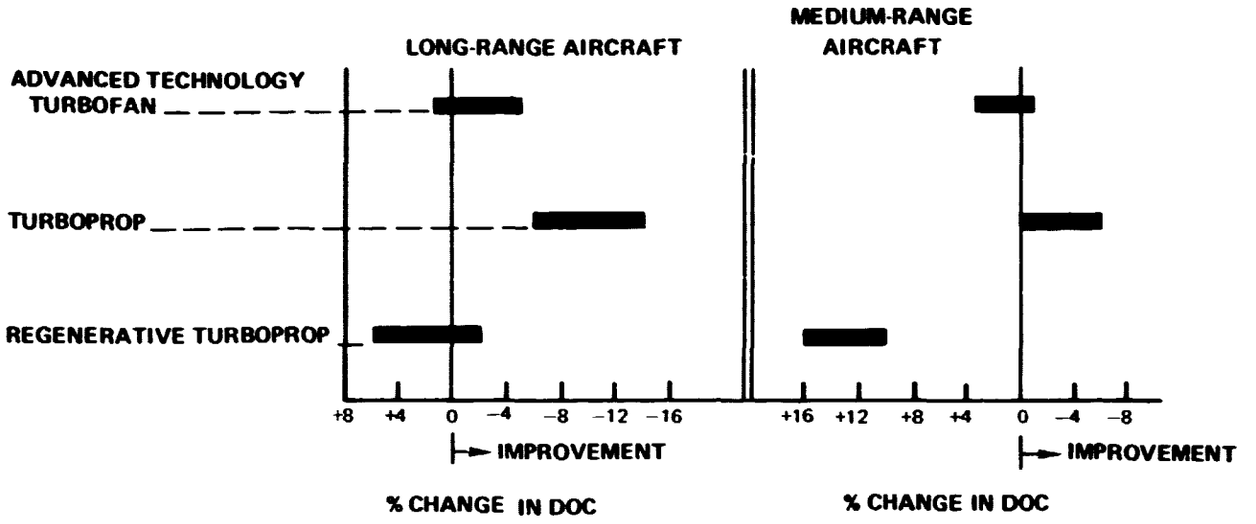

Figure 3.1-1 Direct Operating Cost Benefits Relative to a Current Technology Turbofan

3.2 MOST PROMISING FUEL CONSERVING PROPULSION SYSTEMS

The advanced-technology turbofan engine (ref. 1) and the unconventional turboprop engine offer the best opportunity for conserving fuel in future systems. Each attains substantial fuel conservation while presenting a practical configurational arrangement, attractive economic factors, and reasonable timing (1985 technology).

3.2.1 Advanced-Technology Turbofan Engine

The advanced-technology turbofan engine that was selected under the LEC turbofan contract (ref. 1) served as the baseline in assessing the relative merits of unconventional engine concepts. This engine, designated the STF-477, is representative of a 1985 technology turbofan engine for in-service operation in the 1990's. It embodies those technology advancements which indicate the greatest potential for improved fuel consumption, based on an all-out effort toward fuel economy.

3.2.2 Turboprop Engine

The selected turboprop engine features an advanced primary cycle and propulsion (prop-fan) subsystem.

The primary cycle represents the same level of technology as the advanced turbofan engine (STF-477). This simple Brayton cycle has the greatest potential for increasing thermal efficiency with low system weight. The smaller size of the turboshaft engine relative to the turbofan core increases the difficulty in achieving and maintaining tight clearances in the high pressure region of the engine. A cycle pressure ratio somewhat lower than in a turbofan may be required in the turboshaft engine because of the smaller flow size.

The propulsor subsystem consists of a highly loaded, eight-blade propeller that is used in conjunction with a gearbox. The propeller is assumed to be capable of a cruise Mach number of 0.8 with an efficiency approaching 80 percent. The propeller blades are a spar-and-shell design which uses composite materials.

The recommended technology program is directed towards developing the propulsor subsystem to a state of development readiness. The program would establish an aerodynamic and acoustic technology base to design full-scale 0.8 Mach number prop-fans. Specific emphasis would be placed on the structural integrity of the spar-and-shell composite airfoils.

3.3 OTHER UNCONVENTIONAL SYSTEMS WITH FUEL SAVINGS POTENTIAL

Results of this study showed that the regenerative turboprop and shrouded, variable-pitch fan concepts indicated the potential for a moderate fuel savings relative to the conventional turbofan.

3.3.1 Regenerative Turboprop

The regenerative turboprop concept modifies the primary cycle by adding a regenerator (heat exchanger) which transfers heat from the turbine discharge air to the compressor discharge air. This heat regeneration improves cycle efficiency by reducing the heat rejection temperature.

The success of the regenerative turboprop is dependent on the heat exchanger performance. Several air-to-gas heat exchangers were analyzed leading to the selection of a stationary, plate-fin counterflow matrix arrangement. Although a cycle performance improvement was possible at low cycle pressure ratios with regenerator, the weight and increased nacelle drag of this engine when installed actually resulted in poorer fuel consumption than the turboprop.

Since the regenerative turboprop indicates less fuel savings, has a higher DOC and is more complex than the simple turboprop, no technology programs are recommended for this engine.

3.3.2 Shrouded, Variable-Pitch Fan

The potential advantage of this concept over a conventional turbofan is a short and thin fan cowl which could offer installed engine fuel consumption improvements due to reduced nacelle weight and drag, and a low pressure ratio fan. Analysis of the shrouded fan concept showed the potential for relatively large fuel savings relative to the turbofan. The potential is entirely dependent upon high risk concepts associated with the large diameter stationary shroud. No further work on the configuration is recommended pending the outcome of advanced propeller (prop-fan) testing planned during 1976.

3.4 ENVIRONMENTAL IMPACT

While the jet and core noise for the turboprop concepts are lower than for the turbofan, the total noise level is estimated to be higher because of the high contribution of the propeller. However, with projected advances, both the advanced turboprop and turbofan are expected to offer the potential for meeting the FAR 36 minus 10 EPNdB levels.

The exhaust emissions, on an EPAP basis, are projected to be slightly lower for the turboshaft than the turbofan engine. The CO and THC EPAP's for both engines are projected to be below the proposed EPA standards. The achievement of proposed NO_x emissions would require substantial improvements in burner technology beyond that being presently forecast for advanced burners.

4.0 DISCUSSION OF RESULTS

In this section of the report, the propulsion system unconventional concepts considered in this program as well as the methods of evaluation are discussed in detail. For purposes of discussion and evaluation, the propulsion systems are separated into two subsystems, the primary cycle and the propulsor. To provide a common basis for understanding, Figure 4.0-1 schematically shows the components which are included in each subsystem.

4.1 SURVEY AND ANALYTICAL SCREENING OF UNCONVENTIONAL CONCEPTS

Advanced primary cycle concepts, unconventional propulsor concepts, and unconventional engine installation arrangements were investigated in this study. These concepts, as addressed in this study, incorporated technology advances anticipated for the 1985 time period consistent with the NASA study of turbofan engines designed for low energy consumption (ref. 1).

A total of 12 unconventional concepts in the three categories were screened:

1. Unconventional primary cycles

    a. Regeneration
    b. Intercooling
    c. Regeneration with intercooling
    d. Reheat
    e. Constant volume combustion
    f. Variable compression ratio
    g. Pressure exchange
    h. Compound cycle

2. Unconventional propulsor concepts

    a. Shrouded variable-pitch fan
    b. Advanced propeller

3. Unconventional engine installations

    a. Multiple fans or gas generators
    b. Laminar flow control engine

The first four unconventional primary cycles - regeneration, intercooling, regeneration with intercooling, and reheat – involve the processes of internal heat exchange and/or alteration of external heat addition to the basic Brayton cycle. Regeneration, intercooling, and regeneration with intercooling involve internal heat exchange alone, while reheat is concerned only with additional external heat input at a different point in the cycle. The other cycle concepts – constant volume combustion, variable compression, unconventional primary pressure exchange, and compound cycle -- include a direct substitution of alternate cycle processes which constitute more complex variations of the Brayton cycle, including intermittent flow processes in three of the four concepts.

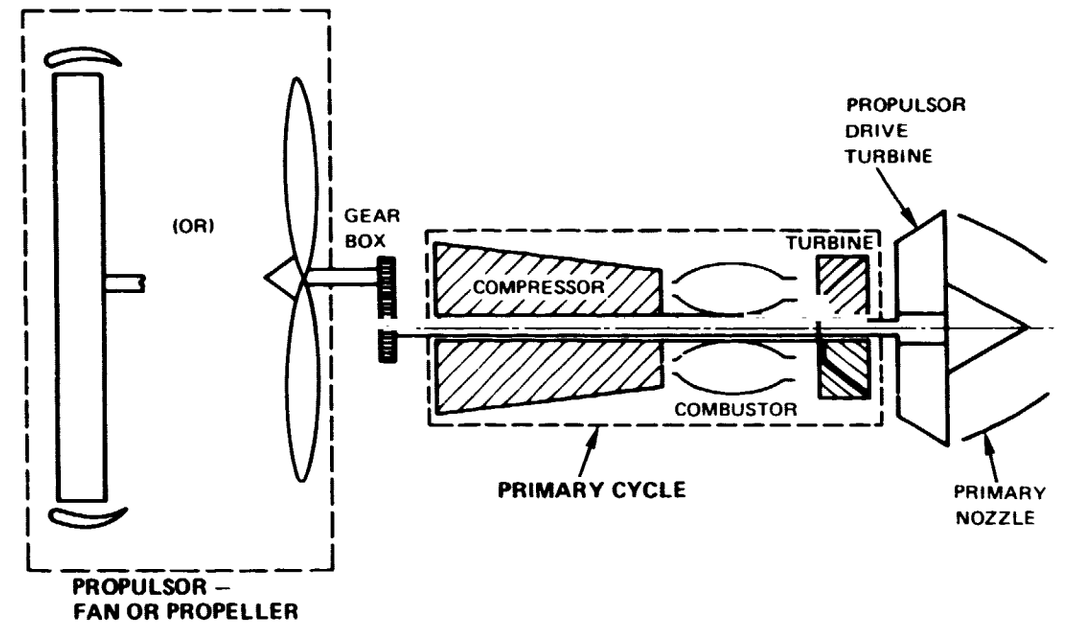

Figure 4.0-1 Schematic Representation of the Basic Propulsion System Components

The unconventional propulsor concepts are alternatives to the conventional 1.6 to 1.8 pressure ratio fan as more efficient methods of converting available primary cycle energy to useful thrust. Efficiency improvements are achieved by lowering the fan pressure ratio while simultaneously utilizing improved aerodynamics and reduced parasitic losses.

Screening of unconventional concepts included consideration of unconventional engine installations such as multiple gas generators (primary cycle) or multiple propulsors. Laminar flow control was evaluated with respect to unconventional propulsion arrangements to provide suction to remove the turbulent boundary layer from the wing surface.

Screening analyses identified promising primary cycle and propulsor concepts and compared the merits of the two unconventional installation approaches. Figures of merit in the screening process included: fuel savings potential (based on cruise TSFC), engine weight, procurement and maintenance cost trends, environmental considerations, and research and development requirements. Fuel savings potential is considered to be the most important of these factors. Qualitative comparison of these figures of merit is shown in Table 4.1-I. In this screening process, quantitative results were obtained where possible. In some areas the results are based on available information surveyed from the literature and analyzed to a degree sufficient to provide a consistent comparison with other concepts. No attempt was made to assess laminar flow control gains associated with airplane improvements.

As a result of these screening analyses three concepts were selected for further detailed analysis: one of the unconventional primary cycles – regeneration – and the two unconventional propulsor concepts – shrouded variable pitch fan and advanced propeller. Examination of Table 4.1-I shows that, in addition to these three concepts, regeneration with intercooling and constant volume combustion also would have lower cruise TSFC than the conventional turbofan. The analysis showed, however, that the simpler regenerative concept has the greater potential for conserving fuel in aircraft engines. The constant volume combustion concept was eliminated from further analysis because the small savings potential of this concept was accompanied by very high risk.

The screening of each of the concepts and the selection processes are described in the following Sections 4.1.1 through 4.1.3.

4.1.1 Primary Cycle Concepts

Improving the primary cycle thermal efficiency is a key factor in reducing fuel consumption. Thermal efficiency (η_{Th}) is defined in equation (1) in terms of heat and also in terms of average temperatures (Figure 4.1.1-1). Average temperatures will be used in this report so that the thermal efficiency of the unconventional concepts may be visualized more readily.

$$\eta_{Th} = \frac{E_O}{Q_A} = \frac{Q_A - Q_R}{Q_A} = 1 - \frac{Q_R}{Q_A} = 1 - \frac{{}_1\int^4 T\,ds}{{}_2\int^3 T\,ds} = 1 - \frac{T_{R\,avg}}{T_{A\,avg}} \qquad (1)$$

TABLE 4.1-I

UNCONVENTIONAL CYCLE SCREENING SUMMARY

	Qualitative Characteristics Relative To Conventional Turbofan					
	Cruise TSFC	Engine Weight	Engine Price	Engine Maintenance Cost	Noise/ Emissions	Additional Fundamental Research Requirements
Unconventional Primary Cycles						
Regeneration*	Lower	Higher	– –	– –	Same	Heat exchanger
Intercooling	Higher	Higher	Higher	Higher	Same	Heat exchanger
Regeneration with Intercooling	Lower	Higher	Higher	Higher	Same	Heat exchangers
Reheat	Higher	Same	Higher	Higher	Same	Additional combustor
Constant Volume Combustion	Lower	Same	– –	Higher	Same	Novel combustor
Variable Compression Ratio	Same	Higher	Higher	Higher	Same	Valve and cooling system
Pressure Exchange	Higher	– –	– –	– –	Same	Pressure exchanger
Compound Cycle	Same	Higher	Higher	Higher	Same	Integrated intermittent flow engine
Unconventional Propulsion Concepts						
Shrouded Variable-Pitch Fan*	Lower	Higher	Higher	– –	Improved	Fan, gear, and drive turbine
Advanced Propeller*	Lower	Higher	– –	– –	Improved	Propeller, gear, and drive turbine
Unconventional Engine Installations						
Multiple Fans or Gas Generators	Same	Higher	– –	– –	Same	Drive systems
Laminar Flow Control Engine	Unknown	Unknown	Unknown	Unknown	Unknown	Unknown

*Selected for further analysis (Section 4.2)

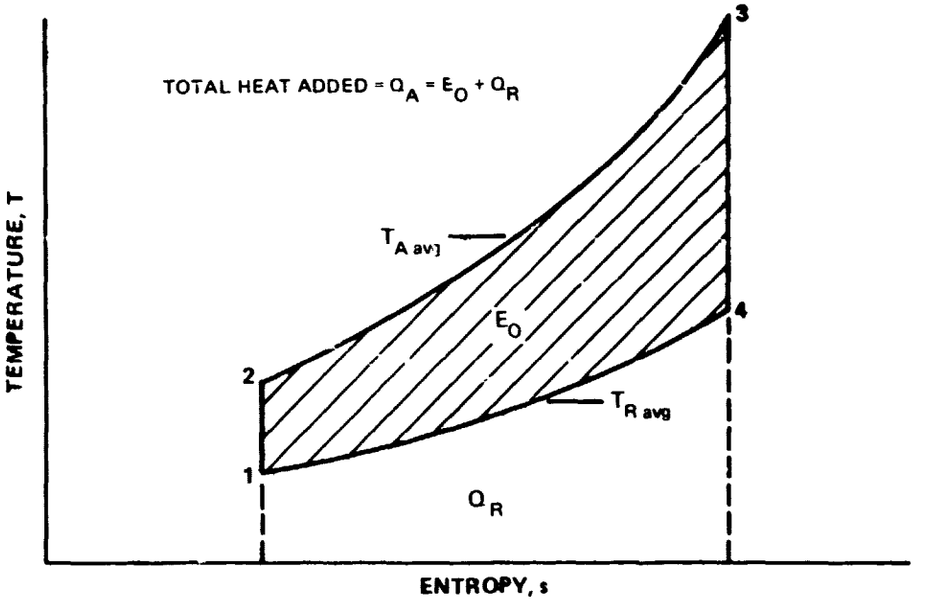

Figure 4.1.1-1 Brayton Cycle Temperature-Entropy Diagram Illustrating Average Temperatures of Heat Addition and Rejection

The expression T_{avg} is defined as being equal to $\int T\,ds$. Also, E_O (shaded area in Figure 4.1.1-1) is the useful energy output, Q_R (area under the line 4-1) is the heat rejection, Q_A is the total heat added and is the total area under 2-3 in Figure 4.1.1-1, $T_{A\,avg}$ is the average gas temperature during external heat addition (point 2 to point 3), and $T_{R\,avg}$ is the average gas temperature during heat rejection (from 4 to 1). Thermal efficiency is increased by raising $T_{A\,avg}$ and/or by reducing $T_{R\,avg}$.

For the purposes of clarity, the temperature-entropy diagram in Figure 4.1.1-1 and all subsequent diagrams of this type are drawn as ideal cycles – that is, the cycles consist of isentropic reversible compression and expansion processes (vertical lines) and constant pressure heating and cooling.

4.1.1.1 Primary Cycle With Internal Heat Exchange

Three internal heat exchange processes were examined to determine the effects of internal heat exchange on the external heat addition and rejection processes of the Brayton cycle. These were regeneration, intercooling, and regeneration with intercooling.

Regeneration. A practical method of internal cycle heat exchange which can both increase the average gas temperature during heat addition and decrease the average gas temperature during heat rejection is regeneration. This concept extracts waste heat from the turbine exhaust gases and transfers it to the air entering the combustor, reducing the amount of fuel required to achieve a given combustor exit temperature level. Referring to the engine schematic diagram in Figure 4.1.1.1-1, heat extracted from the turbine discharge between stations 4 and 4a is transmitted via a working fluid to the burner inlet, raising the temperature from T_2 to T_{2a}. In the ideal case, $T_{2a} = T_4$ because the heat added from 2 to 2a is equal to that extracted from 4 to 4a. With regeneration, external heat is added only from 2a to 3, instead of from 2 to 3, and less heat is rejected (from 4a to 1 instead of from 4 to 1). The average gas temperature during external heat addition is thereby increased and the average gas temperature during heat rejection is decreased as indicated in Figure 4.1.1.1-2, resulting in an increase in efficiency according to $\eta_{Th} = 1 - T_{R\,avg}/T_{A\,avg}$.

Intercooling. The process of intercooling is a form of heat exchange which removes heat from the compressor and rejects it at low temperature to ambient air or to the duct stream (Figure 4.1.1.1-3). Removal of heat from the compressor reduces the compressor work in a turbofan which, in turn, reduces the work required of the compressor-drive turbine. Additional energy is available for thrust at the same combustor exit temperature. In addition, a turbofan's thrust is increased because of the heat transferred to the duct stream. However, since intercooling lowers compressor exit temperature, more fuel must be burned in the combustor to obtain the same combustor exit temperature.

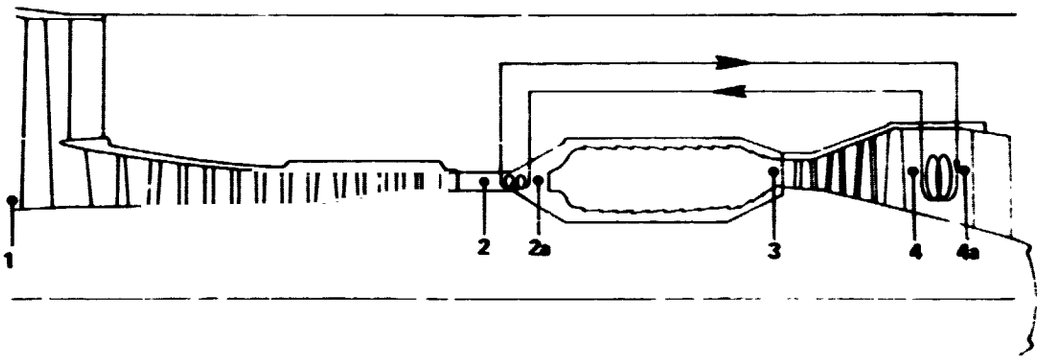

Figure 4.1.1.1-1 Regenerative Engine Concept

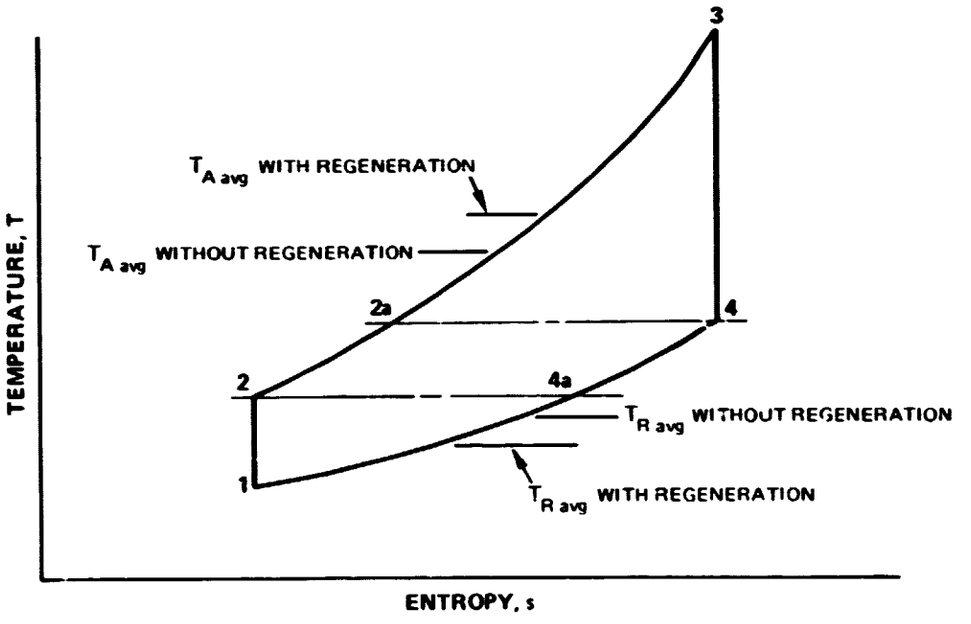

Figure 4.1.1.1-2 Temperature-Entropy Diagram for the Brayton Cycle With Regeneration

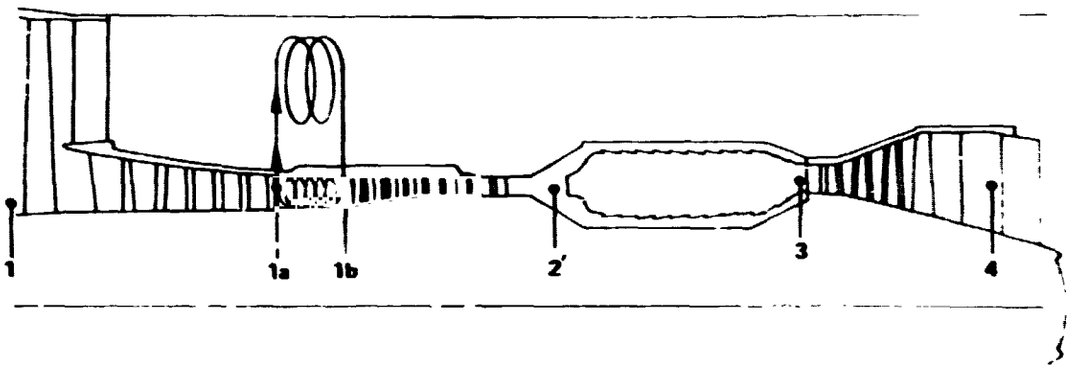

Figure 4.1.1.1-3 Compressor Intercooler Engine Concept

The temperature-entropy diagram for the Brayton cycle with intercooling is depicted in Figure 4.1.1.1-4. The conventional Brayton cycle 1-2-3-4 is shown in the same figure. With an intercooler added, inlet air at station 1 is compressed in the compressor to 1a, then cooled by intercooling to 1b (which is at a temperature almost as low as the temperature at 1), and further compressed in the compressor to 2'. Combustion is along the line from 2' to 3. Combustor exit temperature and pressure are shown at the same level as the comparative conventional Brayton cycle. The expansion process is along 3-4. The area within the intercooling cycle 1-1a-1b-2'-3-4, which is an indication of the available energy, is seen in this ideal intercooling case to be larger than that of the conventional Brayton cycle. With intercooling in the ideal Brayton cycle, both the average temperatures of external heat addition and external heat rejection are lowered. It can be shown that theoretically the average temperature of heat addition drops more than the average temperature of heat rejection. Therefore, thermal efficiency is lower with intercooling.

Regeneration With Intercooling. In the previous paragraphs it was shown that the process of intercooling has certain advantages and disadvantages. The primary advantage of intercooling is the increased power output potential for the same cycle pressure ratio and temperature. The primary disadvantage is the decreased thermal efficiency. A logical and simple means of eliminating the primary disadvantage of intercooling while retaining the advantage is to use both a regenerator and an intercooler.

Referring to the regeneration-intercooling engine schematic (Figure 4.1.1.1-5), inlet air at station 1 is compressed to 1a, cooled to 1b, and compressed further to 2' as with intercooling alone. Now the compressor exit air is heated from 2' to 2a' with the regenerator using the energy extracted from 4 to 4a' at the turbine discharge. As shown in Figure 4.1.1.1-6, the average temperature during heat addition is the same as with regeneration alone. The average temperature during heat rejection is lower than with regeneration alone. Therefore, it is apparent that regeneration with intercooling combines the advantage of regeneration, improved efficiency, with the advantage of intercooling, increased power output potential, and is therefore theoretically better than either regeneration or intercooling used alone.

Comparison of Heat Exchange Processes. The three internal heat exchange processes discussed above were screened based on a number of assumptions with regard to performance (Figure 4.1.1.1-7). Heat exchanger effectiveness and pressure losses were selected as representative levels based on numerous earlier conceptual evaluations. Figure 4.1.1.1-7 is a comparison of thermal efficiency values, as a function of cycle pressure ratio, for the conventional Brayton cycle and each of the three heat exchange processes.

Information on conventional components was based on the 1985 technology definition as considered in the NASA study of turbofan engines designed for low energy consumption (ref. 1). Thermal efficiency improvements of 2.5 and 4.5 percent at the example cruise conditions were indicated for the regenerative and regenerative/intercooled cycles at low pressure ratios relative to a 45:1 pressure ratio conventional cycle. The gains with these cycles are enhanced by the large temperature differential between the hot turbine discharge gases and the compressor discharge air which increases as pressure ratio is reduced.

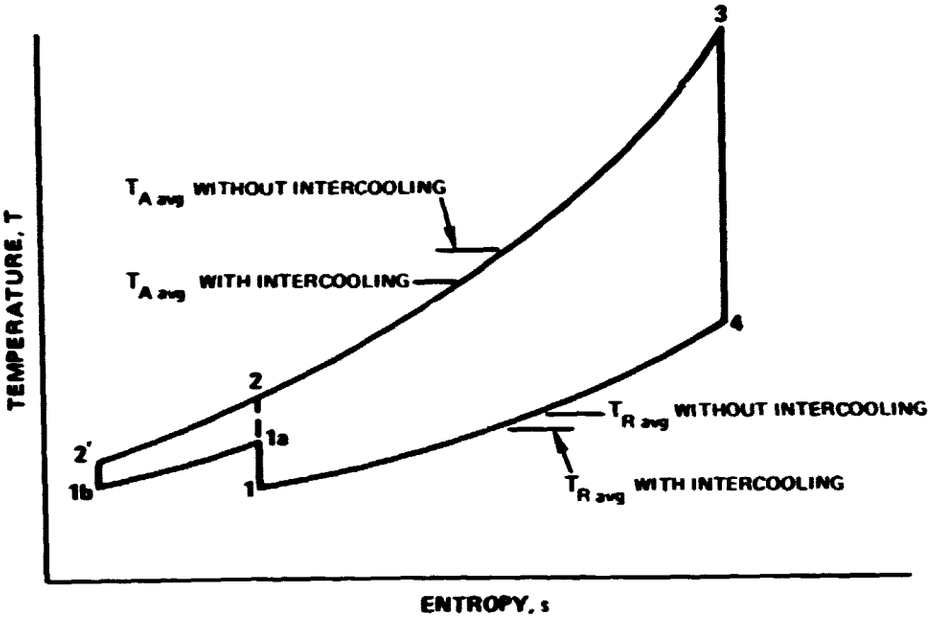

Figure 4.1.1.1-4 Temperature-Entropy Diagram for the Brayton Cycle With Intercooling in the Compressor

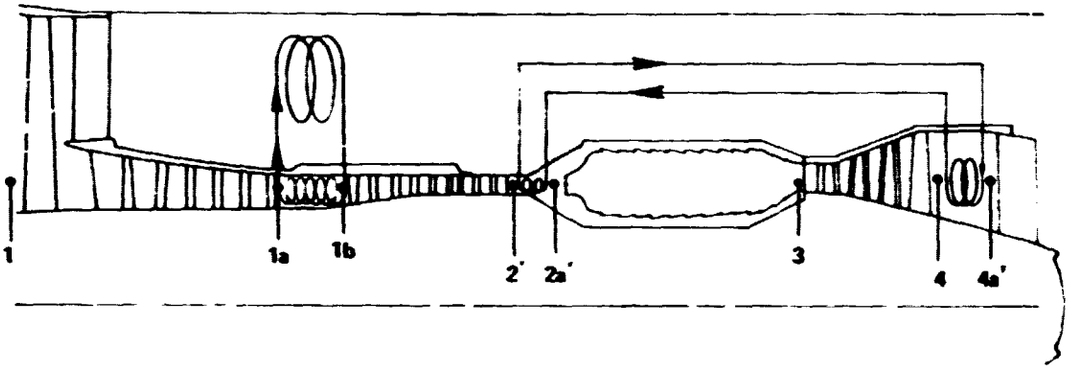

Figure 4.1.1.1-5 Engine Concept With Regeneration and Intercooling

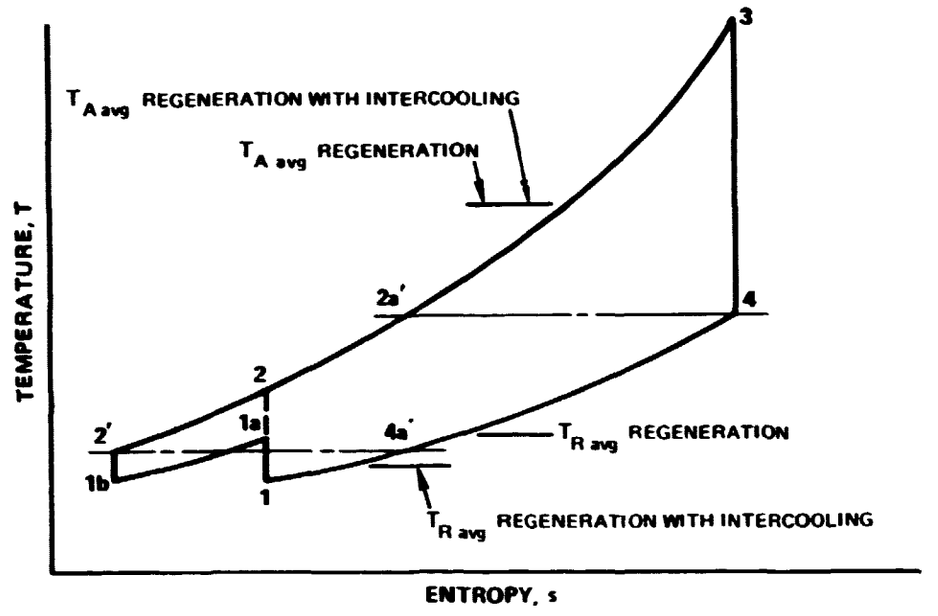

Figure 4.1.1.1-6 *Temperature-Entropy Diagram for the Brayton Cycle With Regeneration and Intercooling*

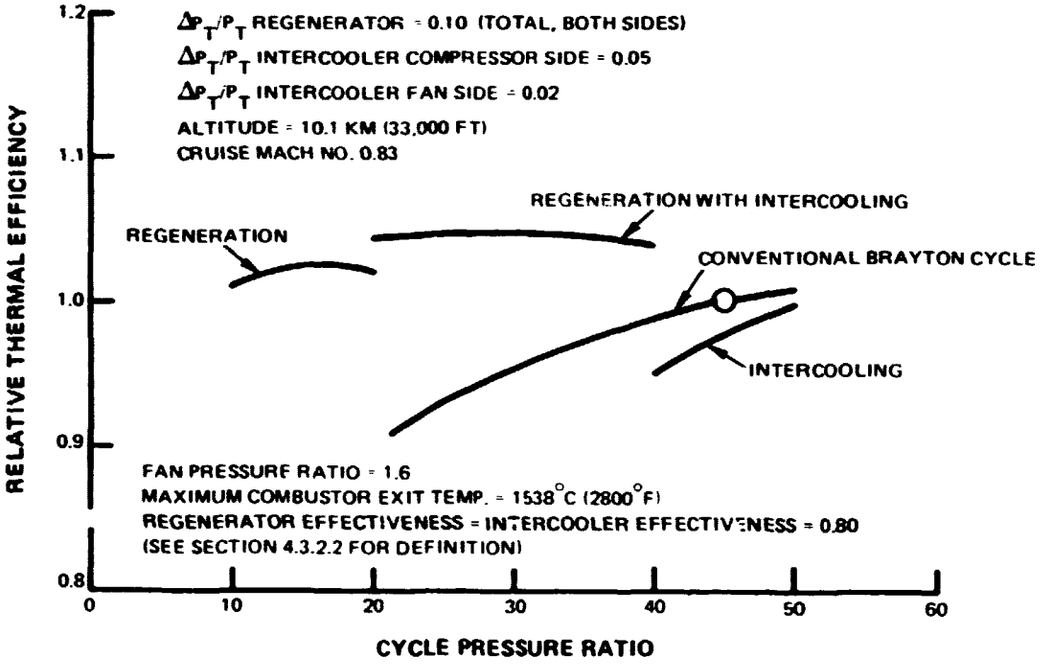

Figure 4.1.1.1-7 *Preliminary Screening of Concepts With Internal Heat Exchange in Turbofan Engine Cycles*

The intercooled cycle, at a 45:1 cycle pressure ratio, provided additional output power sufficient to increase the fan bypass ratio to 13:1 from the conventional level of 11:1 while reducing the thermal efficiency by 2 percent. The small reduction in gas generator weight possible with the higher bypass ratio was not sufficient to offset the loss in thermal efficiency on a fuel weight basis using influence coefficients generated in the study of turbofan engines designed for low energy consumption (ref. 1).

Refined Screening of Two Heat Exchanger Concepts. Based on the above results of preliminary screening of the three heat exchange processes, regeneration and regeneration with intercooling were selected for further screening, in which a set of more refined assumptions were followed. For the purposes of this evaluation, conceptual turbofan installations were determined as shown in Figures 4.1.1.1-8 and -9. In both systems the regenerator was positioned directly behind the turbine to minimize the hot gas ductwork and frontal area requirements.

Turbofan cycles were selected from the preliminary screening analysis to maximize the thermal efficiency potential of the two candidate cycles. Owing to Pratt & Whitney Aircraft prior design and test experience with the PT6 engine with regeneration, rotary toroidal regenerators were evaluated and drawn for the comparison. The geometry and performance characteristics of the regenerators used for refined screening are discussed in more detail in Section 4.3.2 of this report.

A single-pass, counterflow, plate-fin intercooler was conceptually defined for the evaluation. Various combinations of fan duct, cold side intercooler flow rates and heat exchanger effectiveness were examined in an effort to determine the optimum heat exchanger geometry. Various percentages of the fan air to cool the compressor air at an 80 percent effectiveness level were examined analytically, leading to a selected flow rate of 25 percent fan discharge air to maximize the thermal efficiency. Heat exchanger effectiveness was lowered to 70 percent to reduce the intercooler frontal area by 10 percent without significant efficiency loss.

The refined screening of the regenerator and intercooler resulted in a degradation in thermal efficiency for both heat exchangers. The principal cause of the degradation was significantly higher calculated pressure losses in the plumbing relative to the levels assumed in the preliminary screening. As shown in Table 4.1.1.1-I, a regenerative cycle thermal efficiency 2.2 percent lower than the initial screening value and a regenerator with intercooler thermal efficiency 4.0 percent lower than the initial screening value resulted from the reassessment.

Engine performance, weight and nacelle dimensions were also compared using the revised heat exchanger performance (Table 4.1.1.1-II). The following parameters were assumed constant for the data given in the table: 1.6:1 fan pressure ratio, 1538°C (2800°F) maximum combustor exit temperature, 26,700 N (6000 lbf) thrust at maximum cruise, Mach 0.83, and 10.1 km (33,000 ft) altitude.

The simpler regenerative turbofan showed the potential for higher thermal efficiency, lower weight, and lower installation drag than a regenerative/intercooled turbofan. Therefore, the simpler system was found to have the greater potential for conserving fuel in aircraft engines. The level of performance, in terms of cruise TSFC, is essentially the same as a conventional turbofan. The regenerative concept was found to be a low pressure ratio alternative to the higher pressure ratio conventional Brayton cycle engine.

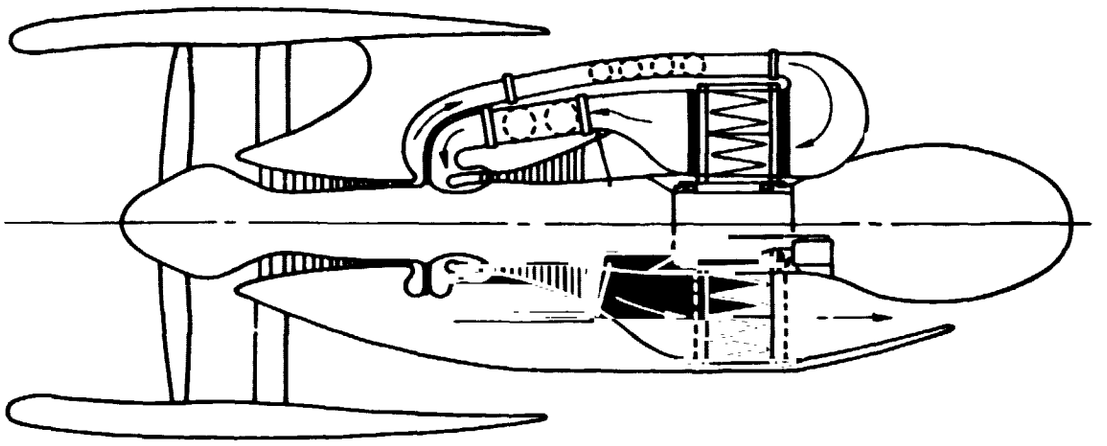

Figure 4.1.1.1-8 Regenerator Configuration for Refined Screening Evaluation

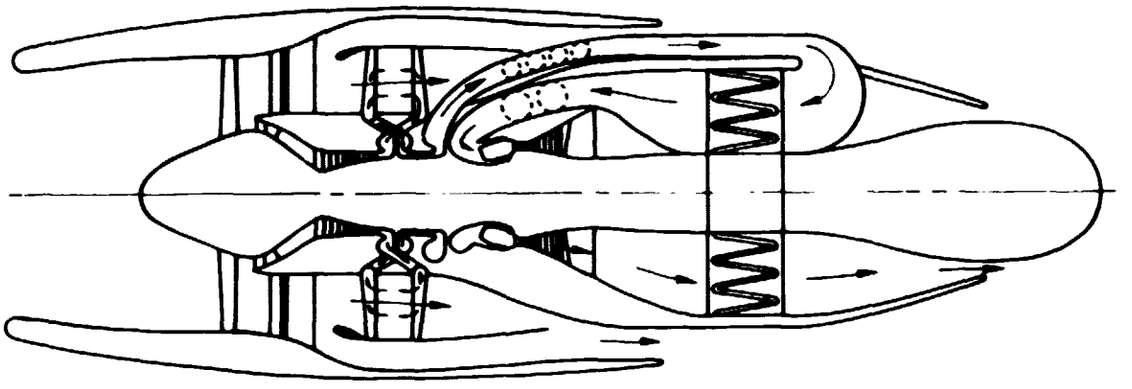

Figure 4.1.1.1-9 Regenerator-Intercooler Configuration for Refined Screening Evaluation

TABLE 4.1.1.1-I

HEAT EXCHANGER REFINED SCREENING RESULTS

	Regenerator		Intercooler	
	Initial	**Refined**	**Initial**	**Refined**
Effectiveness	0.80	0.85	0.80	0.70
Total Pressure Loss, $\Delta P_T/P_T$	0.10	0.153	0.07	0.151
Carryover and Leakage Flow, %	0	3.5	0	0
Percent change in Thermal Efficiency resulting from the above initial-to-refined change in:				
Effectiveness	----	+1.5	----	−0.2
Total Pressure Loss	----	−1.6	----	−1.6
Carryover and Leakage Flow	----	−2.1	----	----
Total		−2.2		−1.8

TABLE 4.1.1.1-II

REFINED SCREENING RESULTS FOR THE REGENERATIVE TURBOFAN AND THE REGENERATIVE TURBOFAN WITH INTERCOOLER

	Regenerative Turbofan	**Regenerative Turbofan With Intercooler**
Cycle Pressure Ratio	15:1	20:1
Relative Base Engine Weight	1.00	1.20
Relative Maximum Nacelle Diameter	1.00	1.07
Relative Nacelle Length	1.00	1.03
Relative Cruise Thermal Efficiency	1.000	0.996

4.1.1.2 Primary Cycle With Reheat

If a second burner is added between turbine stages, the Brayton cycle engine with reheat results as shown in Figure 4.1.1.2-1. Compression and combustion 1-2-3 is as in the conventional Brayton cycle. Following partial expansion 3-3a in the high pressure turbine, heat is added in the second burner between 3a and 3b ($T_{3b} = T_3$), and low pressure turbine expansion occurs between 3b and 4'. Adding reheat to the Brayton cycle increases the average temperature during heat addition (2-3-3a-3b) but increases the average temperature during heat rejection (4'-1) even more, resulting in the cycle diagram of Figure 4.1.1.2-2. Therefore, the efficiency of the reheat cycle is lower than that of the conventional Brayton cycle. The advantage of an engine which uses the reheat principle is that added power output is obtained for the same size gas generator.

The reheater was evaluated in several different positions among the turbine stages to determine the performance sensitivity to reheater location. The reheater exit temperature was set equal to the primary combustor exit temperature to maximize the power output of the system. The additional power output was utilized by reducing the gas generator size and weight needed to power the fan in a turbofan engine. The engine bypass ratio was increased accordingly. The TSFC of the reheated turbofan is compared with a conventional turbofan in Figure 4.1.1.2-3. The increased air bleed needed to cool turbine parts behind the reheater resulted in a TSFC penalty of 8 percent; this penalty increased as the reheater was moved aft through the turbine. Gas generator size was reduced simultaneously. Table 4.1.1.2-I illustrates the TSFC and gas generator size (weight) effects as related to fuel use by a domestic trijet using sensitivity factors generated under the NASA study of turbofan engines designed for low energy consumption (ref. 1).

No further evaluation of reheat was conducted, as it was determined that even a 100 percent engine weight saving could not offset the large specific fuel consumption penalty in terms of the fuel savings potential.

4.1.1.3 Unconventional Thermodynamic Processes

In addition to internal heat transfer and reheat, direct substitution of alternate processes was considered for improving thermal efficiency. Variations to the Brayton cycle that were surveyed included constant volume combustion, variable compression, pressure exchange, and a compound cycle.

Constant Volume Combustion. The nonsteady combustor, of which the constant volume combustor (Figure 4.1.1.3-1) is a special case, is essentially a tube of constant cross-sectional area with a valve at each end.

Since combustion is accompanied by a pressure rise in the nonsteady combustor, its application as a primary burner presents the possibility of achieving effective compression ratios in excess of those achieved through the compressor section of the engine. Thus the potential benefit of constant volume combustion would be to achieve a higher cycle pressure ratio for a given number of compressor and turbine stages. This could lead to a reduction in engine TSFC, with a consequent reduction in the airplane fuel requirement.

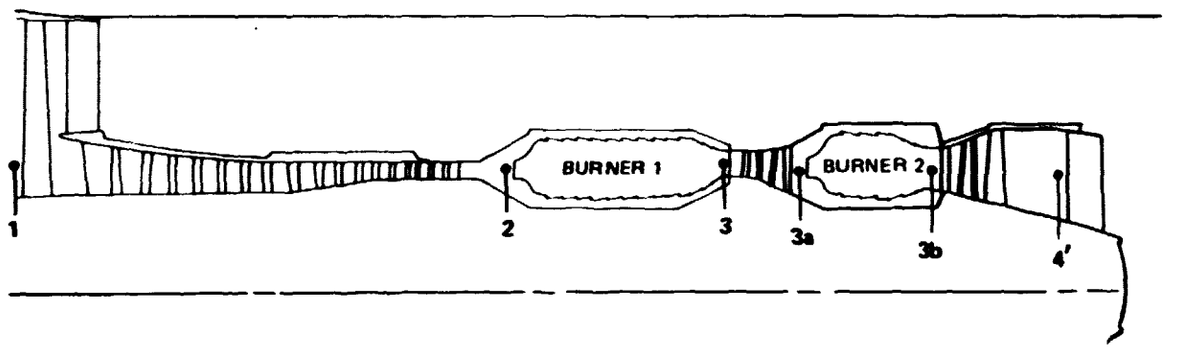

Figure 4.1.1.2-1 *Engine Concept With Reheat Burner Between Turbine Stages*

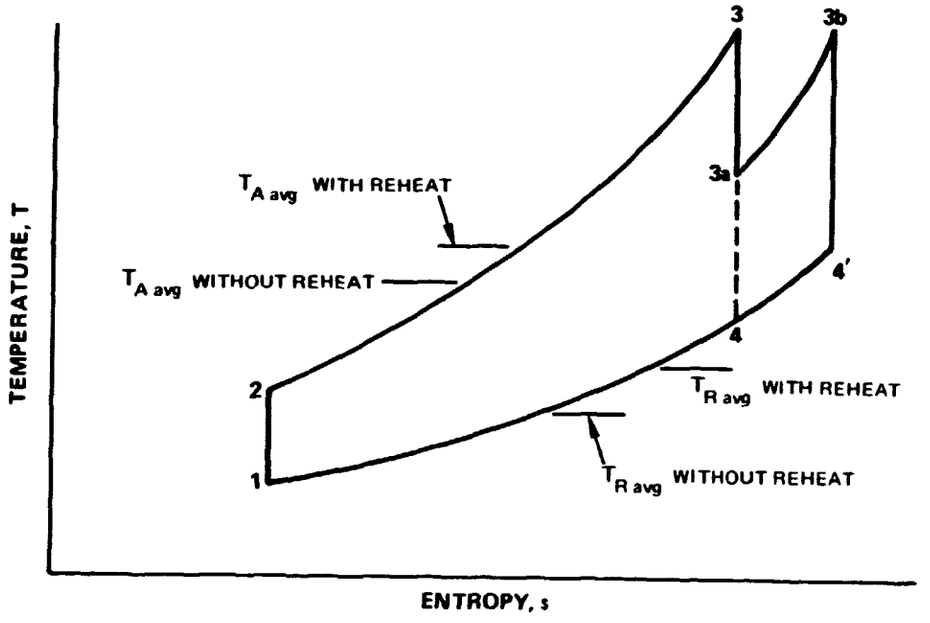

Figure 4.1.1.2-2 *Temperature-Entropy Diagram for the Brayton Cycle With Interturbine Reheat*

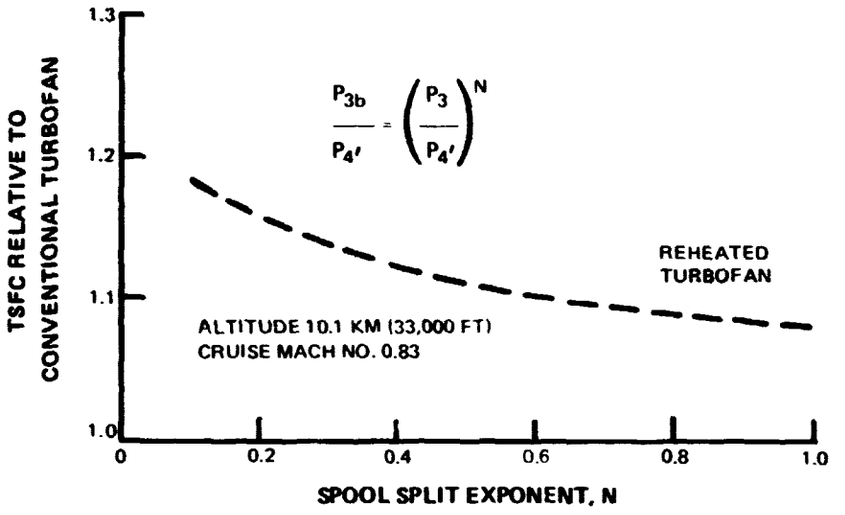

Figure 4.1.1.2-3 Reheat Cycle Preliminary Screening Results

TABLE 4.1.1.2-I

REHEAT CYCLE FUEL SAVINGS POTENTIAL RELATIVE TO CONVENTIONAL TURBOFAN

Spool Split Exponent, N*	0.9	0.5	0.1
Relative Installed TSFC	1.08	1.11	1.17
Relative Gas Generator Airflow	1.00	0.77	0.69
Relative Fuel Use	1.27	1.30	1.38

*See Figure 4.1.1.2-3

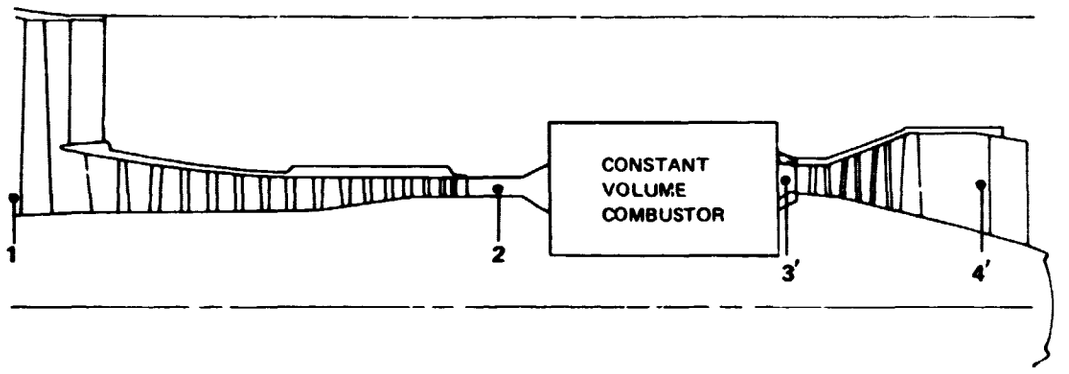

Figure 4.1.1.3-1 Constant Volume Combustor Turbofan Concept

In the temperature-entropy diagram for the constant volume combustion cycle (Figure 4.1.1.3-2), compression is along 1-2. Combustion 2-3′ results in further compression to station 3′, which is drawn at the same temperature as station 3 in the conventional Brayton cycle (dashed lines). From examination of this diagram it can be seen that the average temperature during external heat addition is essentially the same as the conventional Brayton cycle, but the average temperature of external heat rejection is lower, resulting in a higher thermal efficiency potential for the constant volume combustion cycle.

The pressure rise that can be achieved in a practical combustor design provides the key to the potential of this concept. For the performance estimates in the screening, a pseudo-detonation process was assumed with a combustor pressure ratio of 1.2 based on valving dynamic limit considerations. The background information for assessment of this concept was based on ref. 2.

A 2 to 4 percent cruise thermal efficiency improvement over a conventional Brayton cycle was calculated. The small return for the significantly increased engine complexity does not currently appear to justify the further development of these devices. This conclusion is the same as was reached in ref. 3.

Variable Compression Ratio. A variable compression ratio turbofan such as that illustrated in Figure 4.1.1.3-3 employs a flow diverter valve located in the compression system. A high overall compression ratio is achieved during cruise operation by positioning the flow diverter valve to direct the discharge from the low-pressure compressor into the high-pressure compressor. A lower overall compression ratio is obtained by positioning the flow diverter valve such that the discharge from the low-pressure compressor is diverted into the fan duct and a portion of the fan discharge flow is directed into the high-pressure compressor.

Very high cycle pressure ratios (40 to 60) can reduce the fuel consumption of a turbofan cycle. However, these very high compression ratios create a severe metal-temperature and pressure problem in the rear of the high-pressure compressor at sea level on high ambient temperature days. A cycle which has a variable compression ratio can use a high compression ratio at cruise, where fuel consumption is of prime importance and where the ambient temperature and pressure are low, and use a low compression ratio at sea level where the ambient temperature and pressure are high, thus reducing the metal temperatures and pressures in the rear stages of the high-pressure compressor.

In the temperature-entropy diagram (Figure 4.1.1.3-4) cycle 1-2-3-4 is the variable compression ratio cycle for cruise operation. The cycle would apply to a similar conventional engine which does not employ the variable compression principle. With the flow diverter valve positioned for take-off operation of the compressors, the compression can be reduced from conventional operation. The attendant reduced compressor discharge temperature levels at take-off can be used to reduce the cooling air bleed requirement based on a given hot parts metal temperature with the lower temperature cooling air. Reduced cooling air could improve the cycle thermal efficiency both at take-off and during cruise operation.

The de-supercharging associated with the diverter valve operation during take-off results in a lowering of the gas generator airflow and resultant loss in thrust potential. To make up

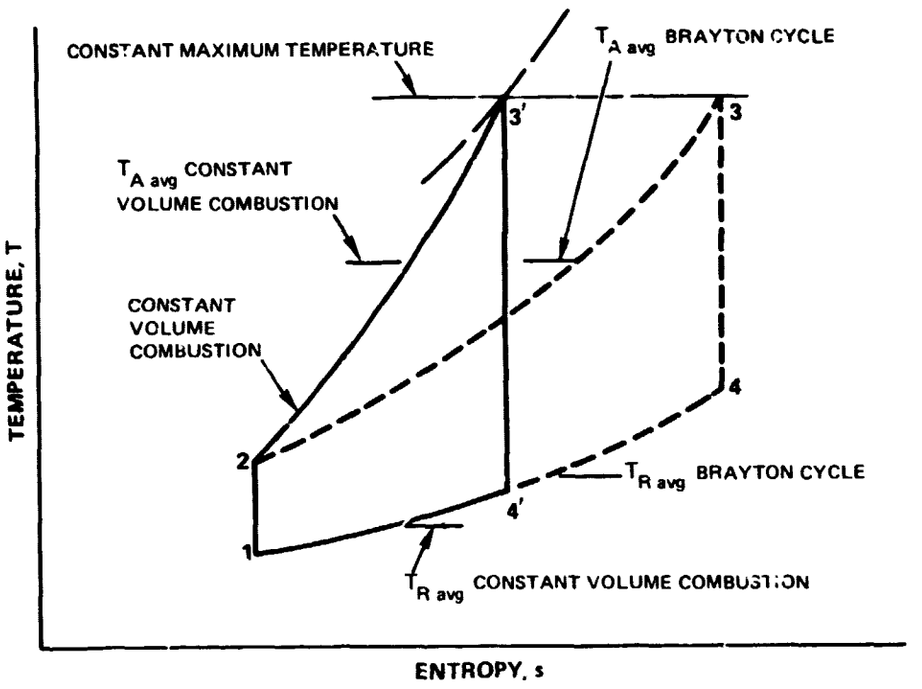

Figure 4.1.1.3-2 *Temperature-Entropy Diagram for the Constant Volume Combustion Process Compared to the Conventional Brayton Cycle With the Same Combustor Exit Temperature*

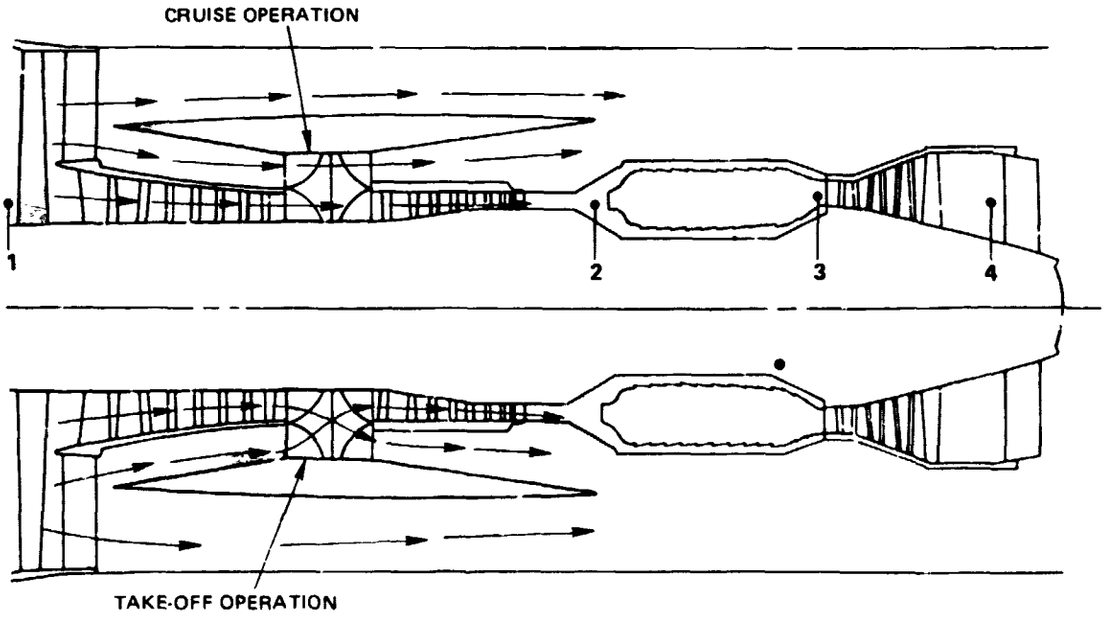

Figure 4.1.1.3-3 *Variable Compression Ratio Turbofan Concept*

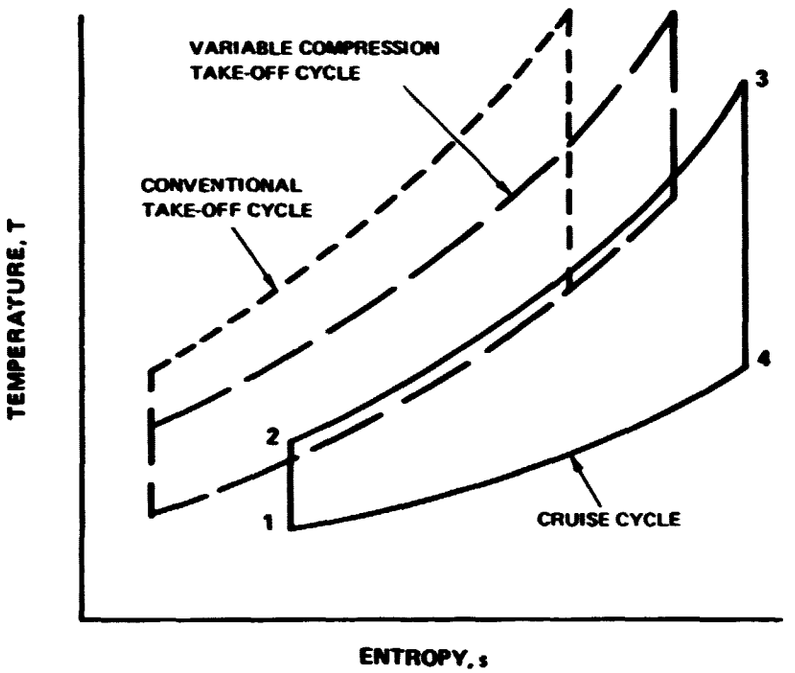

Figure 4.1.1.3-4 Temperature-Entropy Diagram for a Variable Compression Cycle Engine

the loss, the engine size must be increased substantially or run at higher combustion exit temperature levels during take-off. Of the two alternatives, the latter was determined to have a smaller detrimental effect on fuel savings potential. When used in this manner, the utility of variable compression lies in the cooling air bleed requirements as affected by the cooling air and gas temperature levels. These effects were evaluated as shown in Figure 4.1.1.3-5. The variation in temperatures shown was accomplished by varying the division of compression between the low-pressure and high-pressure compressors. The cooling air variation over a wide range of compression splits was estimated to be far less than ±0.5 percent of compressor air to achieve a given level of thrust at take-off when assuming 1985 cooling and materials technology. The added complexity of the valving system is not justified based on these results.

Pressure Exchange. Pressure exchange is the compression of one fluid at the expense of the expansion of another fluid. This process could theoretically replace a portion of the compressor-turbine combination normally used to achieve compression.

Pressure exchange is a well known phenomenon and there have been several proposed applications for it, such as the Comprex®* (Figures 4.1.1.3-6 and -7 and ref. 4). The efficiency of the pressure exchange process relative to the displaced turbomachinery was assessed in order to determine the relative fuel savings potential. Investigators in the past have estimated a maximum theoretical compression-expansion efficiency of slightly over 70 percent to be possible with the practical application of wave mechanics to the pressure exchange process. This efficiency level is substantially below an equivalent compressor-turbine efficiency of approximately 80 percent, which is projected for 1985. Therefore, the conventional turbomachinery will offer significantly higher future fuel savings than pressure exchange devices.

Compound Cycle. Another means of increasing the average temperature of external heat addition of a gas turbine engine is compounding. The type of cycle compounding considered combines a gas turbine engine with an intermittent flow engine (Figure 4.1.1.3-8). An example of this type of engine is the Napier Nomad aircraft engine (refs. 5, 6). Referring to the figure, intake air is compressed 1-2 as in a conventional gas turbine engine. This compressed air is further compressed 2-2a in the intermittent flow engine chambers, burned 2a-2b, expanded 2b-3, then further expanded 3-4 in the turbine. The average temperature during heat rejection is the same as in the conventional Brayton cycle, but the average temperature during heat addition is higher, resulting in a higher thermal efficiency (see Figure 4.1.1.3-9). Since combustion is not continuous, a higher combustor exit temperature is possible without exceeding material limits.

Historically, the compound engine, as exemplified by the Napier Nomad engine, has exhibited the highest efficiency among applicable engine cycles, i.e., the lowest brake specific fuel consumption (Figure 4.1.1.3-10). This historical evidence also shows that the use of very high pressure ratios in general has resulted in the highest efficiencies. On an equal output power basis, the Napier Nomad weighed approximately two to three times more than smaller first-generation turboshaft engines while providing one-third higher thermal efficiency.

*This is a trademark of BBC Brown, Boveri & Company, Ltd., 5401 Baden, Switzerland.

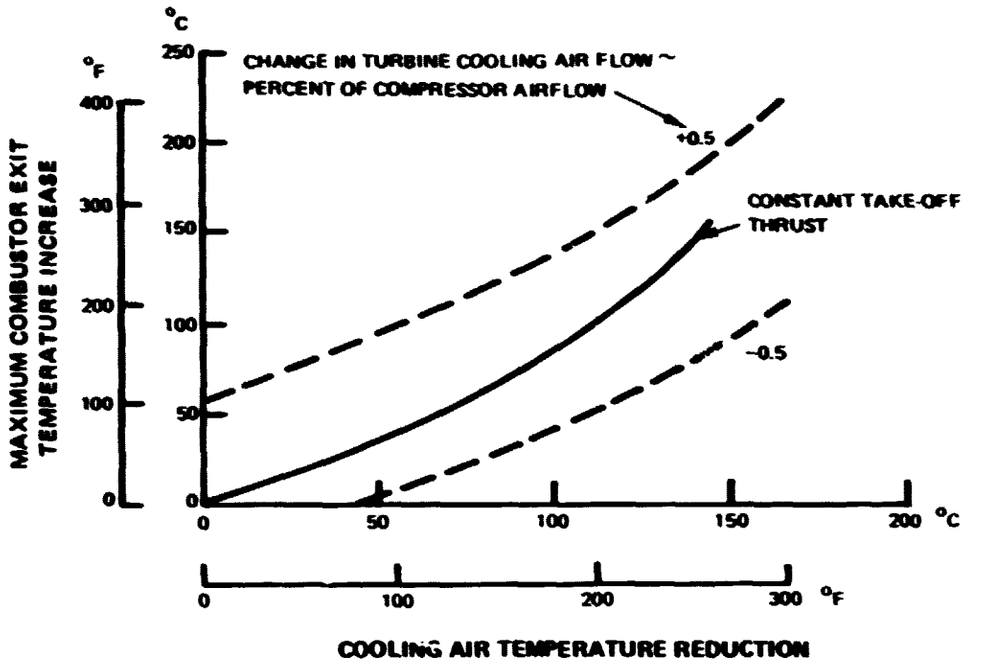

Figure 4.1.1.3-5 *Effect of Variable Compression on Cooling Air Requirements Based on 1985 Cooling Technology*

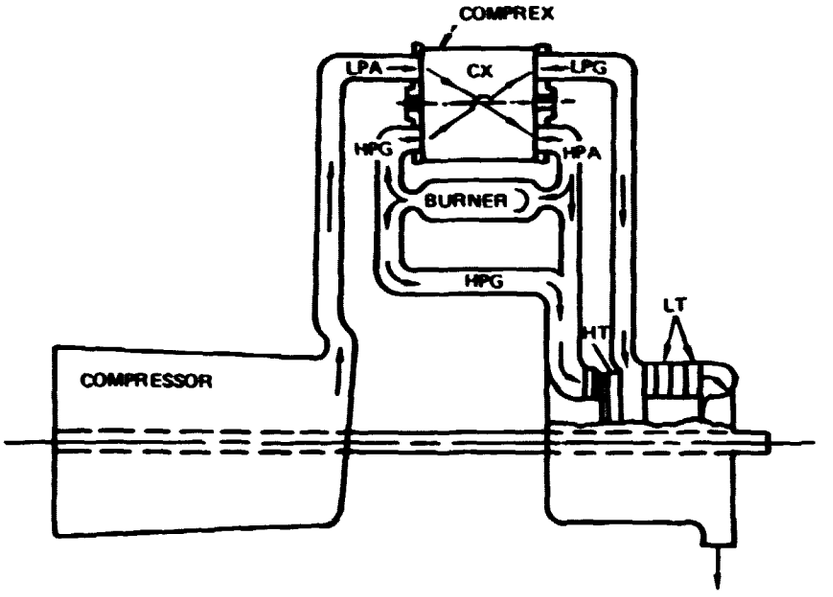

Figure 4.1.1.3-6 *Schematic Diagram of the Comprex® Pressure Exchange Engine*

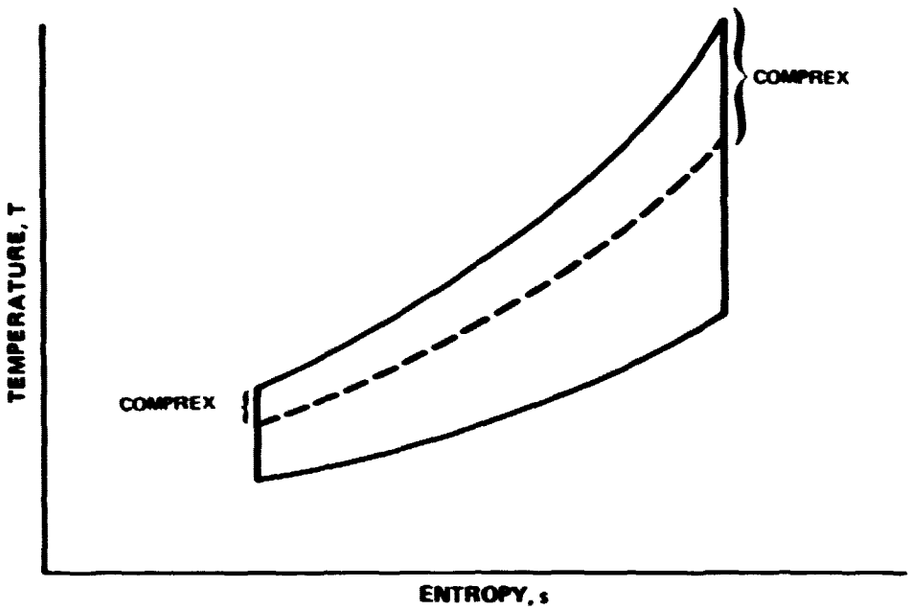

Figure 4.1.1.3-7 Temperature-Entropy Diagram for the Comprex® Pressure Exchange Engine

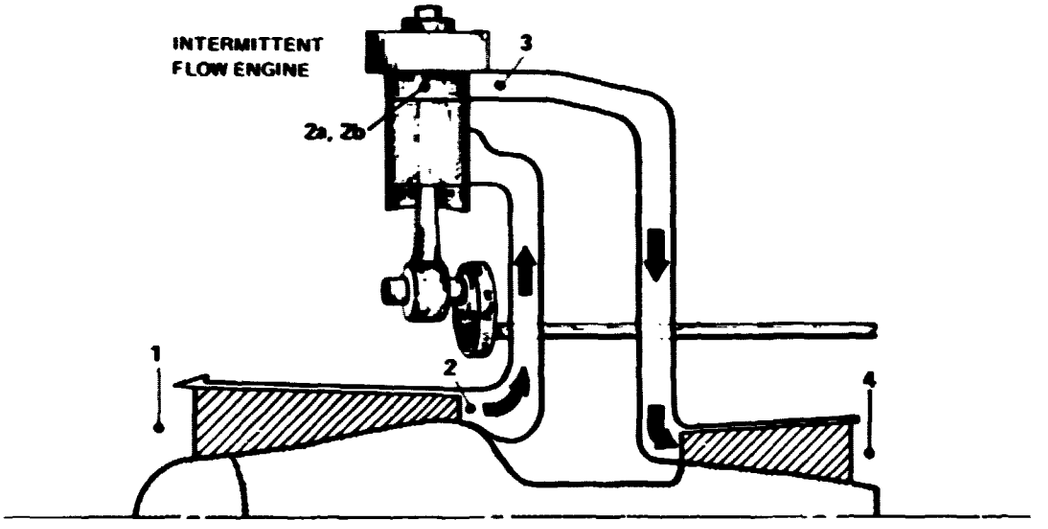

Figure 4.1.1.3-8 Compound Gas Turbine and Intermittent Flow Engine

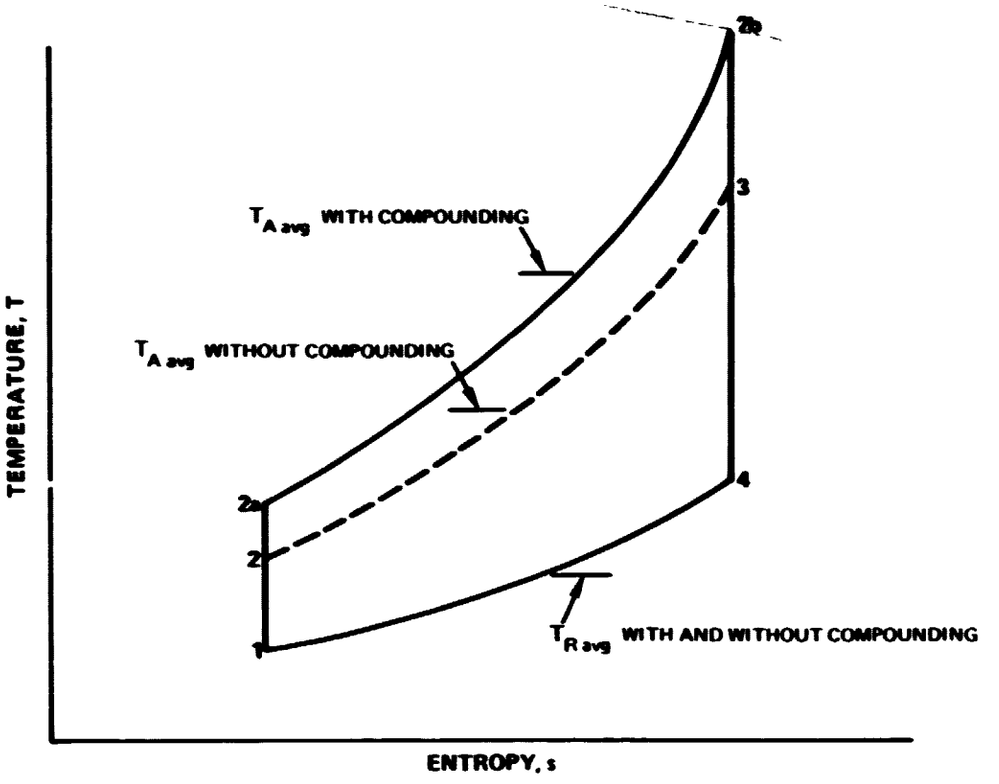

Figure 4.1.1.3-9 Temperature-Entropy Diagram for the Compound Brayton/Intermittent Flow Engine Cycle

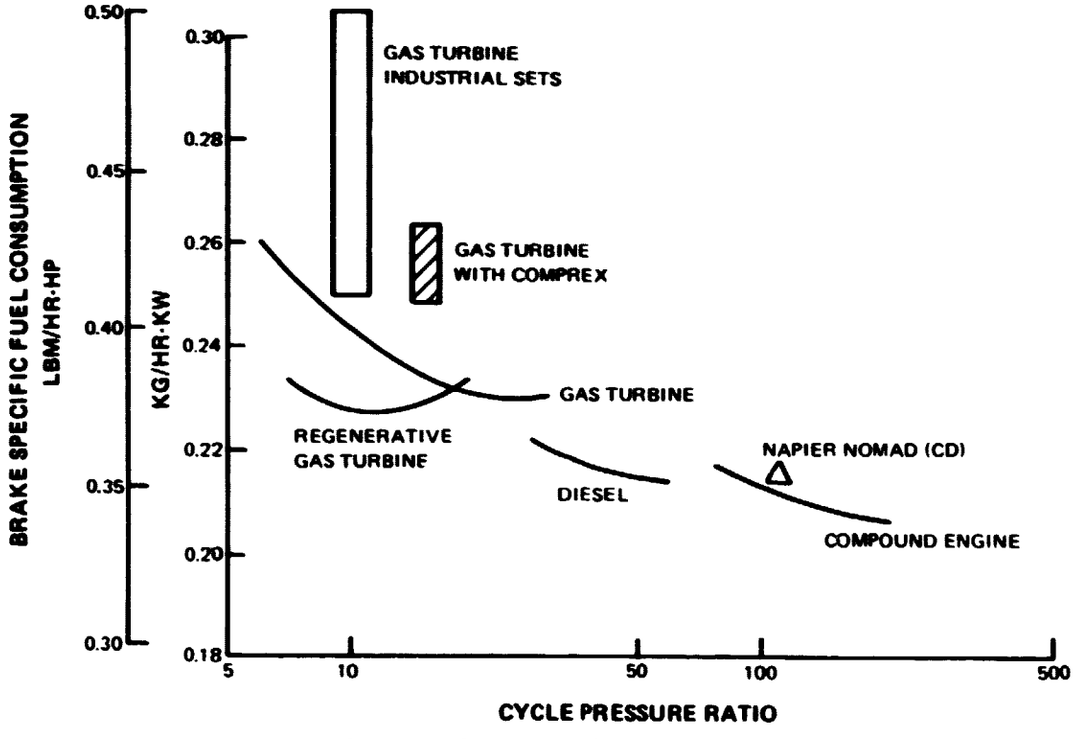

Figure 4.1.1.3-10 Historical Sea Level Static Fuel Consumption Data for Various Engine Cycles

Recent studies indicate that this weight difference could now be significantly narrowed by proper selection of the pressure ratio of an advanced technology compressor and a modern rotary engine (ref. 7). Improvements in thermal efficiency could also be obtained by utilizing advanced technology turbomachinery and by insulating the rotary engine to limit the heat loss to 10 or 15 percent of the external heat input. By 1985, it is possible that the rotary engine, compressor, and turbine technologies will advance to the point where a compound cycle thermal efficiency 10 or 15 percent greater than the Napier Nomad level would be possible.

With this improvement, advanced compound gas turbines with projected 1985 technology levels can provide thermal efficiency levels similar to the advanced simple gas turbine cycle. However, the risk involved in the development of the complex nonsteady flow engine together with its greater weight and cost prevented selection of this concept for further study.

4.1.2 Propulsor Concepts

The propulsor is that part of the propulsor subsystem which converts available power into useable propulsive power (net thrust times flight velocity). In an effort to increase propulsive efficiency (net thrust times flight velocity divided by primary cycle available energy), the effects of incorporating unconventional propulsors were analyzed.

Two unconventional propulsors were selected for special emphasis because of their theoretical potential fuel savings. One was an advanced propeller; the other was a shrouded fan. Both were analyzed for propulsive efficiency potential and compared to the efficiency potential of an advanced turbofan propulsor incorporating 1985 technology. The baseline turbofan was the STF 477 (ref. 1). Propulsor performance comparisons are based on a Mach 0.8, 9.14 km (30,000 ft) altitude cruise capability. These conditions were selected because a future transport with this capability could readily merge into the currently established air traffic system.

4.1.2.1 Conventional Propulsor Characteristics

Shaft power is converted to propulsive power when the propulsor (fan or propeller) increases the velocity of a given mass of air. For a given level of propulsive power, the fan, in combination with an air inlet and an exhaust nozzle, imparts a relatively large velocity increase to a small mass of air, while the propeller imparts a small velocity increase to a substantial amount of air.

Figure 4.1.2.1-1 presents a comparison of the installed efficiencies of the baseline conventional fan, incorporating 1985 technology, and current operational propellers relative to the pressure ratio across the propulsor. Also shown is the ideal efficiency which theoretically can be achieved. As can be seen, the lower the pressure ratio, the higher the ideal propulsive efficiency. Consequently, the potential for improving the propulsive efficiency would be best achieved by reducing the pressure ratio across the propulsor, i.e., by reducing the velocity increase across the propulsor.

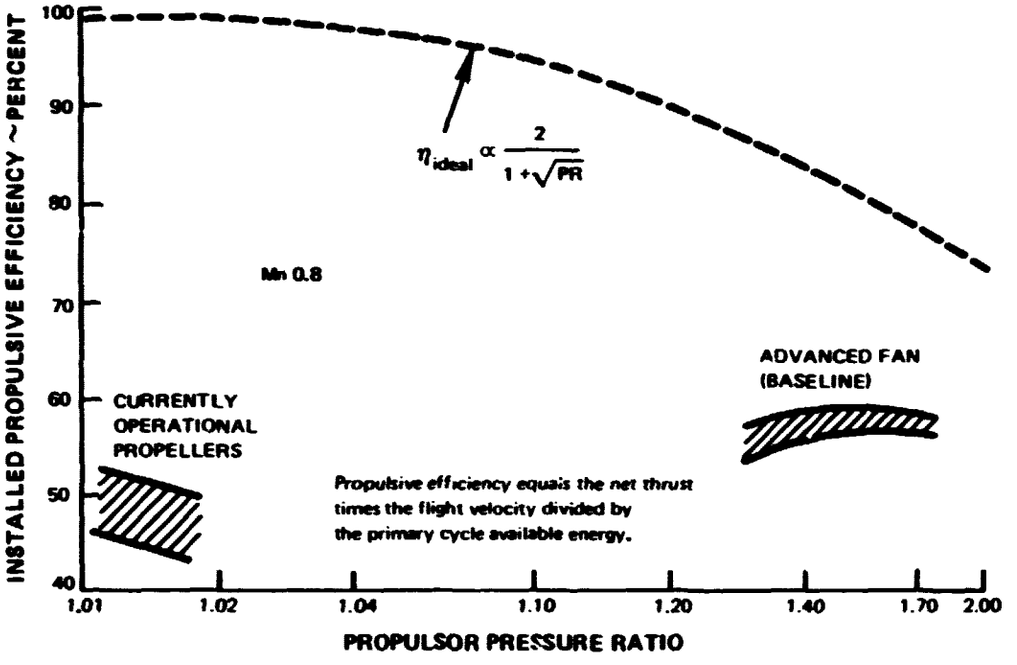

Figure 4.1.2.1-1 *Installed Propulsive Efficiency of the Baseline Conventional Advanced Fan (1985 Technology) and Currently Operational Propellers Compared to Ideal Propulsive Efficiency*

Well-designed advanced conventional fans may achieve adiabatic efficiencies of 85 percent or higher. However, installation losses such as inlet and exit ducting (parasitic) losses, fan cowl drag, and afterbody scrubbing drag account for significant reductions in propulsive efficiency. Current propellers, by comparison, can achieve only a 50 to 55 percent equivalent adiabatic efficiency at high subsonic cruise Mach number (0.8) due to high blade profile losses, compressibility losses, and tip vortex losses associated with propeller blading.

Since thrust output is proportional to mass flow rate and the velocity increase through the propulsor, propulsor diameter increases with reduced pressure ratio (i.e., higher mass flow rate, lower velocity increase). Figure 4.1.2.1-2 shows the relationship between diameter and pressure ratio for these propulsors.

From this comparison it was decided that to achieve the full propulsive efficiency potential, unconventional fan development should be directed toward reducing parasitic losses. In addition, performance improvement for the unconventional propeller can best be achieved by redesign of propeller blading.

4.1.2.2 Shrouded Fan Concept

The shrouded fan propulsor consists of the fan, a static shroud which forms the outer diameter of the ducting including the nozzle, and the exit guide vanes. The three major factors affecting low pressure ratio fan propulsive efficiency potential are internal ducting pressure losses, nozzle losses, and fan cowl drag. Sensitivity of propulsive efficiency to these three factors is shown in Figure 4.1.2.2-3. The propulsive efficiency sensitivity increases by a factor of five or greater between pressure ratios of 1.7 and 1.1 for these parameters (left side of figure). Fan cowl drag could easily increase by a factor of four between pressure ratios of 1.7 and 1.1 for conventional nacelle geometry because of the increased wetted area associated with larger fan diameter (right side of Figure 4.1.2.2-3). The estimated performance benefits for a reduction in nacelle length to diameter (L/D) from 1.55 to 0.50 are also shown in Figure 4.1.2.2-3, right side.

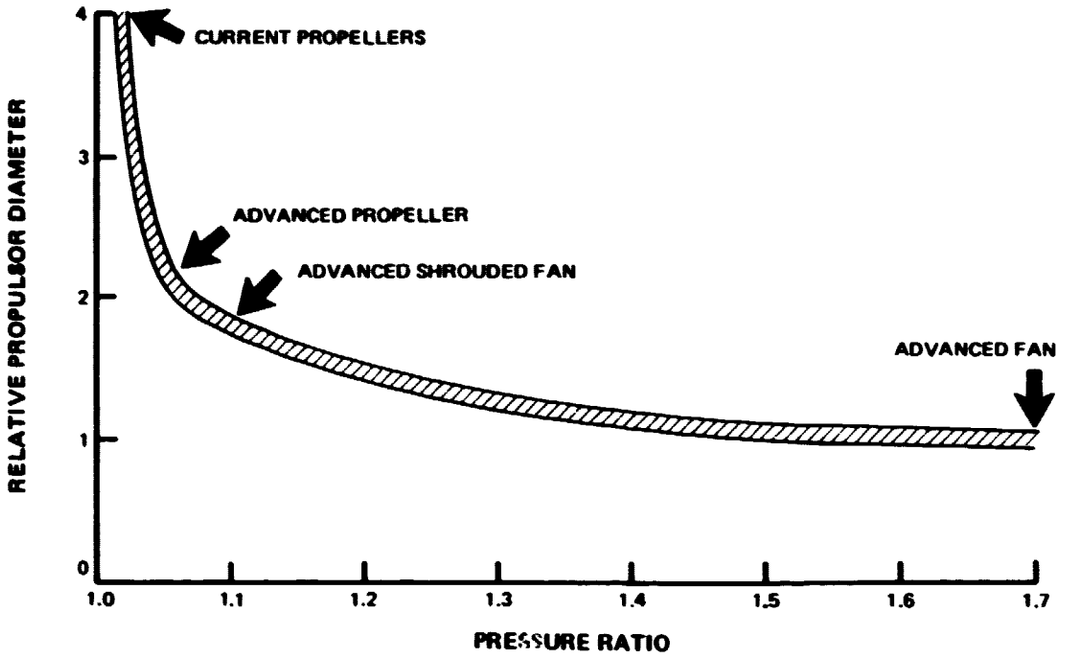

Figure 4.1.2.1-2 Relationship Between Propulsor Diameter and Pressure Ratio

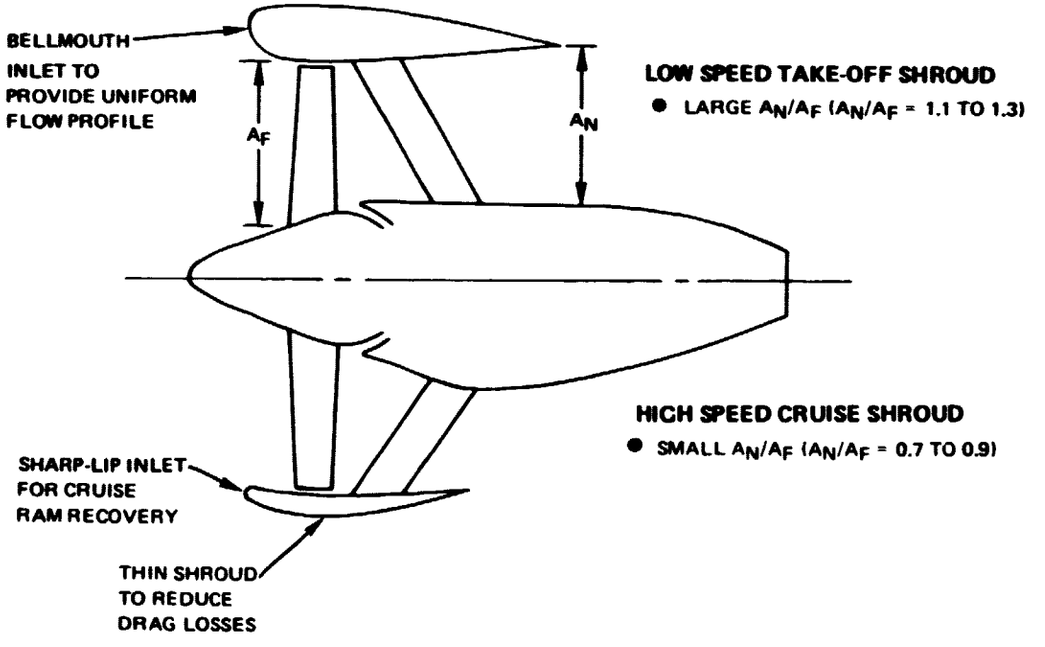

Figure 4.1.2.2-1 Schematic Comparison of Take-Off and Cruise Fan Shrouds

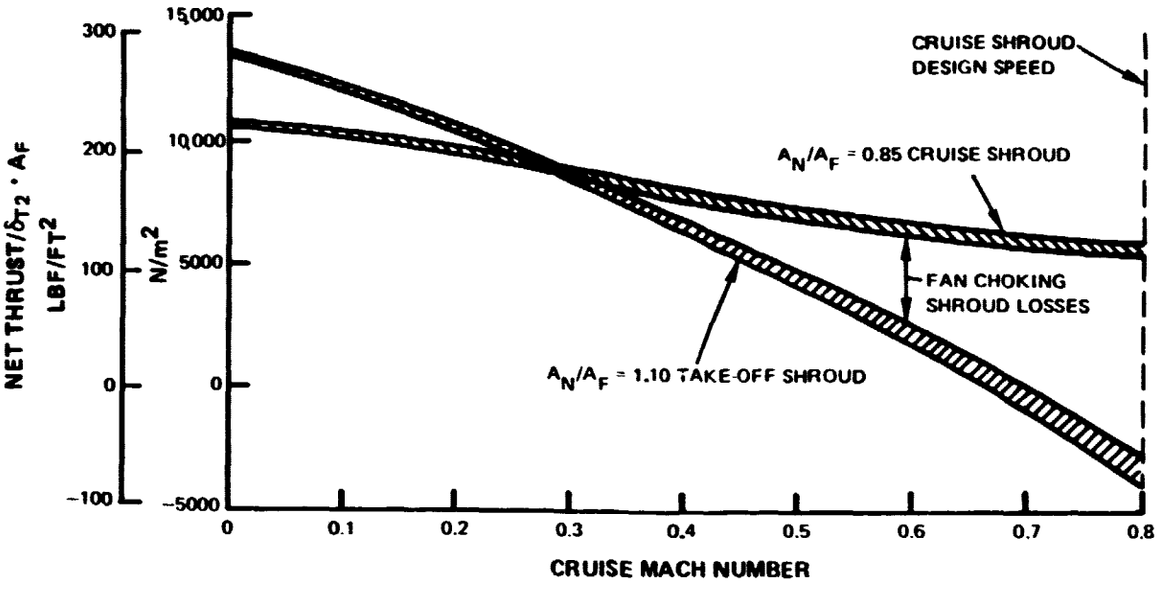

Figure 4.1.2.2-2 *Comparison of Thrust Capability of Take-Off and Cruise Fan Shrouds As a Function of Flight Speed*

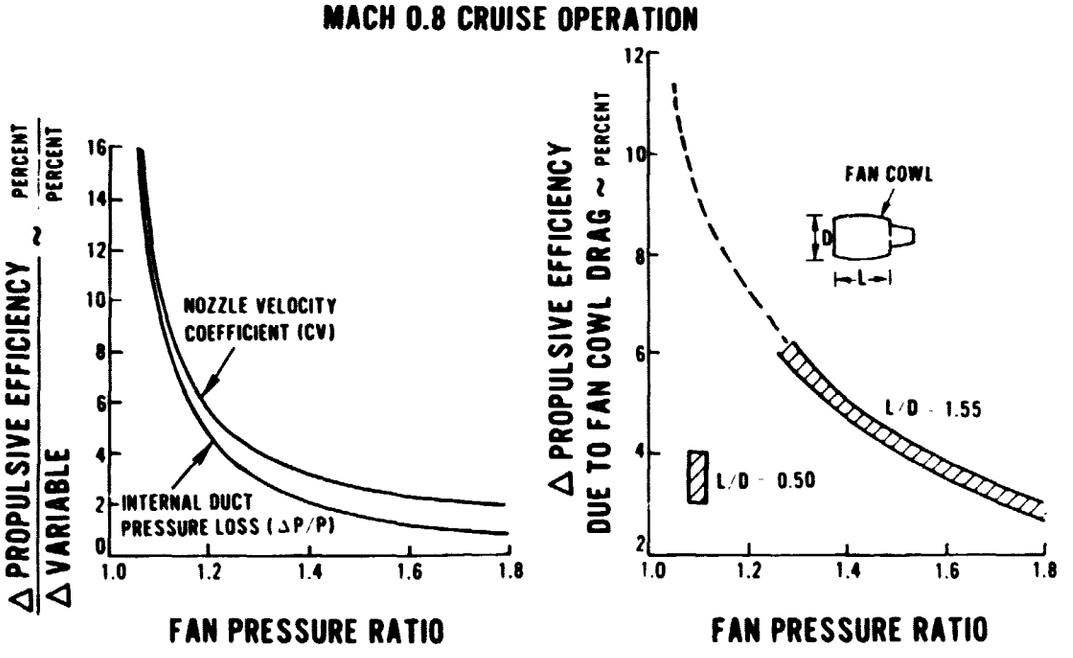

Figure 4.1.2.2-3 *Propulsive Efficiency Sensitivity to Internal Ducting Pressure Losses, Nozzle Losses, and Fan Cowl Drag*

In selecting the cruise shrouded fan cycle, parametric studies were conducted to determine the relationships between the relative fan diameter and pressure ratio as well as the sensitivity of TSFC, and hence of propulsive efficiency, to changes in selected parameters for a range of pressure ratios.

The adiabatic efficiency of the 1.1 pressure ratio, 12-bladed fan was estimated to be within 0.5 percent of the conventional 1.7 pressure ratio fan. Based on the trends shown in Figure 4.1.2.2-3, a cowl, or static shroud, with a 0.5 ratio of length to maximum diameter was needed to provide a minimum desirable inlet length, adequate blade-to-stator acoustic spacing and nozzle ducting allowance. Variable pitch was included to achieve reverse thrust during landing and also to improve the stability margin at take-off, where the sharp-lip inlet imposes a highly distorted fan face flow field.

Figure 4.1.2.2-4 shows the effect of the sharp lip of the cruise shroud on take-off thrust potential compared to the advanced conventional turbofan. Static thrust, normalized to design point conditions, is slightly less for the unconventional shrouded fan design. The thrust capability significantly exceeds that of the turbofan at Mach 0.2 because of the improved ram recovery characteristics.

To provide the thrust and performance needed at take-off and other off-design conditions, variable pitch was incorporated into the unconventional shrouded fan concept. Figure 4.1.2.2-5 shows the resulting configuration together with the shroud and fan physical characteristics. The tip speed of the fan was selected to provide aerodynamic loadings consistent with the conventional turbofan. Fan geometry was based on structural requirements extrapolated from the base Hamilton Standard design. The number of airfoils (12) was set by aerodynamic loading and structural constraints.

Figure 4.1.2.2-6 presents estimated reverse thrust potential for the unconventional shrouded fan. The data were extrapolated from the Hamilton Standard variable (changeable) pitch fan. The figure compares the relative reverse thrust generated by a fixed-pitch fan with a cascade reverser to the relative thrust of the variable-pitch fan which rotates its blades to a reverse thrust setting either through feather or through flat pitch. Rotating to reverse through feather offers more reverse thrust potential due to more effective camber at full reverse pitch. Both methods of blade pitch rotation to reverse thrust result in transient conditions such as overspeed due to blade unloading while going through flat pitch or blade stall and shaft overload while going through feather. Rotation through flat pitch may have the additional problem of mechanical interference of adjacent blades.

The performance potential of the unconventional shrouded fan concept was compared to that of the baseline turbofan (Table 4.1.2.2-I). As shown in the table, the propulsive efficiency of the shrouded fan is 8 percentage points higher than that of the baseline turbofan. Note the reductions in parasitic losses necessary for the shrouded fan to achieve this improvement.

The propulsor drive system losses as well as the remainder of the nacelle drag losses are considered in relation to propulsive efficiency in Section 4.2.2.1 of this report.

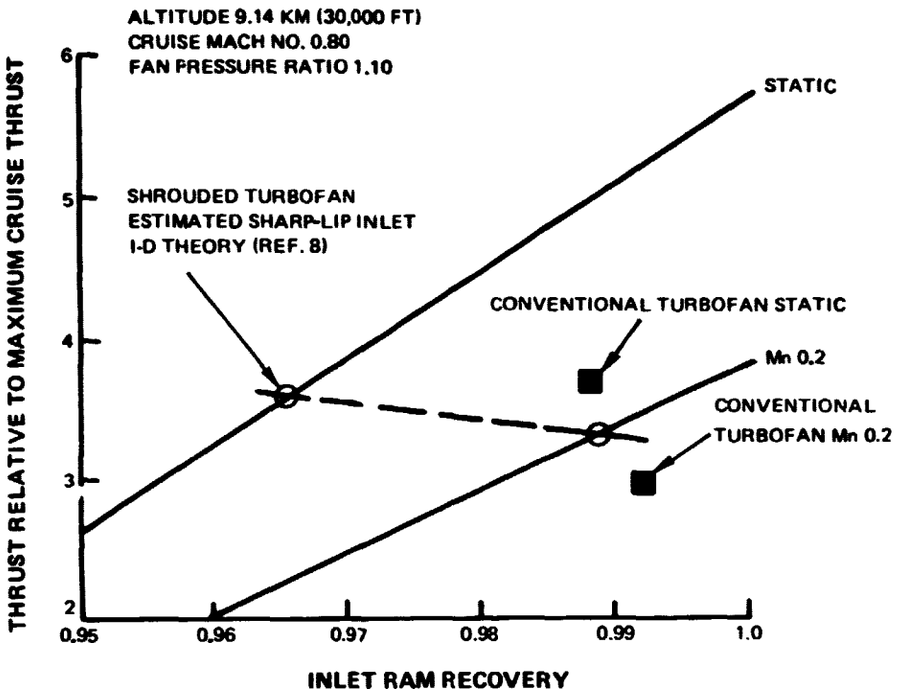

Figure 4.1.2.2-4 *Take-Off Thrust Potential of the Sharp-Lip Cruise Shroud With Fixed Nozzle Area As a Function of Inlet Ram Recovery*

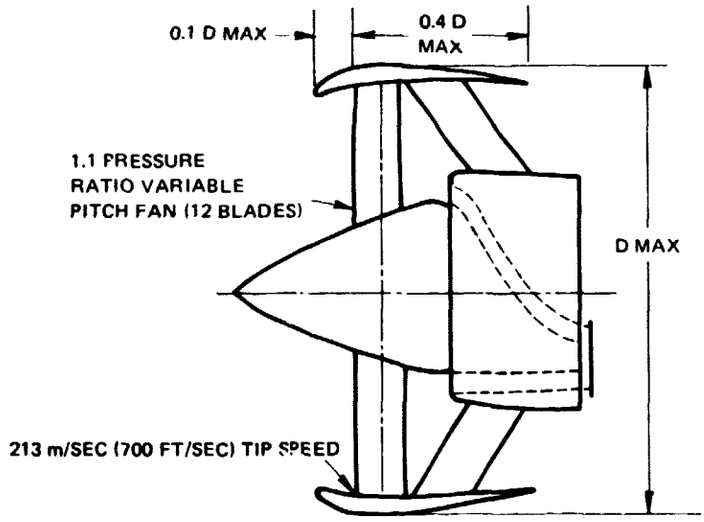

Figure 4.1.2.2-5 *Schematic Diagram of High Speed Sharp-Lip Cruise Shroud, Variable Pitch Advanced Fan Configuration*

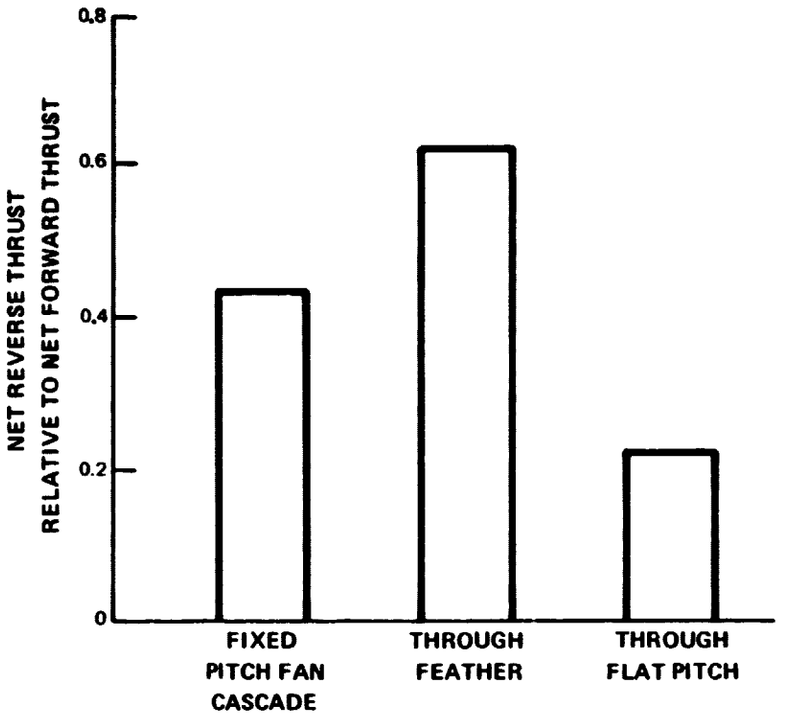

Figure 4.1.2.2-6 *Reverse Thrust Potential of the High Speed Sharp-Lip Cruise Shroud, Variable Pitch Advanced Fan*

TABLE 4.1.2.2-I

COMPARISON OF UNCONVENTIONAL SHROUDED FAN AND ADVANCED CONVENTIONAL TURBOFAN PERFORMANCE POTENTIAL

Mach 0.8 9.14 km (30,000 ft) Cruise Capability

	Baseline Turbofan	Unconventional Shrouded Turbofan
Fan Nozzle Velocity Coefficient	0.995	0.997
Inlet Ram Recovery	0.993	0.998
Duct Pressure Loss	0.012	0.0013
Ratio of Fan Cowl Drag to Thrust	0.031	– –
Ratio of Fan Shroud Drag to Thrust	– –	0.038
Propulsive Efficiency, percent	65	73

4.1.2.3 Unconventional Advanced Propeller Concept

The small diameter, eight-blade advanced propeller concept evaluated in this program is based on 1950 research testing conducted by Hamilton Standard. The advanced propeller would have a pressure ratio of 1.05 with all performance comparisons based on a Mach 0.8, 9.14 km (30,000 ft) altitude cruise capability.

Conventional (circa 1950) propeller blades traditionally incorporated blades with high thickness ratios to provide strength. The camber levels (design lift coefficient) were also high to meet climb requirements which, because of engine power limits, usually were the prime criteria for sizing the propeller diameter. Analysis shows that the high levels of these parameters adversely affect airfoil section critical Mach numbers (M_{CR}) and consequently increase compressibility losses. These propellers exhibit good efficiency up to a flight speed of approximately Mach 0.6 to 0.65 (Figure 4.1.2.3-1). Above this speed, compressibility loss sharply decreases the efficiency.

Thin cross-section, lightly cambered two bladed research propellers, tested in 1950, demonstrated high efficiency at the higher flight speeds. The thinnest model had an 80 percent measured efficiency at Mach 0.8. However, these models were structurally inadequate. Their demonstrated efficiency combined with composite structural technology form the basis for advanced propeller characteristic projections.

The two-blade efficiency data were converted to an eight-blade configuration by established techniques which halved propeller diameter. Cruise efficiency was estimated to be 73 percent for the smaller diameter eight-bladed propeller using ideal efficiency trends with diameter and blade number.

In the advanced propeller concept composite blades incorporate thin, advanced airfoil sections and tip sweep. The blades are integrated with the spinner and contoured nacelle to reduce the axial Mach number through the blading. Structural constraints still impose practical limitations on how much the thickness of the composite blades can be reduced in an effort to reduce compressibility losses. Consequently, other concepts such as supercritical airfoils, spinner and nacelle contouring, and blade sweep were investigated. The estimated effects of these concepts on propeller efficiency are shown in Figure 4.1.2.3-2. The results of the analysis indicate that the potential propulsive efficiency of an eight-bladed unconventional advanced propeller is 14 percentage points higher than the baseline advanced turbofan. In this comparison, installation losses such as engine nacelle drag, pylon and/or wing interference drag, gearbox losses, and drive turbine losses were not considered. These losses are considered for selected installations in Section 4.2. Although the advanced propeller offers the potential for considerable performance improvement, Figure 4.1.2.3-3 shows that there are technological requirements which must be addressed before it can be considered as a practical concept.

4.1.2.4 Comparison of Unconventional Propulsor Efficiency Potential With Baseline

As shown in Figure 4.1.2.4-1, the advanced propeller shows significant additional potential when compared to either the baseline fan or shrouded fan propulsors. In addition, the analytical efforts already conducted on this concept indicate that the development effort could be

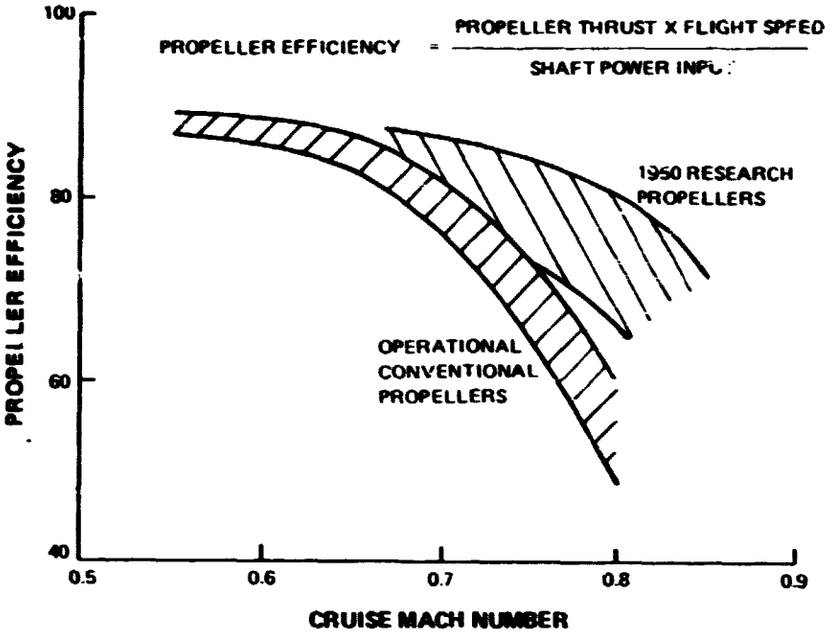

Figure 4.1.2.3-1 Advanced Propeller Performance Derived From 1950 Test Data

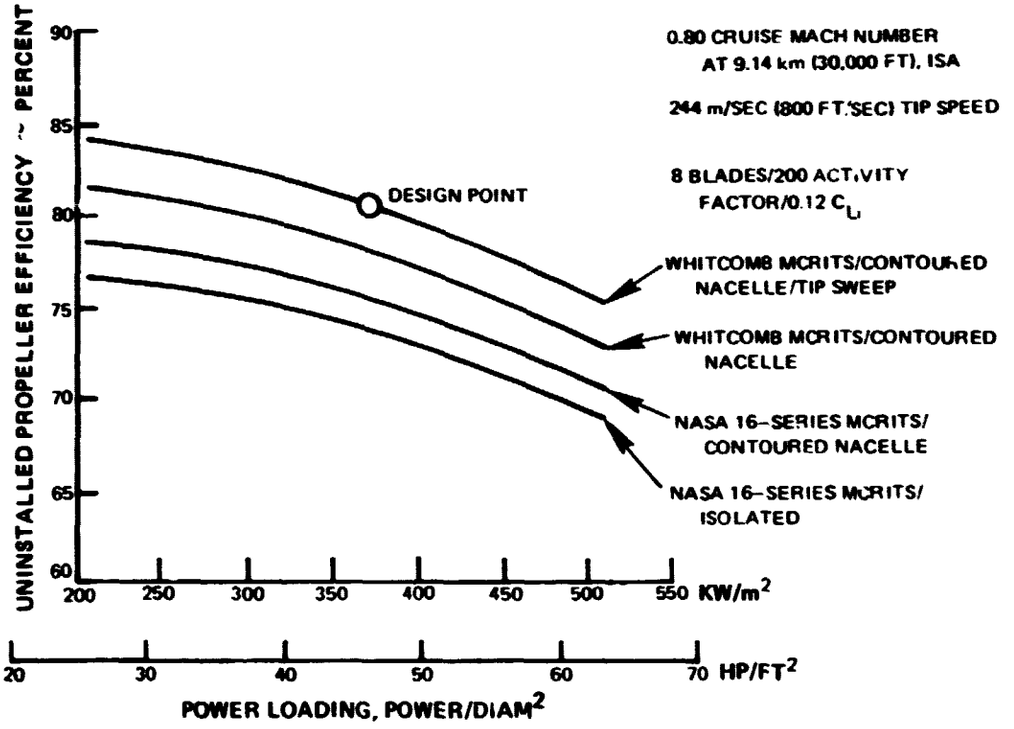

Figure 4.1.2.3-2 Advanced Propeller Uninstalled Efficiency Variation With Power Loading

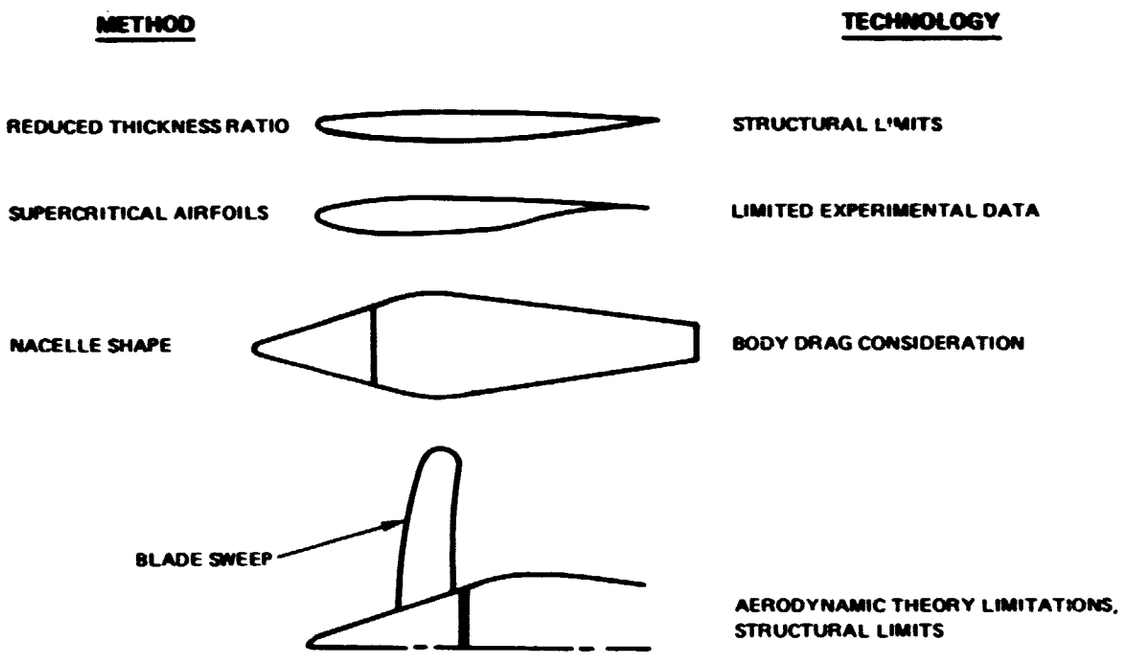

Figure 4.1.2.3-3 Technological Requirements for Improved Propeller Performance

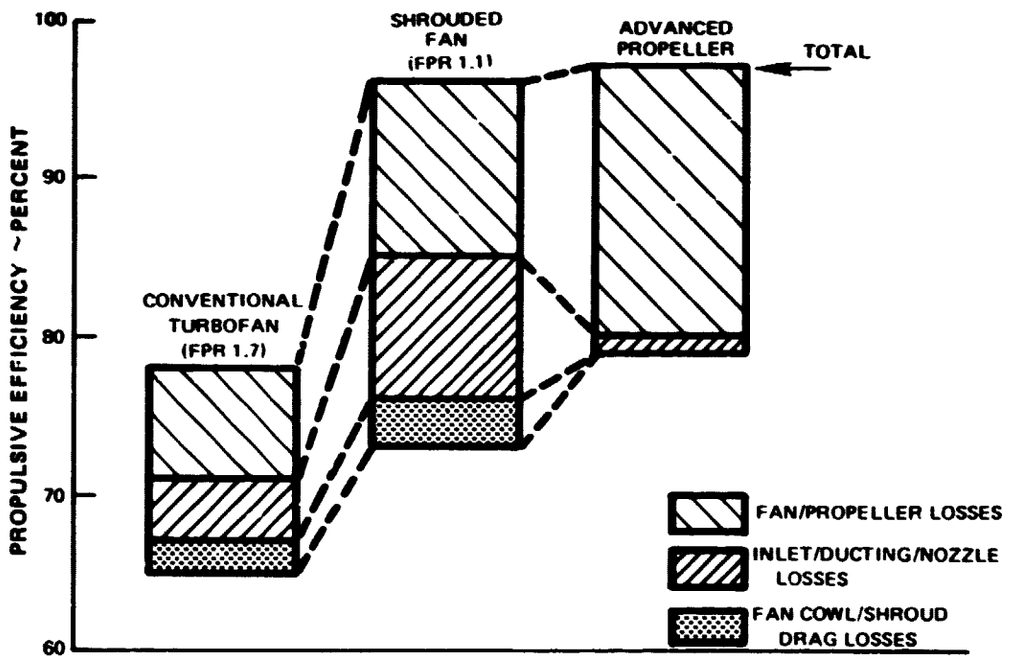

Figure 4.1.2.4-1 Propulsive Efficiency Potential of the Baseline Conventional Turbofan, the Advanced Shrouded Fan, and the Advanced Propeller

shorter and involve considerably less risk than the effort required for the shrouded fan concept.

Although substantially improved efficiency is theoretically achievable through the use of a shrouded fan, major aerodynamic and structural constraints must be overcome. The sensitivity of performance to parasitic losses require substantiation of the assumptions used in this study to ensure that shroud designs will reduce these losses. In addition, the increased diameter of the shrouded fan compared to the conventional baseline turbofan adds substantially to the weight of the installation. This added weight could seriously impact supporting structure design.

4.1.3 Unconventional Installations

As a part of this program, unconventional arrangements of propulsion systems in an aircraft were investigated to determine the applicability to this study. Figure 4.1.3-1 shows schematically the arrangements considered. In the multiple engine arrangement, shutting down the two outboard propulsion systems during portions of the flight was considered. The second arrangement incorporates multiple propulsors driven by a single gas generator, and the third arrangement shows single, large propulsors driven by multiple gas generators. The portions of the flight considered in the investigation were loiter and cruise to alternate landing site because of theoretical potential for fuel saving at the lower engine powers required at these flight conditions. The programmed propulsion system element shutdown would allow the operating components to operate more nearly on-design or to provide an improved thermodynamic cycle at the flight segments examined.

Rather than conduct a detailed evaluation of the many possibilities, the savings that could ideally be obtained by achieving the minimum thrust specific fuel consumption levels at the two flight conditions were determined. These were then converted into block fuel savings (Figure 4.1.3-2) using influence coefficients applied to a selected system in the NASA study of turbofan engines designed for low energy consumption (ref. 1). A combined theoretical block fuel savings of 0.6 percent was estimated, excluding the effects of power transmission losses and system weight increases. The in-flight use of multiple fans or multiple gas generators in subsonic transports does not offer the potential for significant fuel savings.

Laminar flow control (LFC) propulsion systems were also surveyed. The potential of LFC lies mainly in improved airplane performance with reduced drag. A suction source is required to remove the boundary layer over significant portions of the airplane wing and/or fuselage. A possible suction device could be a suction compressor driven by the main propulsion system or by an auxiliary gas generator. The two possibilities are shown in Figure 4.1.3-3. The performance characteristics of the two alternates are estimated to be similar. Neither alternative presents unique problems requiring unconventional propulsion system approaches. The major questions are associated with the airplane and, as such, fall outside the scope of this study program.

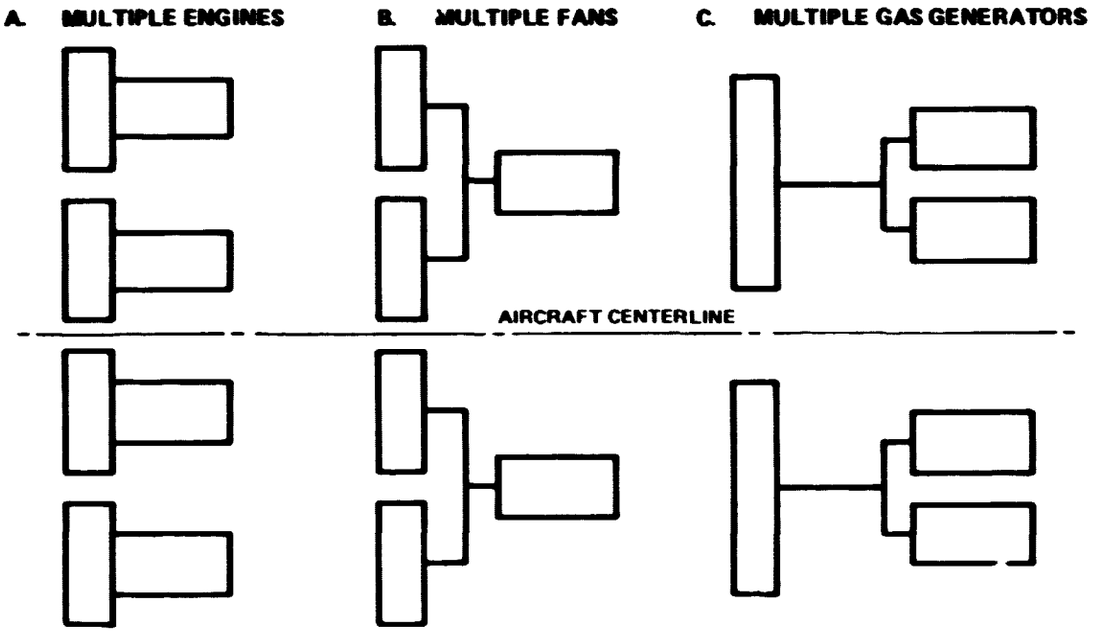

Figure 4.1.3-1 *Conventional Arrangement of Multiple Engines and Unconventional Arrangement of Multiple Fans and Multiple Gas Generators*

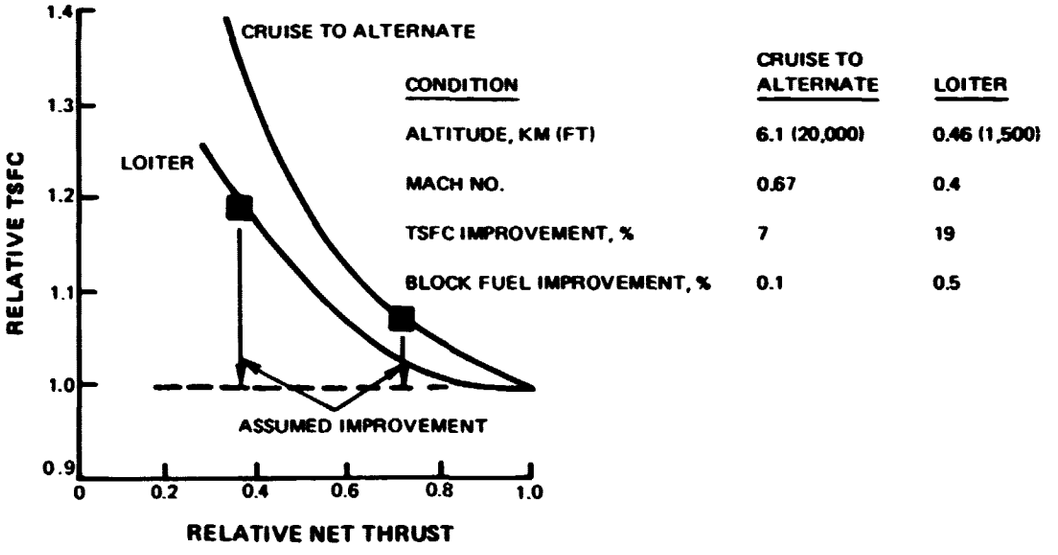

Figure 4.1.3-2 *Fuel Consumption Improvements From Shutdown of Outboard Fans or Gas Generators During Loiter and Cruise to Alternate on an International Quadjet Aircraft Equipped With Multiple Fans or Multiple Gas Generators*

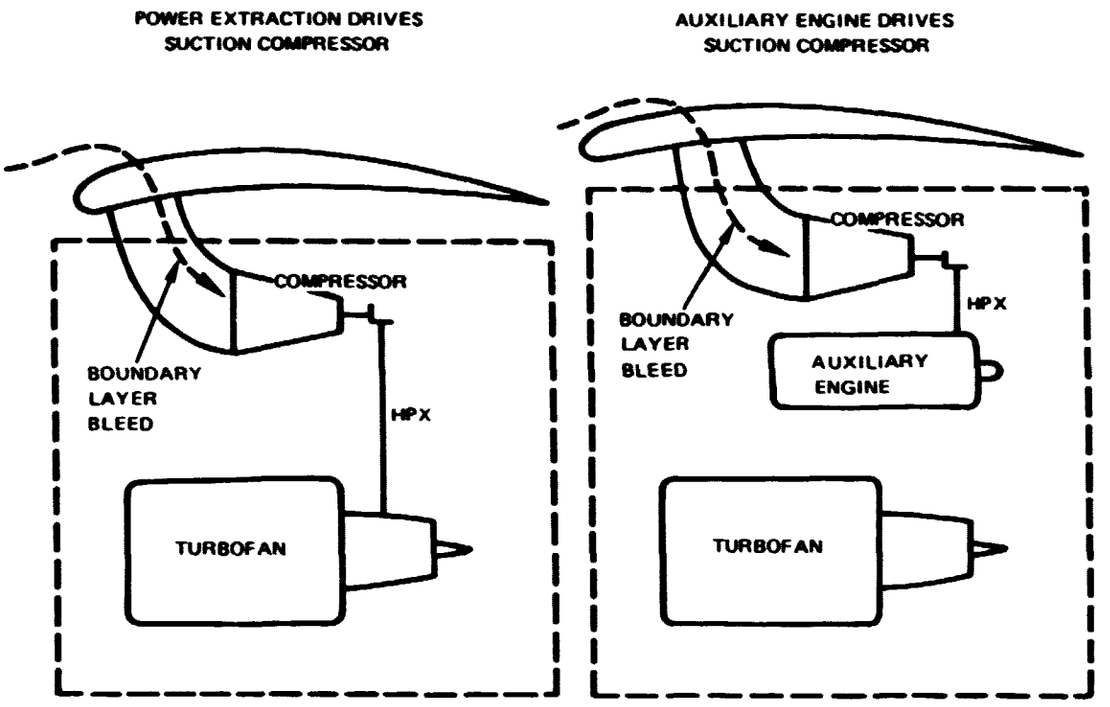

Figure 4.1.3-3 Laminar Flow Control Propulsion Systems

4.2 EVALUATION OF SELECTED UNCONVENTIONAL PROPULSION SYSTEMS

Propulsion systems studied under the Low Energy Consumption, Unconventional Engine Program consisted of conventional or unconventional primary cycles combined with unconventional propulsor concepts. Table 4.2-I lists the three unconventional propulsion systems selected for study and identifies the primary cycle and propulsor that make up each system. Also listed in this table is the advanced technology turbofan (Ref. 1) used as the baseline engine to compare results of the unconventional engine studies.

The regenerative turboprop was selected over a regenerative turbofan engine primarily because the better propulsive efficiency of the advanced propeller results in a smaller gas generator. The smaller core is an important consideration because the regenerator size is a direct function of gas generator size and the regenerator weight is a significant portion (≈ 40%) of the total propulsive system weight.

4.2.1 Propulsion System Parameters

The cycle and propulsor cruise design parameters for the primary cycles and propulsors of the selected propulsion systems are compared in Table 4.2 .1-I. The maximum combustor exit temperatures occurs at a climb rating on a standard +10°C (18°F) day.

Figure 4.2.1-1 presents the thermal efficiencies for the primary cycles of the selected unconventional concepts relative to the baseline turbofan cycle and shows the thermal efficiencies for the unconventional concepts to be within 1.[illegible]% of the baseline turbofan. The baseline turbofan had been refined (Ref. 1) to optimize the primary cycle (simple Brayton cycle) thermal efficiency to minimize fuel consumption. A combustor exit temperature (CET) of 1427°C (2600°F) and an overall pressure ratio (OPR) of 45:1 were the cycle parameters that attained the potential of the simple Brayton cycle in an ungeared turbofan configuration. The 45:1 OPR is an aggressive goal and was established based on an analysis of blade clearance and pressure seal requirements at the maximum pressure point of the engine.

Because of the smaller gas generator size for the turboprop and shrouded turbofan concepts, the OPR had to be reduced to 40:1. This was necessary to provide a gas path height in the critical compressor exit region comparable to the turbofan engine so that comparable compressor and turbine blade tip clearances and losses could be assumed. As shown on the right side of Figure 4.2.1-1, reducing the OPR would also reduce the thermal efficiency if CET were held constant. Increasing the CET to 1538°C (2800°F) for the turboprop and shrouded turbofan cycles results in thermal efficiencies nearly equal to the baseline turbofan; therefore a comparable thermal efficiency potential is attained for all three applications.

A gear driven conventional fan cycle was also evaluated in reference 1 with a CET of 1538°C (2800°F). The result was a reduction in fuel consumption of under 1.0% relative to the direct drive system with a 1427°C (2600°) CET and a higher fan pressure ratio (lower propulsive efficiency). This improvement is considered to be insignificant in context with the added mechanical complexities of the gear system. Therefore, the gear driven conventional turbofan was not considered for further evaluation.

The high bypass ratios of the turboprop and shrouded turbofan engines preclude the use of a direct drive system with these concepts.

The regenerative turboprop concept uses a modified Brayton cycle which incorporates an air to air heat exchanger. The plate-fin recuperator was used in this evaluation since it was found to maximize engine performance based on the selection process discussed in Section 4.3.3.2. As shown in Figure 4.2.1-1, the cycle benefits for regeneration are greatest at relatively low cycle pressure ratios (≈ 15: 1).

If the optimum CET for the simple Brayton cycle, 1538°C (2800°F), is used with the regenerative modified cycle, a significant loss in thermal efficiency results. In an effort to increase thermal efficiency, the CET was increased to 1760°C (3200°F), where the optimum thermal efficiency for the regenerative cycle is achieved. Above this CET, cycle efficiency suffers from the increased turbine cooling air requirement.

TABLE 4.2-I

CYCLE/PROPULSOR COMBINATIONS EVALUATED IN LOW ENERGY CONSUMPTION, UNCONVENTIONAL ENGINES

Propulsion System Designation	Primary Cycle	Propulsor (Drive)
Turbofan (baseline)	Simple Brayton	Conventional Fan (direct)
Turboprop	Simple Brayton	Advanced Propeller (gear)
Regenerative Turboprop	Modified Brayton	Advanced Propeller (gear)
Shrouded Turbofan	Simple Brayton	Shrouded Fan (gear)

TABLE 4.2.1-I
UNCONVENTIONAL ENGINE EVALUATION CRUISE DESIGN PRIMARY CYCLE AND PROPULSOR CYCLE PARAMETERS

Propulsion System	Maximum Combustor Exit Temperature °C (°F)	Overall Pressure Ratio	Propulsor Pressure Ratio	Bypass Ratio
Turbofan (baseline)	1427 (2600)	45:1	1.7	8.0
Turboprop	1538 (2800)	40:1	1.05	≈ 100
Regenerative Turboprop	1760 (3200)	15:1	1.05	≈ 100
Shrouded Turbofan	1538 (2800)	40:1	1.1	57

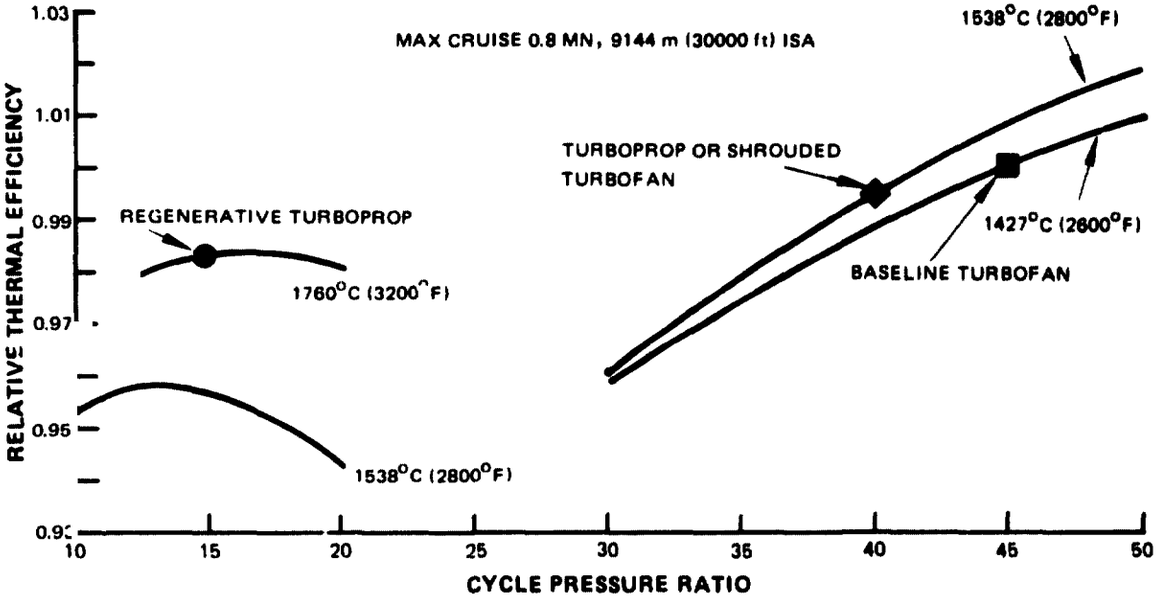

Figure 4.2.1-1 Thermal Efficiency Comparison

4.2.2 Engine Installation Considerations

Installation considerations included cabin noise and vibration, engine-out and roll stability margins, wing root bending moments, nacelle and slip stream drag effects, ground clearance and propeller tip clearance requirements, and engine accessibility for maintenance. The four-engine intercontinental range aircraft was used in this evaluation. Figure 4.2.2-1 presents installation schematics of the baseline turbofan and three selected unconventional concepts. Figure 4.2.2-2 is a front view of the aircraft showing clearance requirements.

The baseline turbofan was assumed to be a conventional under-the-wing, pylon mounted configuration. Vertical placement of the engines, relative to the wing, and spanwise location of the engines are similar to the Boeing 707 and 747 engine locations. The fan cowl length is 1.55 times the maximum cowl diameter to provide adequate length for efficient inlet diffusion and sufficient acoustically treated wall area to attenuate fan noise to FAR 36 minus 10 EPNdB at take-off, sideline and approach conditions. Reverse thrust is provided by a cascade thrust reverser in the fan stream only.

The installation arrangements for the shrouded turbofan, turboprop and regenerative turboprop are shown in Figure 4.2.2-1 and feature under-the-wing mounting of the turboshaft portion of the engines with the full nacelle gloved to the wing. Further study would be required to provide complete justification for this installation scheme; however, it appears that this arrangement can provide adequate ground clearance, drag and internal pressure recovery characteristics comparable to over-the-wing installations, and ready access to the engine modules. Thrust reverse is accomplished by altering the pitch of the two propulsors; blading ballrace retention and hydro-mechanical (mechanical) pitch change system have been assumed for this purpose.

Inboard turboprops were placed to provide 0.8 of the propeller diameter clearance between the fuselage and the blade tips. In reference 2, this placement was indicated to provide cabin noise levels comparable to turbofan aircraft by adding fuselage wall treatment equal to 0.25% of the aircraft gross weight. A blade tip clearance between inboard and outboard propeller of 0.33 propeller diameter was assumed. The aircraft wing weight, tail size and weight, and landing gear weight calculations were all based on these engine placement criteria.

The axial distance between the wing quarter chord and propeller planes was set at a value of approximately 1.0 times the propeller diameter to minimize the tendency for nacelle whirl flutter and vibration transmission to the cabin. Chin inlets were placed well out in diameter from the blade roots in the turboprop to benefit from the pressure rise through that section of the propeller. A total pressure recovery to the gas generator face of 1.0 is possible by carefully contouring the spinner and inlet for minimum loss. The maximum nacelle diameter on the turboprop was set equal to 35% of the propeller diameter to provide sufficient back-pressure and avoid blade root choking. While an attempt has been made to account for all of these phenomena, it is recognized that much additional analyses and testing is required to weigh the many factors involved in selecting a final installation arrangement.

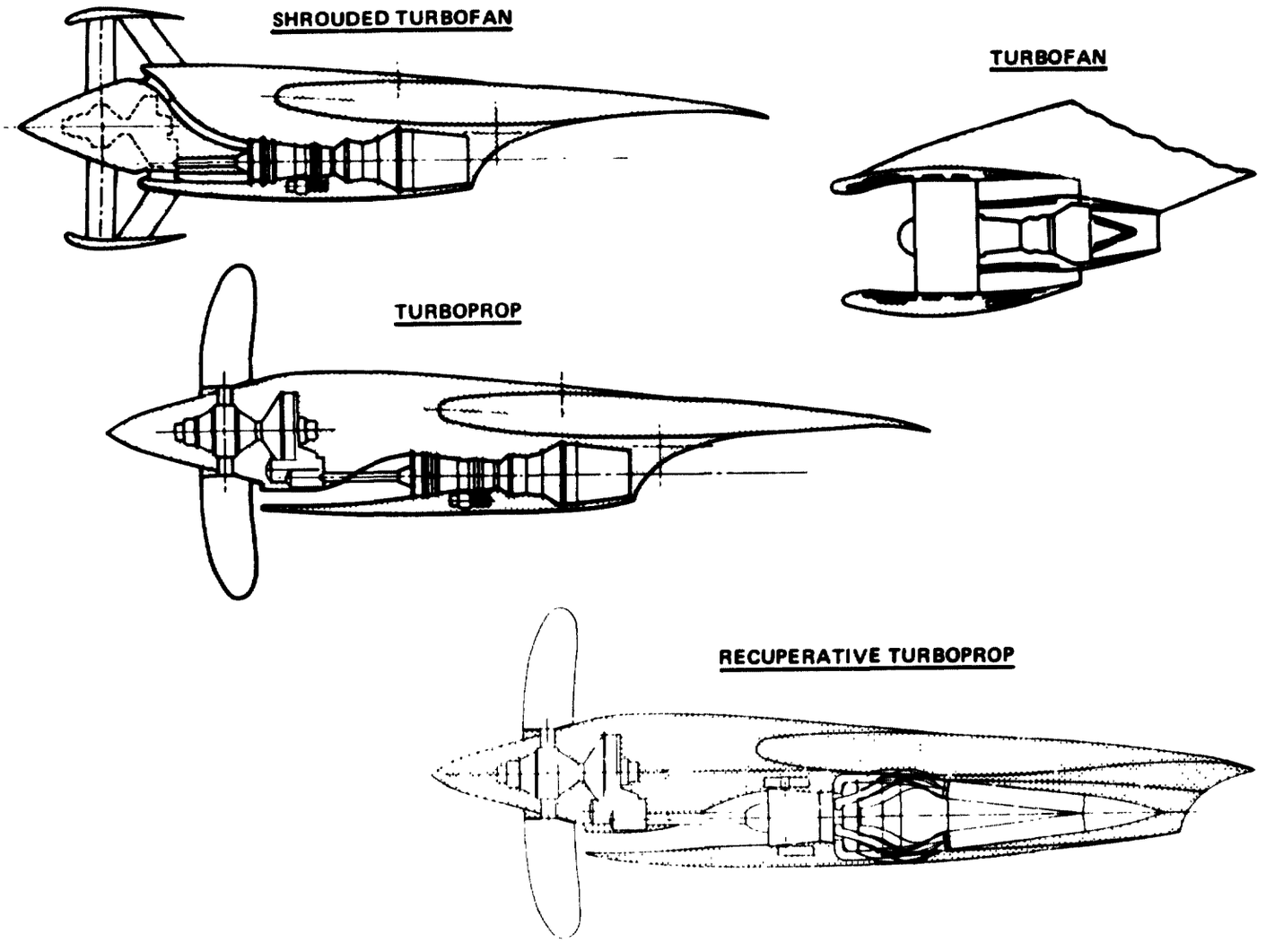

Figure 4.2.2-1 Engine Installation Schematics

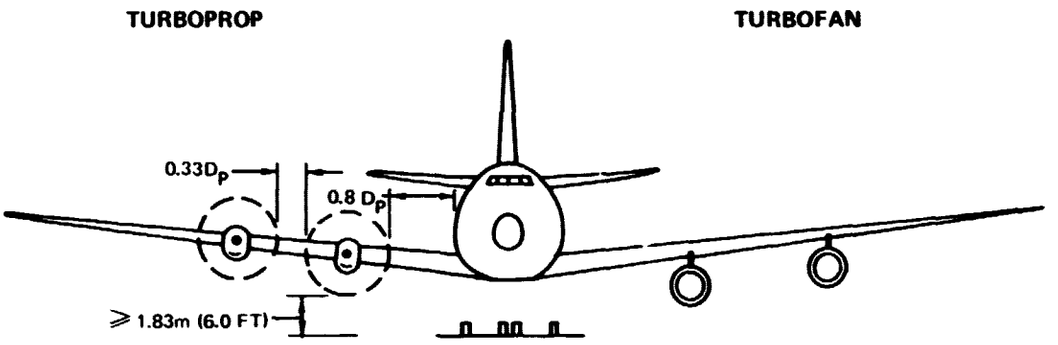

Figure 4.2.2-2 Four Engine Installation-Clearance Requirements

The results of the drag analyses, presented in Table 4.2.2-I, show that the nacelle drag of the pylon mounted turbofan is somewhat higher than either turboprop configuration during cruise operation. The large fan cowl of the shrouded turbofan results in this configuration having a slightly higher drag than the baseline turbofan.

At the Mn 0.8 cruise condition, the propulsor induced slipstream Mach number for the turboprop configurations is 0.84, and 0.9 for the shrouded turbofan. The magnitude of the drag increase due to the high slipstream Mach numbers and the effects of drag reducing fixes (such as increased local wing sweep,thinner wing section, etc.) on fuel consumption are uncertain. The possibility of reduced drag because of the wing's ability to operate at lower angles of attack in a higher dynamic pressure environment add to the uncertainties surrounding quantitative estimates of propulsor slipstream effects. Because of uncertainties, no drag penalty for propulsor slipstream effect was used, other than the increased friction drag, in the evaluation of the unconventional engines. A detailed discussion of the techniques used in the drag analyses along with a comprehensive review of the results are presented in Appendix A.

TABLE 4.2.2-I

NACELLE DRAG SUMMARY

0.8 Mn, 9144 m (30,000 ft) Altitude, Maximum Cruise Rating

	Drag-To-Thrust Ratio			
Drag Element	Baseline Turbofan	Turboprop	Regenerative Turboprop	Shrouded Turbofa.
Fan Cowl or Shroud	.031	–	–	.038
Scrubbed Afterbody and Pylon	.012	–		
Pylon	.022	–	–	–
Interference	.015	.010	.010	.011
Scrubbed Nacelle Surfaces		.036	.056	.022
Wing Scrubbing	–	.007	.007	.012
Total	.080	.053	.073	.083

4.2.2.1 Installed Propulsive Efficiency Comparison

Installation losses were estimated for each of the engine concepts to compare the fully installed propulsive efficiency. Propulsor blading efficiency, internal ducting losses, and fan cowl or shroud drags were taken from the evaluation discussed in Section 4.1.2. The remainder of the installation drag was obtained from Table 4.2.2-I. The power transmission losses through the propulsor drive turbine and gear set were calculated as shown on Figure 4.2.2.1-1. The large installed propulsive efficiency gains calculated for the turboprop engines indicate that installation loss effects are small in relation to the improved propulsor performance. The shrouded fan is a third less effective in increasing propulsive efficiency than is the advanced propeller.

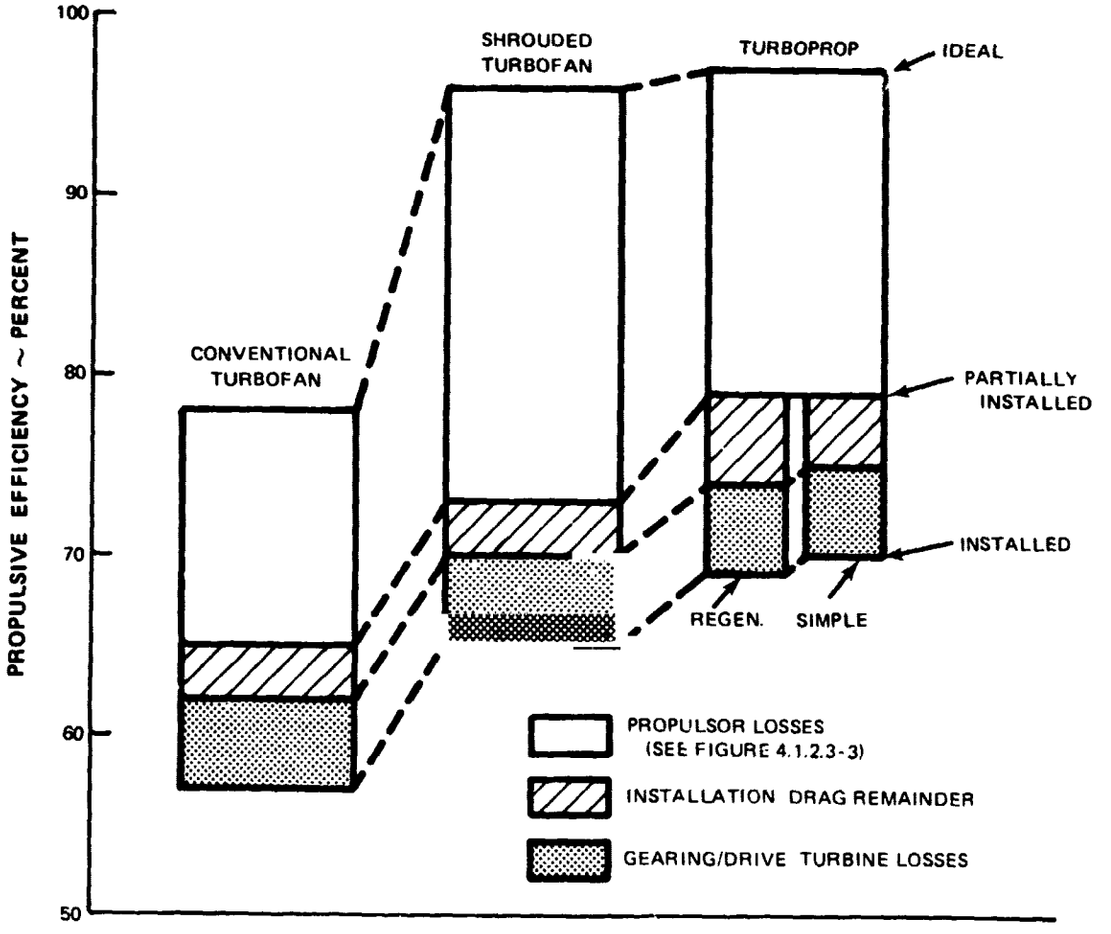

Figure 4.2.2.1-1 Installed Propulsive Efficiency Comparison

4.2.3 Thrust Specific Fuel Consumption Trends

Thrust specific fuel consumption (TSFC), which is inversely proportional to the product of the thermal and propulsive efficiencies, is a convenient parameter for expressing improvements in the unconventional approaches to low energy consumption. Table 4.2.3-I presents a comparison of the TSFC values for the unconventional concepts relative to the baseline turbofan. The relative installed TSFC, shown on the third line of the table, includes engine installation effects (drag), drive turbine loss and gearbox loss but does not include the effect of customer power requirements. The customer power requirements are based on anticipated needs for the 1985 time period. These requirements are equivalent for all four engines shown in the table; however, the means for extracting this power varies.

As indicated in Table 4.2.3-I, customer power is provided from the baseline turbofan engine by direct extraction of 4119 watts (150 hp) from the high rotor, 0.908 kg/sec (2.0 lbm/sec) compressor discharge bleed and 0.454 kg/sec (1.0 lbm/sec) fan duct bleed. This results in a 5% increase in TSFC. Bleeding a similar amount of compressor discharge air, 0.908 kb/sec (2.0 lbm/sec), from the relatively small core of the unshrouded prop engine would result in a significant increase in engine size to maintain the same thrust. However, extracting an equivalent total customer power of 17300 watts (23 hp) from the free turbine rotor would result in an engine size about 11% smaller than if compressor discharge bleed were used. Therefore, customer service for the turboprop engine is supplied by direct power extraction alone. An auxiliary compressor to convert the power to pressurized air is required with this system. A TSFC penalty (5%) comparable to that for the baseline turbofan was noted for the shrouded turbofan and turboprops. The relative TSFC (energy consumption improvement) for the unconventional concepts was not changed by customer power requirements, as indicated by the bottom line in Table 4.2.3-I.

TABLE 4.2.3-I

RELATIVE INSTALLED MAXIMUM CRUISE TSFC
0.8 MN, 9144 m (30000 Ft) ALTITUDE

	Baseline Conventional Turbofan	Shrouded Turbofan	Regenerative Turboprop	Turboprop
Relative Thermal Efficiency	1.00	.995	.983	.995
Relative Installed Propulsive Efficiency	1.00	1.14	1.21	1.23
Relative Installed TSFC (without customer power requirements)	1.00	0.88	0.84	0.82
Customer Power Requirements	.908 kg/sec (2.0 lb/sec) Compressor discharge bleed .454 kg/sec (1.0 lb/sec) Fan duct bleed 4119 watts (150 hp) extracted from high rotor	17300 watts (630 hp) Extracted from low rotor	17300 watts (630 hp) Extracted from free turbine rotor	17300 watts (630 hp) Extracted from free turbine rotor
Relative installed TSFC (including customer power requirements)	1.00	0.88	0.84	0.82

4.2.4 Weight Trends

Table 4.2.4-I presents a comparison of the estimated weights for the unconventional concepts relative to the baseline advanced technology turbofan engine. The weight of items such as accessories, controls and engine mount system are included in the various component weights listed in the table. The weigh: estimates in Table 4.2.4-I are expressed as percentages of the total weight of the baseline propulsion system to facilitate the comparison.

The weight estimates for the gas generator and power turbine portions of the unconventional concepts are based on weight trends derived from reference 1. The variable pitch shrouded fan weight estimate is based on an extension of fan data from the same study. Propeller and gearbox weights were estimated using data from Hamilton Standard Division (Ref. 9). Information for the heat exchanger weight estimates was provided by AiResearch Manufacturing of California while under subcontract to P&WA for this study. The procedure used to calculate nacelle geometry and weight is discussed in Appendix A of this report. Advanced technology materials were assumed in the engine weight estimates: carbon epoxy was used for the fan blades and stators, composite shell and metal spar construction for the propellers, and advanced titanium and nickel base alloys for the compressor and turbine sections.

The weight comparisons in Table 4.2.4-I are based on equal maximum cruise thrust at 0.8 MN, 9144 m (30,000 ft) altitude for each engine. The unconventional concepts have higher bypass ratios and therefore smaller, lighter core engines (gas generator and power turbine). The higher cycle temperature for the unconventional concepts (higher specific power output) also contribute to the lower core engine weight; however, this factor does not significantly reduce the total propulsion system weight since the shrouded fan/propeller and gearbox increase in size and weight to absorb the higher power output.

Nacelle and thrust reverser weights for the turboprop and shrouded turbofan are lower than the baseline because the nacelle cross sections are smaller and a cascade type thrust reverser is not required with variable pitch blading. The higher weight for this component in the regenerative turboprop is due to the larger nacelle envelope required for the heat exchanger and associated plumbing.

The turboprop concept is the lightest of the unconventional concepts as well as offering the largest cruise TSFC improvement potential.

TABLE 4.2.4-I

INSTALLED ENGINE WEIGHT COMPARISON
Equal Thrust @ 0.8 MN,
9144 m (30,000 ft) Altitude, Maximum Cruise Rating

Component	Baseline Turbofan	Shrouded Turbofan	Turboprop	Regenerative Turboprop
Gas Generator and Power Turbine	41	34	35	37
Propeller/Fan	15	52	28	26
Gearbox		15	24	20
Recuperator and Plumbing				56
* Nacelle and Thrust Reverser	32	30	26	38
Pylon	12	–		–
Total	100	131	113	177

*Includes fan duct wall acoustical treatment for baseline turbofan.

4.2.5 Fuel Savings Trends By Using Influence Coefficients

The fuel burned influence coefficient relates the change in fuel burned to a given change in an independent parameter such as TSFC or engine weight. For example, percent change in fuel burned = λ times percent change in TSFC where λ is the fuel burned influence coefficient of TSFC. Influence coefficients are assumed to be independent and the separate responses of fuel burned to changes in TSFC and engine weight are assumed to be additive (coupling effects are ignored).

The TSFC influence coefficient was determined by computing the change in fuel burned resulting from a selected change in TSFC. Other parameters such as engine weight, range, payload, approach speed and take-off field length were held constant. The computer program used to estimate the fuel burned response accounted for all airframe and engine parameter changes (i.e., structural weights, drag, engine size, etc.) associated with the resized airplane. Similarly, the engine weight influence coefficient was computed by varying the engine weight holding TSFC constant, and determining the resultant fuel burned change. The influence coefficients for TSFC and engine weight are listed in Table 4.2.5-I. The baseline turbofan values of TSFC, engine weight and fuel burned were used as reference values. The predominance of TSFC over weight in affecting fuel burned is evident by comparing the relative magnitude of the influence coefficients.

Table 4.2.5-II presents the results of the influence coefficient analysis applied to the unconventional concepts. These trends were determined by applying the influence coefficients listed in Table 4.2.5-I to the relative installed TSFC and weight values presented in Tables 4.2.3-I and 4.2.4-I. As shown, the highly efficient turboprop engine exhibits the greatest potential for reducing energy consumption.

4.2.6 Propulsion Systems Selected for Conceptual Design

Based on the evaluation of unconventional propulsion systems discussed in the previous sections, the turboprop and regenerative turboprop concepts were selected for refined analysis and conceptual design. While all three concepts evaluated show potention for significant fuel savings relative to the baseline turbofan, the turboprop configurations show the greater potential. Further, the shrouded turbofan is highly sensitive to system parasitic losses associated with ducting the air through the propulsor and there are major unanswered aerodynamic and structural questions related to the large diameter shroud. For these reasons, evaluation of the shrouded turbofan concept was discontinued.

TABLE 4.2.5-I

FUEL BURNED INFLUENCE COEFFICIENTS FOR TYPICAL MISSION

a) Mn 0.8 Cruise, Intercontinental Range Aircraft
[3704 km (2000 n.mi.) range, 55% load factor]

Independent Variable (% Change)	Fuel Burned Influence Coefficient
Installed TSFC (± 1.0)	± 1.35
Installed Engine Weight (± 1.0)	± 0.105

b) Mn 0.8 Cruise, Transcontinental Range Aircraft
[1296 km (700 n. mi.) range, 55% load factor]

Independent Variable (% Change)	Fuel Burned Influence Coefficient
Installed TSFC (± 1.0)	± 1.18
Installed Engine Weight (± 1.0)	± 0.09

TABLE 4.2.5-II

TYPICAL MISSION FUEL BURNED TRENDS USING INFLUENCE COEFFICIENTS

a) Four Engine Intercontinental Range Aircraft

[Design Mission: 200 passengers, 10,186 km (5,500 n. mi.) stage length]
[Typical Mission: 110 passengers, 3,704 km (2,000 n. mi.) stage length]

	% Change in Fuel Burned Relative to Baseline Turbofan		
	Turboprop	Regenerative Turboprop	Shrouded Turbofan
Change Due to Δ Installed TSFC	– 24.3	– 21.6	– 16.2
Change Due to Δ Installed Engine Weight	+ 1.4	+ 8.1	+ 3.3
Total Change	– 22.9	– 13.5	– 12.9

b) Transcontinental Range Aircraft

[Design Mission: 200 passengers, 5,556 km (3000 n. mi.) stage length]
[Typical Mission: 110 passengers, 1296 km (700 n. mi.) stage length]

	% Change in Fuel Burned Relative to Baseline Turbofan		
	Turboprop	Regenerative Turboprop	Shrouded Turbofan
Change Due to Δ Installed TSFC	– 21.0	– 18.9	– 14.2
Change Due to Δ Installed Engine Weight	+ 1.2	+ 6.9	+ 2.8
Total Change	– 19.8	– 12.0	– 11.4

4.3 CONCEPTUAL DESIGN

Two unconventional engine concepts were selected for conceptual design and are designated the STS-487, a turboprop engine, and the STS-488, a regenerative turboprop engine. These study engines are described in detail in this section. The baseline engine for this study program, the advanced technology turbofan (STF-477) is also described.

4.3.1 STF-477 Component and Mechanical Description

A detailed discussion of the STF-477 is contained in reference 1. This section provides a brief description of this baseline engine for background information.

The STF-477 is a two rotor design based on technology projected for the 1985 time frame. The low spool consists of a high speed, single stage 1.7 pressure ratio fan, a three stage low-pressure compressor with a 2.47 pressure ratio and a five stage uncooled low-pressure turbine. The high spool consists of an 18.2 pressure ratio high-pressure compressor and two-stage cooled high-pressure turbine. The combustor is a two stage, low emissions vorbix design with aerating pilot nozzles with a maximum combustor exit temperature of 1427°C (2600°F). The design parameters, performance, and installation parameters for the STF-477 are summarized in Table 4.3.1-I.

Figure 4.3.1-1 presents a cross section of the STF-477. As shown, the two rotors are supported by six bearings: three on the low spool and three on the high spool, which includes an intershaft bearing at the rear of the engine. A bearing is located at the mid-engine section to provide additional support to minimize rotor deflections and to help minimize running clearances in the rear of the compressor and high-pressure turbine.

Advanced materials providing improved strength-to-weight and high temperature capabilities are assumed throughout the engine definition. The fan blades are of spar and shell construction with carbon epoxy shell and titanium spar. Improved titanium alloys are used in the high stress, high temperature regions (rear stages) of the compressors and cases. High temperature titanium is also used for the last turbine stage and exhaust case. Monocrystal or eutectic alloys are used in the high-pressure turbine airfoils and an oxide dispersion strengthened alloy is used in the burner liners.

4.3.2 Turboprop Engine (STS-487) Component and Mechanical Description

The turboshaft portion of the STS-487 turboprop engine employs advanced technology features comparable to the STF-477. The propeller and drive gear system are also based on advanced technology projections. Table 4.3.2-I presents a summary of the STS-487 design parameters. A discussion of the engine components is contained in the following sections.

4.3.2.1 Turboshaft Configuration Selection

A number of options are available in the selection of the propeller drive mechanism. One approach is to use a free turbine to drive the propeller at a speed schedule that can be optimized for both components. The gas generator compression system can then be split between the high- and low-pressure compressors in a manner that minimizes the number of compressor and turbine stages. This approach was selected for the STS-487.

TABLE 4.3.1-I

STF 477 ENGINE PARAMETERS

PARAMETRIC DESCRIPTION

Base Size, Thrust, N (lbf)*	118100 (26550)
Scaling Range, Thrust, N (lbf)*	71200-178000 (16000-40000)
Nominal Cruise Design Cycle at Mn 0.83 and 10,058m (33,000 ft)	
Fan Pressure Ratio	1.70:1
Bypass Ratio	8.0:1
Overall Pressure Ratio	45:1
Maximum Combustor Exit Temperature, °C (°F)	1427 (2600)
Inlet Flow (corrected), kg/sec (lbm/sec)	472 (1040)
Acoustics (Engine Plus Nacelle)	FAR 36 minus 10 EPNdB

PERFORMANCE (Representative Conditions)

Condition	Altitude		Mach No.	Net Thrust		TSFC	
	km	(ft)		N	(lbf)	kg/hr/N	(lbm/hr/lbf)
Take-off**	0	(0)	0.147	93635	(21050)	0.0358	(0.351)
Max. Climb***	9.14	(30000)	0.8	32912	(7399)	0.0588	(0.577)
Max. Cruise***	9.14	(30000)	0.8	29910	(6724)	0.0586	(0.575)

WEIGHTS AND DIMENSIONS

Base Engine Weight, kg (lbm)	1787 (3940)
Dimensions	
Maximum Diameter, m (in.)	1.92 (75.6)
Overall Length, m (in.)	2.88 (113.2)
Nozzle Throat Areas	
Duct, m^2 ($in.^2$)	1.150 (1783)
Primary, m^2 ($in.^2$)	0.303 (470)

*Sea level static take-off, 28.9°C (84°F) ambient temperature; U.S. Standard Atmosphere, 1962; 100% ram recovery; no customer bleed or power extraction; representative nozzle thrust coefficients.

**Estimated performance calculated on basis of: U. S. Standard Atmosphere, 1962; 100 percent ram recovery; 1.04 kg/sec (2.3 lbm/sec) mid-compressor bleed; 1.01 kg/sec (2.4 lbm/sec) duct bleed; 112 kw (150 hp) extraction; standard day; representative nozzle thrust coefficients.

***Same conditions as take-off except bleed: 0.91 kg/sec (2.0 lbm/sec) mid-compressor; 0.45 kg/sec (1.0 lbm/sec) duct bleed.

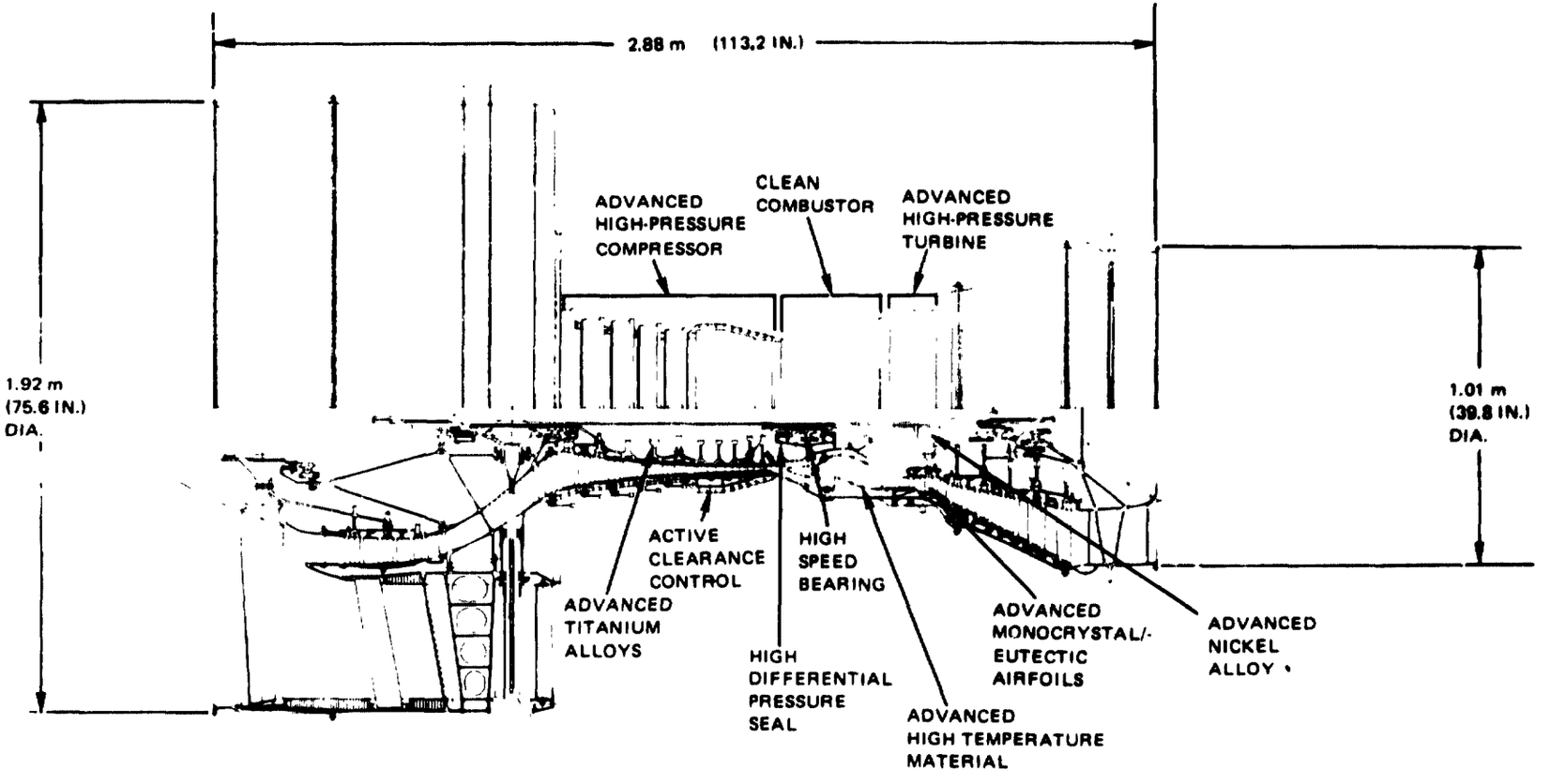

Figure 4.3.1-1 STF 477 Engine Cross Section With High Spool Advanced Technology Concepts Identified

TABLE 4.3.2-I

STS-487 ENGINE PARAMETERS

CYCLE DESCRIPTION

Base Size, Shaft power, Watts (hp)*	$1.538X10^7$ (20628)
Scaling Range, Shaft power, Watts (hp)*	$0.895X10^7$ - $2.237X10^7$ (12000-30000)
Nominal Cruise Design Cycle at Mn 0.8 and 9, 144m (30,000 ft)	
Overall Pressure Ratio	40:1
Maximum Combustor Exit Temperature °C (°F)	1811 (2800)
Inlet Airflow (corrected), kg/sec (lbm/sec)	31.75 (70)
Acoustics (Propeller, Engine plus Cowl)	FAR 36 minus 10 EPNdB

PERFORMANCE

Condition	Altitude km	Altitude (ft)	Mach No	Net Thrust N	Net Thrust (lbf)	TSFC kg/hr-N	TSFC (lbm/hr-lbf)
Take-off**	0	(0)	0.147	106757	(24000)	.0264	(.259)
Max. Climb***	9.14	(30000)	0.8	27845	(6260)	.0512	(.502)
Max. Cruise***	9.14	(30000)	0.8	25400	(5710)	.0500	(.490)

PROPELLER

Number of blades	8
Integrated lift coeff. (CLi)	0.12
Tip speed, m/sec (ft/sec)	243.8 (800)
Base diameter, m (ft)	4.40 (14.44)
Power loading, Watts/m^2 (HP/ft^2)****	$3.69x10^5$ (46)
Efficiency, percent****	79.7

*Sea level static, take-off power, 28.9°C (84°F) ambient temperature; U.S. Standard Atmosphere, 1962; 100% ram recovery; no customer bleed or power extraction; representative nozzle thrust coefficients.

**U.S. Standard Atmosphere, 1962; 100 percent ram recovery; 470 kw (630hp) extraction; 28.9°C (84°F) ambient temperature day.

***Same conditions as take-off except temperature is standard day.

****Maximum cruise, 0.8 Mach number, 9.14km (30000 ft); 470 kw (630 hp) extraction; standard day.

TABLE 4.3.2-1 (Cont'd)

STS-487 ENGINE PARAMETERS

REDUCTION GEAR

Gear ratio	8.24
Efficiency, percent	99.0

WEIGHTS – kg (lbm)

Turboshaft	968 (2134)
Propeller	747 (1647)
Reduction gear system	655 (1444)
Total engine	2370 (5225)

DIMENSIONS - m (in.)

Length	– Compressor inlet to turbine exhaust flange	2.24 (88.2)
Diameter	– Compressor inlet flange	0.64 (25.0)
Diameter	– Turbine mount flange	0.91 (36.0)

A second approach would be to gear the propeller directly to the low spool and drive both the propeller and LPC with a multi-stage LPT. The major drawback to this scheme is that the propeller speed (rpm) must be varied in a manner which results in less than optimum efficiency to prevent the LPC from being driven into or toward surge at part power. Figure 4.3.2.1-1 compares the off-design cruise performance for the first two approaches. The loss in performance (increased TSFC) is due almost entirely to the reduced propeller and LPT performance. Most, if not all, of the performance could be recovered by adding several stages of variable geometry stators to the front of the LPC to obtain a flow-speed schedule more favorable to the propeller and LPC.

A third approach would be to revise the compression system split by increasing the compression accomplished by the HPC. This approach has been taken in turbofan engine design recently. The reduced pressure ratio LPC may reduce the need for variable geometry stators to match the optimum efficiency speed schedule of the propeller and LPC.

The detailed analysis necessary to identify the optimum configuration was beyond the scope of this program but would not significantly affect the comparisons with other unconventional engine concepts or the conclusions of this study. Therefore, the free turbine arrangement is considered to be a good representative approach.

4.3.2.2 Turboshaft Description

The STS-487 advanced technology turboshaft consists of a two spool gas generator and a free turbine driven power shaft. A cross section of this configuration is shown in Figure 4.3.2.2-1. The low spool consists of a high speed five-stage LPC with a 5:1 pressure ratio driven by a single stage cooled LPT. The high speed seven-stage 8:1 pressure ratio HPC is also driven by a single stage cooled HPT. The burner is a low emissions two-stage vorbix combustor with aerating pilot nozzles and a maximum average CET of 1538°C (2800°F). An uncooled four-stage constant speed free turbine drives the power shaft.

The three spools are supported by four support struts and seven bearings. There are two bearings for the high spool, three bearings for the low spool and two bearings for the power shaft. Advanced technology materials were selected to provide the required temperature capability, oxidation/corrosion resistance, etc. The technology advances and related benefits are discussed in more detail in Section 4.3.4.

4.3.2.3 Reduction Gear System

Many gear train systems, such as compound offset with idler, epicyclic in-line and offset star system, are available for the reduction gears. A two-stage compound offset with idlers gear system was selected for the STS-487 turboprop engine because it provides good accessibility to the engine in an underwing installation, provides flexibility in designing the gearbox/gas generator mount and presents fewer design problems for the propeller pitch control mechanism. While this gear system is neither the smallest nor the largest of the various types available, it is believed that it could be designed to have acceptable size and weight. A final decision on the type of gear system and engine mount location would have to be coordinated through engine/airframe integration studies.

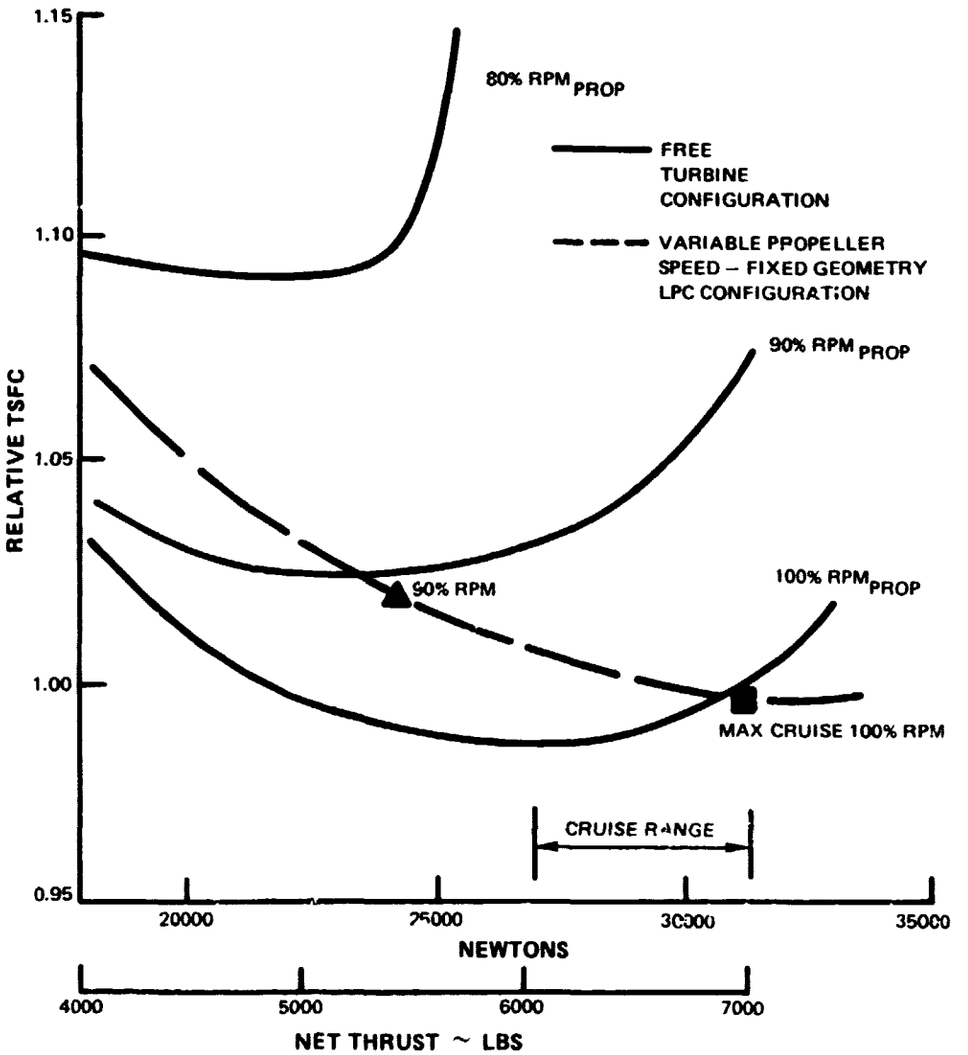

Figure 4.3.2.1-1 Turboshaft Off-Design Cruise Performance Comparison

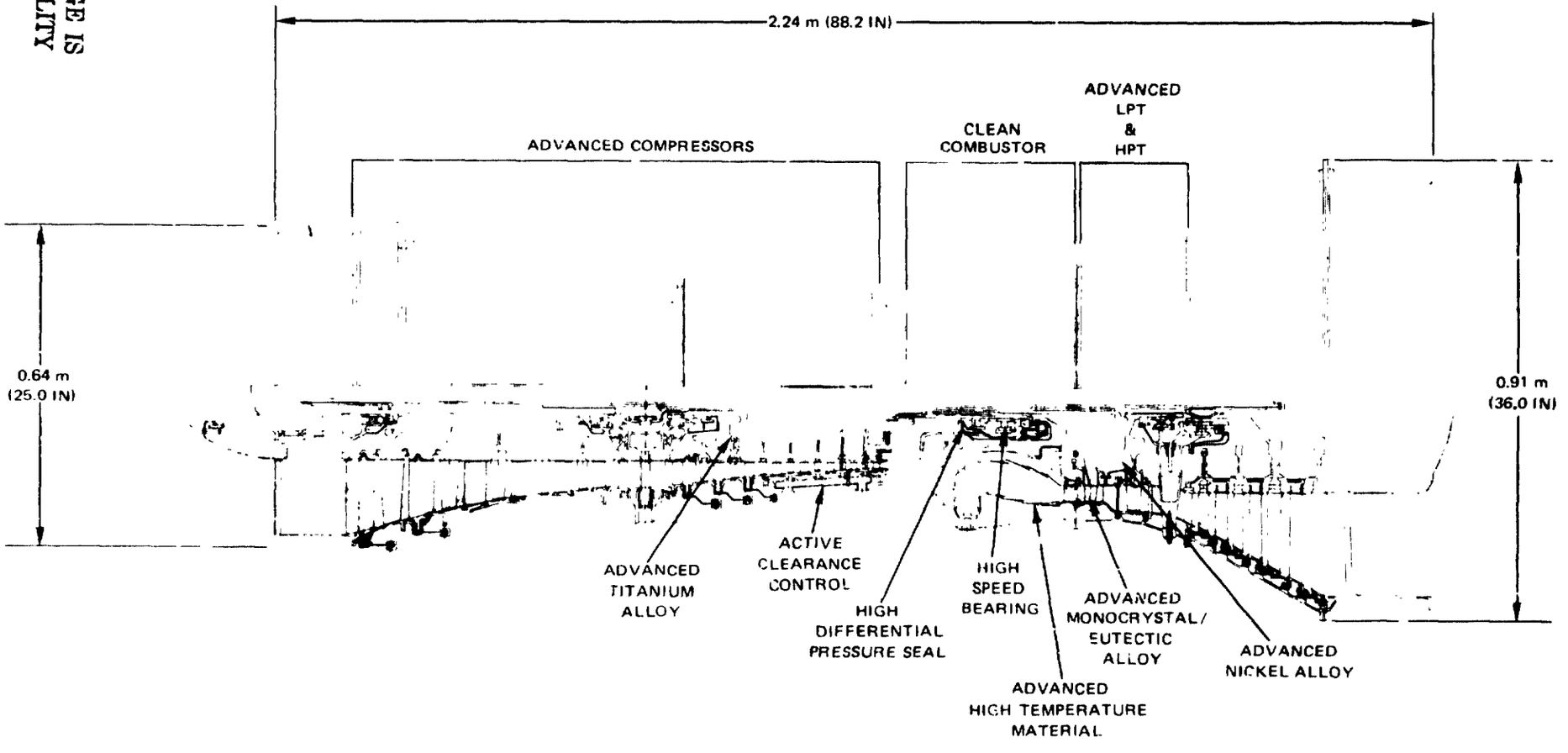

Figure 4.3.2.2-1 STS 487 Turboshaft Cross Section With Advanced Technology Concepts Identified

The reduction gear system uses advanced technology design features to effect a 6% weight reduction over current designs. The design transmission efficiency of 99% reduces the heat rejection rate below current levels to permit a 47% reduction in oil, tankage and air/oil cooler weight relative to current designs.

4.3.2.4 Propeller

The propeller selected for the STS-487 engine has eight blades with advanced technology aerodynamic and structural design features. At all radial locations, the blades have thin, low loss airfoil sections relative to conventional designs. In addition, the blade is swept rearward starting at about the 50% radial location with the sweep angle increasing to about 30° at the blade tip. The blade is swept to increase the blade Mach number at which losses start to increase rapidly. The blades are assumed to be constructed with a carbon epoxy airfoil shell filled with honeycomb material and a hollow titanium spar. A titanium clad leading edge provides added protection against foreign object damage. The blade shape and construction features are shown in Figure 4.3.2.4-1.

The estimated efficiency of the advanced propeller is shown in Figure 4.3.2.4-2 for variations in tip speed and power loading*. At the design altitude and Mach number, a power loading of 3.7×10^5 watts/m^2 (46.0 SHP ft^{-2}) was selected for the propeller. A 243.8 m/sec (800 ft/sec) maximum blade tip speed was selected to limit far field, low speed and near field, high speed noise. Blade structural and flutter design are also simplified at this relatively low tip speed.

Efficiency gains appear possible at lower power loadings than the level used in this evaluation; however, an increase in propeller tip diameter would be required. The larger propeller would result in weight increases for the propeller, gearbox, mounting system and nacelle, as well as increased nacelle drag. Studies would have to be conducted to determine the optimum power loading.

*Power loading for a propeller can be considered analogous to fan pressure ratio. At the design condition of 0.8 Mn and 9144 m (30000 ft), a power loading of 3.7×10^5 watts/m^2 (46.0 SHP/ft^2) is equivalent to a pressure ratio of about 1.05.

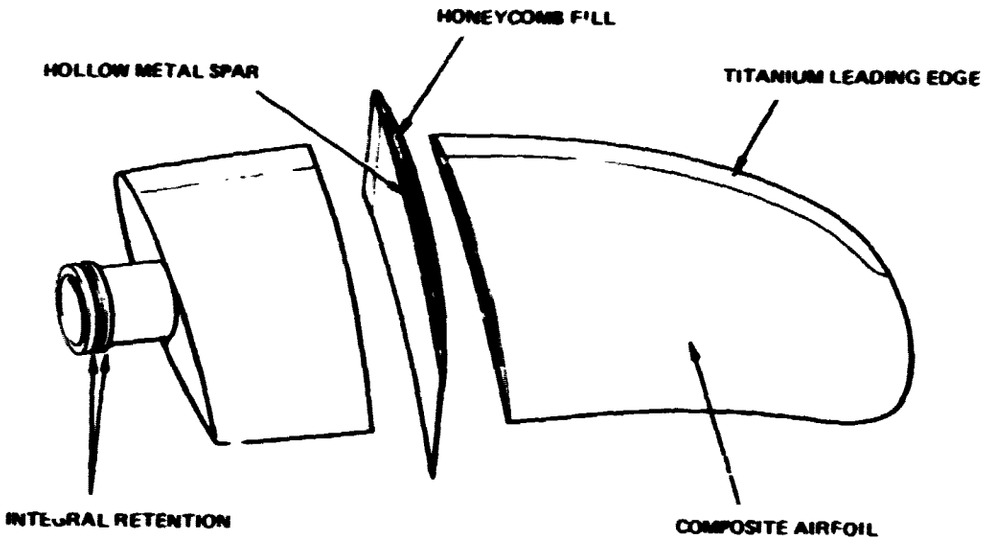

Figure 4.3.2.4-1 Advanced Propeller Blade Shape and Construction Features

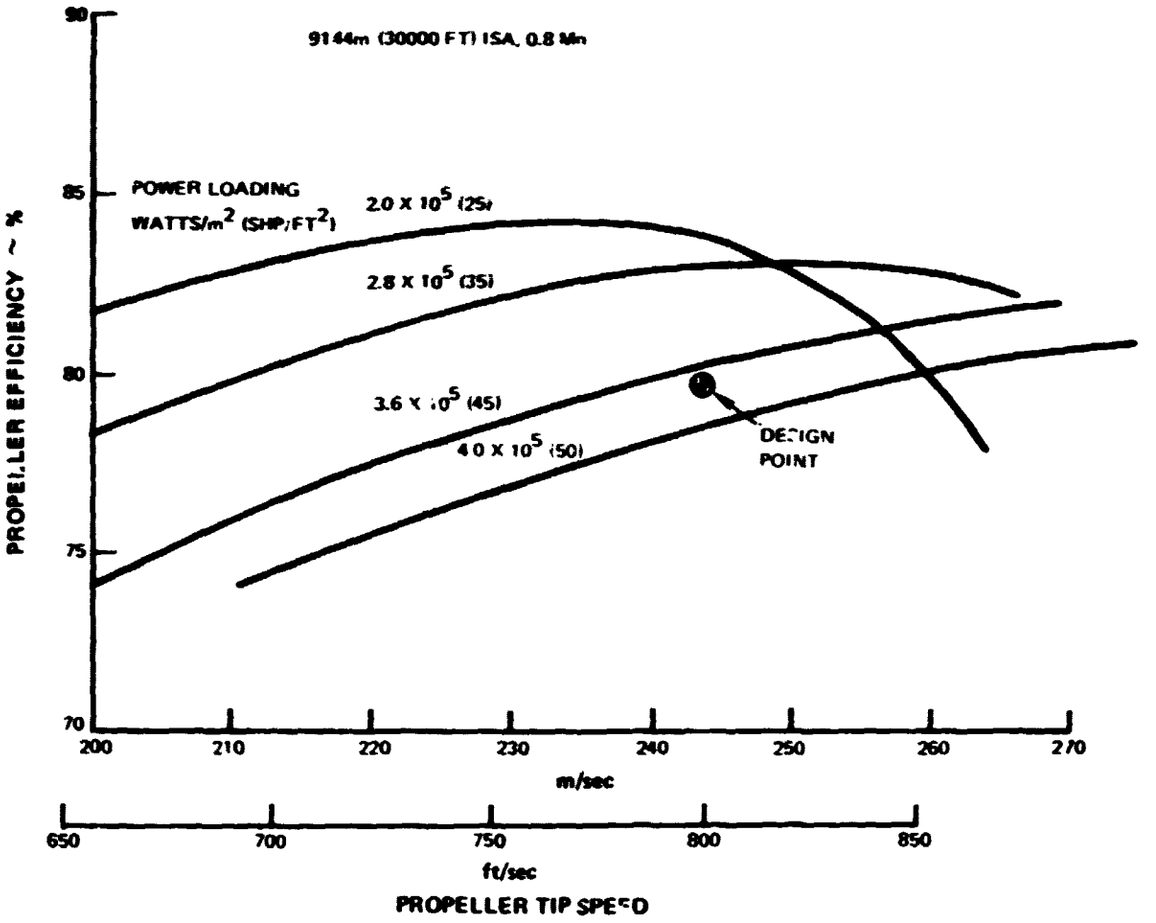

Figure 4.3.2.4-2 Advanced Propeller Efficiency

4.3.3 Regenerative Turboprop Engine (STS-488) Component and Mechanical Description

The primary difference between the STS-488 and the STS-487 is that the STS-488 employs a modified Brayton cycle which incorporates internal heat exchange. Other aspects of the two engines are similar and are based on the same advanced technology projections. A summary of the cycle and performance characteristics and the significant design parameters are presented in Table 4.3.3-1. The following sections describe the components of the STS-488.

4.3.3.1 Turboshaft

Because the OPR of the STS-488 (15:1) is much lower than the STS-487 (40:1), a single spool configuration was selected for the STS-488. A conceptual cross section of this engine is shown in Figure 4.3.3.1-1. The high tip speed nine-stage compressor is driven by a single stage cooled turbine. Compressor discharge air passes through a radial out flow diffuser and is ducted rearward through eight pipes to a heat exchanger located aft of the free turbine. The heat exhanger selected for the regenerative turboprop engine is a counterflow plate-fin recuperator which will be discussed in the next section. The heated air is ducted forward from the heat exchanger through eight pipes to a low emissions, two-stage vorbix combustor with aerating pilot nozzles and a maximum average exit temperature of 1760°C (3200°F). The power output shaft is driven by a cooled two-stage constant speed free turbine.

The support concept for this engine includes three support struts and four bearings. Two bearings support the gas generator spool and two bearings support the power output shaft. The STS-488 uses advanced high strength/high temperature materials as were projected for the STF-477 and STS-487 engines.

4.3.3.2 Heat Exchanger Selection

Several types of air-to-air heat exchangers were screened in the early phases of the study. These heat exchangers generally fall into two categories - rotary and stationary. Figure 4.3.3.2-1 is a drawing of a rotary concept. Both wire screen and ceramic matrices were evaluated. Two types of the stationary concept were considered: a plate-fin counterflow recuperator (shown in Figure 4.3.3.2-2) and a two-pass cross-counterflow tubular recuperator.

Selection Criteria - The heat exchangers were evaluated on the basis of their impact on the fuel consumption characteristics of the installed engine. The heat exchanger parameters considered were effectiveness, total pressure loss of the heat exchanger, system weight, and the geometric parameters of frontal area and volume.

TABLE 4.3.3-I

STS-488 ENGINE PARAMETERS

CYCLE DESCRIPTION

Base Size, Shaft power, Watts (hp)*	$1.424X10^7$ (19100)
Scaling Range, Shaft power, Watts (hp)*	$0.895X10^7$ - $2.237X10^7$ (12000-30000)
Nominal Cycle	
Overall Pressure Ratio	15:1
Maximum Combustor Exit Temperature, °C (°F)	(2033) 3200
Inlet Airflow (corrected), kg/sec (lbm/sec)	32.36 (71.34)
Acoustics	Not evaluated

PERFORMANCE

Condition	Altitude km	(ft)	Mach No.	Net Thrust N	(lbf)	TSFC kg/hr-N	(lbm/hr-lbf)
Take-off*	0	(0)	0.147	104600	(23515)	.0261	(256)
Max. Climb**	9.14	(30000)	0.8	29400	(6610)	.0509	(.499)
Max. Cruise***	9.14	(30000)	0.8	26890	(6045	.0503	(.493)

PROPELLER

Number of blades	8
Integrated lift coeff. (CLi)	0.12
Tip speed, m/sec (ft/sec)	243.8 (800)
Base diameter, m (ft)	4.40 (14.45)
Power loading, Watts/m^2 (hp/ft^2)****	$3.69X10^5$ (46)
Efficiency, percent****	79.7

*Sea level static, take-off power, 28.9°C (84°F) ambient temperature.

**U.S. Standard Atmosphere, 1962; 100 percent ram recovery; 470 kw (630 hp) extraction; 28.9°C (84°F)

***Same conditions as take-off except temperature is standard day.

****Maximum cruise, 0.8 Mach number, 9.14km (30000 ft); 470 kw (630 hp) extraction; standard day.

TABLE 4.3.3-1 (Cont'd)

STS-488 ENGINE PARAMETERS

REDUCTION GEAR

Gear ratio	7.75
Efficiency, percent	99.0

WEIGHTS - Kg (lbm)

Turboshaft	1070 (2358)
Recuperator System	1615 (3560)
Propeller	748 (1648)
Reduction gear system	590 (1302)
Total engine	4023 (8868)

DIMENSIONS - m (in.)

Length	– Compressor inlet to turbine exhaust flange	1.78 (70.1)
	– Compressor inlet to recuperator rear header	4.32 (170.1)
Diameter	– Compressor inlet flange	0.75 (29.4)
	– Turbine mount flange	1.10 (43.2)
Width	– Maximum, recuperator front header	1.52 (60.0)
Height	– Maximum, recuperator front header	0.97 (38.0)

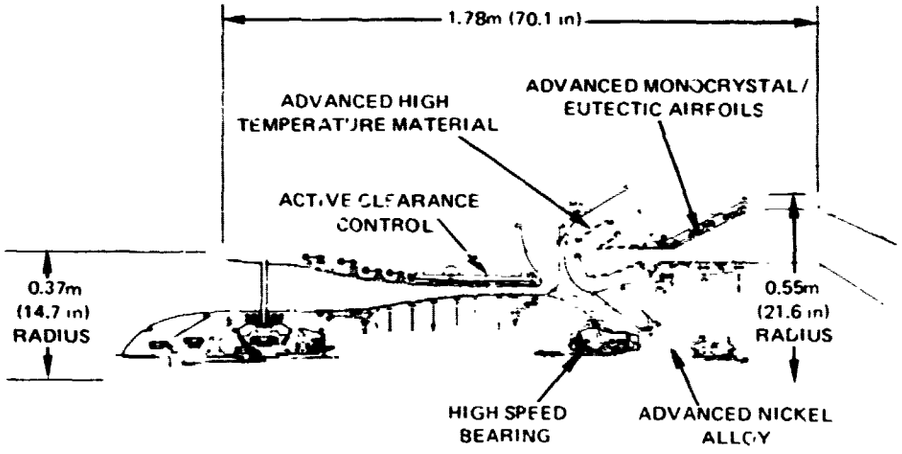

Figure 4.3.3.1-1 *STS 488 Regenerative Turboshaft Cross Section With Advanced Technology Concepts Identified*

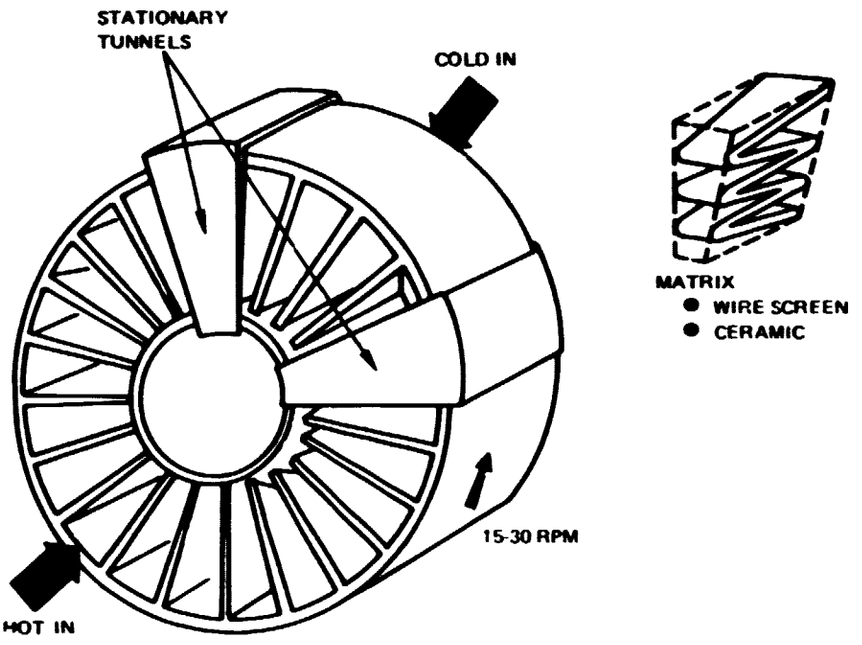

Figure 4.3.3.2-1 Rotary Regenerator Concept

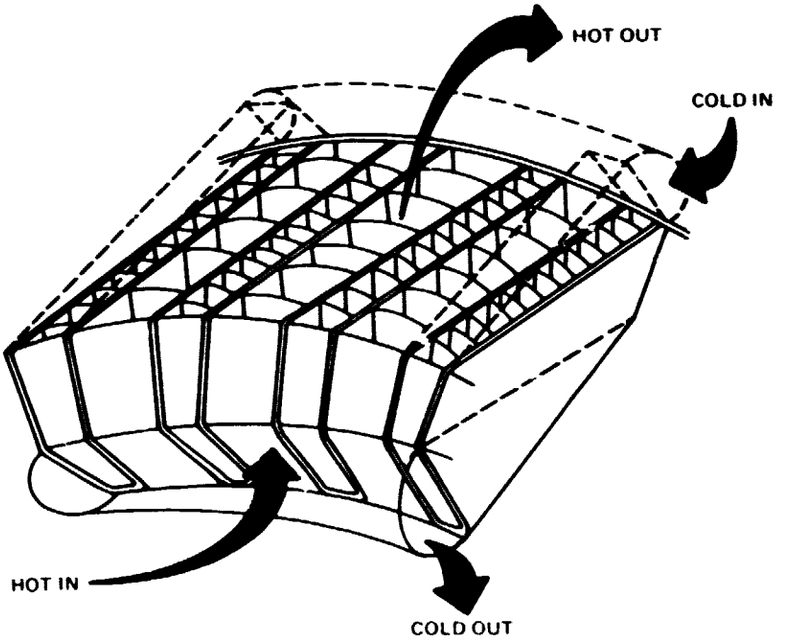

Figure 4.3.3.2-2 Stationary Plate-Fin Counterflow Recuperator Concept

The effectiveness ($\in$) of the heat exchanger is defined by the following equation:

$$\in = \frac{T_{2A} - T_2}{T_4 - T_2}$$

where: T = temperature, °C (°F)

and subscripts: 2 = cold side inlet
2A= cold side exit
4 = hot side inlet

The simplified schematic in Figure 4.3.3.2-3 shows the heat exchanger arrangement and identifies the temperature measuring locations used in calculating effectiveness. Figure 4.3.3.2-4 illustrates the impact of heat exchanger effectiveness on cycle thermal efficiency.

Total heat exchanger pressure loss includes compressor exit collector losses, duct losses, matrix entrance and exit losses and internal matrix losses. The heat exchanger weight is based on these same components.

Table 4.3.3.2-I lists the sensitivity factors that were used to compare the performance of the various heat exchangers evaluated. Carryover is the mass of gas entrained in a rotary heat exchanger as it rotates through the sealing tunnel separating the high pressure, cold gas from the low pressure, hot gas.

TABLE 4.3.3.2-I

Heat Exchanger Sensitivity Factors

Factor	ΔTSFC (%)
0.01 Δ Effectiveness	0.3
0.01 Δ Pressure Loss	0.3
1.0% Carryover	0.6
45.4 kg (100 lbm) Δ Weight	0.11

Refined Analysis Results – Analysis of the performance, geometry and weight characteristics of the rotary regeneators was conducted by P&WA. The capability to accomplish this analysis was acquired during design and experimental testing of similar unit for the PT6 engine. Rotary regenerators with three different types of matrix geometry were analyzed: a folded wire matrix in an annular cylinder, a folded matrix in a torus and conically shaped matrix in an annular cylinder. Figure 4.3.3.2-5 contains a sketch of each type of rotary configuration along with the parameters of each and the effective TSFC. Based on TSFC alone, the folded cylinder configuration gives the lowest fuel consumption. It also has the smallest packaging requirement and was, therefore, selected for comparison with the stationary recuperators.

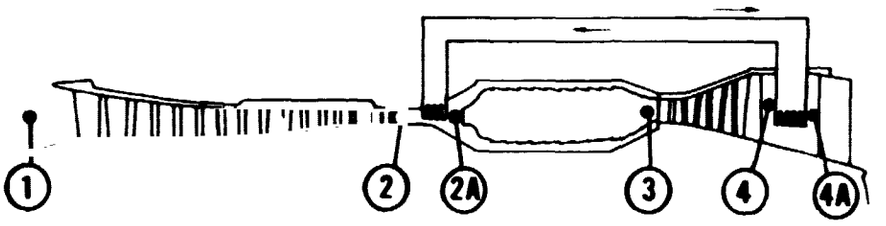

Figure 4.3.3.2-3 *Simplified Heat Exchanger Schematic Showing Temperature Measuring Points for Effectiveness Calculation*

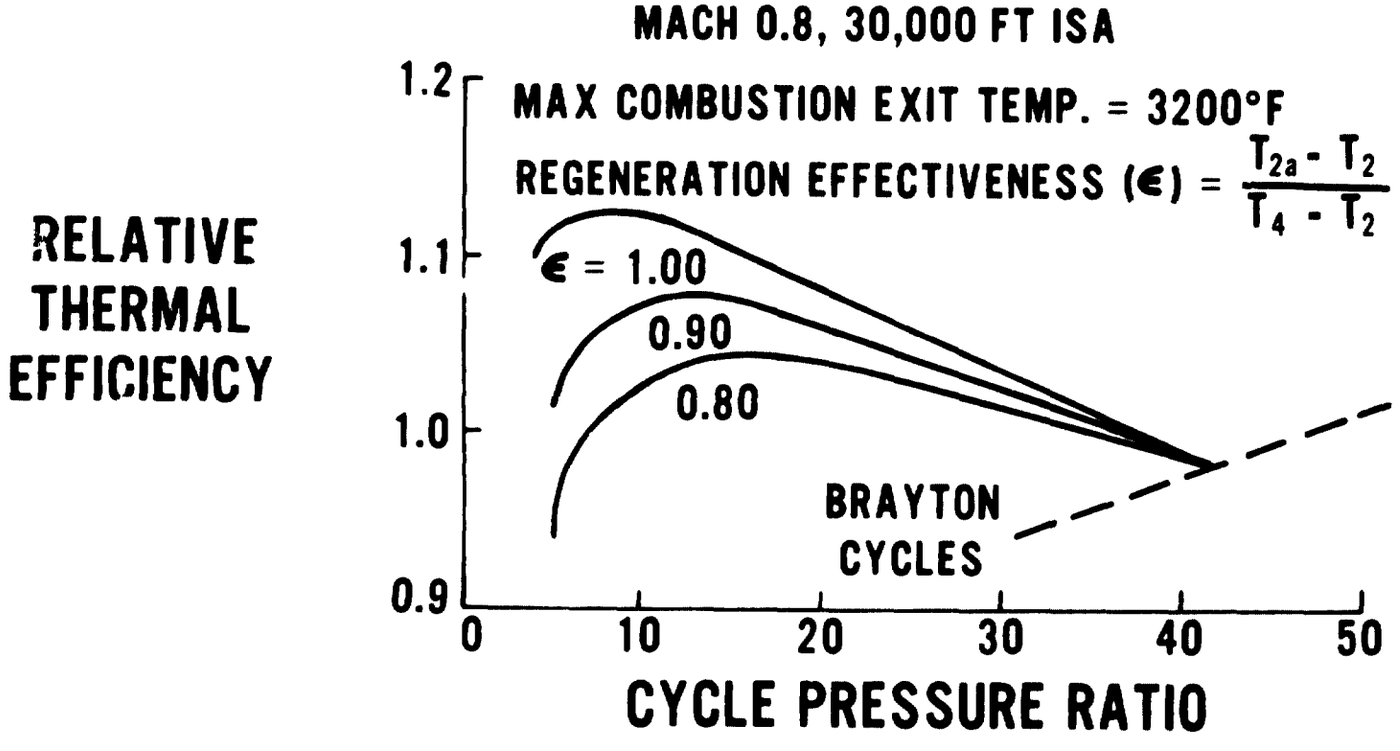

Figure 4.3.3.2-4 Heat Exchanger Effectiveness Effect on Thermal Efficiency

ROTARY GENERATOR

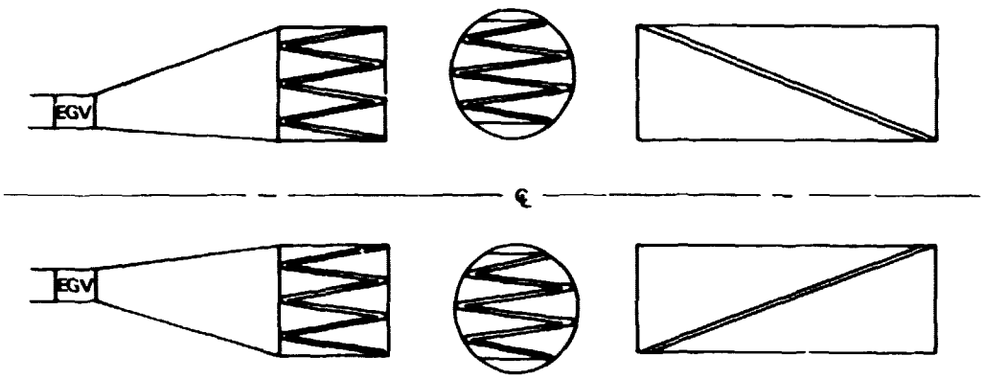

	FOLDED CYLINDER	FOLDED TORUS	CONICAL CYLINDER
RPM	15.7	15.7	15.7
EFFECTIVENESS, ~%	85.0	85.0	85.0
SYSTEM PRESSURE LOSS, $\Delta P/P$ ~%	15.3	15.3	15.3
CARRYOVER ~%	3.6	3.6	10.0
LEAKAGE ~%	1.5	2.0	1.5
MATRIX FRONTAL AREA ~m^2 (ft^2)	1.89 (20.3)	1.89 (20.3)	1.89 (20.3)
PACKAGE DIAMETER ~m (in)	1.64 (64.5)	1.78 (70.0)	1.64 (64.5)
LENGTH ~m (in)	0.56 (22.0)	0.61 (24.0)	1.52 (60.0)
TOTAL REGENERATOR WEIGHT ~Kg (lbm)	1334 (2940)	1334 (2940)	≈2220 (4900)
EFFECTIVE TSFC	BASE	+0.3%	+5.9%

Note: All dimensions and weights based on engine size described in Table 4.3.3-I.

Figure 4.3.3.2-5 Rotary Regenerator Configurations and Characteristics

AiResearch conducted the analysis of the stationary recuperators. This extensive effort included 56 different plate-fin and 100 different tube-shell types of matrices. For equal performance, the tube-shell concept was found to be larger, heavier and more costly than the plate-fin concept and was therefore dropped from further consideration. Three of the plate-fin recuperators were selected for further analysis and comparison with the best of the rotary regenerators. Table 4.3.3.2-II presents the characteristics of the selected plate-fin configurations. The higher effectiveness heat exchangers were generated by increasing the matrix axial approach and through flow Mach number and flow length at the expense of increased matrix pressure loss. The higher Mach number reduces the matrix frontal area and the overall heat exchange package size.

Figure 4.3.3.2-6 shows the sensitivity of the regenerative engine TSFC to changes in heat exchanger effectiveness and system pressure loss. The best of the rotary regenerators and the three stationary recuperators listed in Table 4.3.3.2-II are plotted on this figure. As shown the differences in heat exchangers effectiveness and pressure losses for the three plate-fin recuperators trade-off and result in almost equal engine TSFC. The configuration with 90% effectiveness (SR3) was selected as the best recuperator based on packaging considerations. The smaller axial projected frontal area results in a smaller and lighter nacelle with less drag than the other two configurations. The better installation characteristics offset slightly higher equivalent TSFC caused by the higher weight at the SR3 heat exchanger.

A comparison of the best rotary regenerator and best stationary recuperator is presented in Table 4.3.3.2-III. The stationary recuperator has a higher pressure loss and is heavier than the rotary recuperator, however, it has a lower equivalent TSFC because of a higher effectiveness and a low leakage rate (0.3%) compared to the 5.1% carryover for the rotary concept. The stationary recuperator also requires a much smaller nacelle cross section as illustrated in Figure 4.3.3.2-7. Therefore, the stationary counterflow plate-fin recuperator was selected as the best exchanger for use in the conceptual design of the regenerative turboprop (STS-488).

A sketch showing the details of the selected heat exchanger is presented in Figure 4.3.3.2-8. This sketch shows the modular design with eight identical heat exchangers arranged in a wedge shaped package. A hot gas approach Mach number of 0.2 requires a flow area which, along with the matrix blockage area, results in a heat exchanger height less than the rear turbine flange diameter and a width 0.56m (20 in) greater than the rear turbine flange. The additional nacelle interior volume is used for the ducting required to carry the compressor discharge air to and from the heat exchanger.

4.3.3.3 Reduction Gear System

The STS-488 uses a two-stage compound offset with idlers gear system which, except for a slightly lower gear ratio, is similar to that used with the STS-487. A detailed discussion of the gear system is contained in Section 4.3.2.3.

TABLE 4.3.3.2-II

STATIONARY PLATE-FIN RECUPERATOR CHARACTERISTICS

Configuration	SR1	SR2	SR3
Effectiveness (ϵ) ~ %	80	85	90
Axial Projected Frontal Area, (HxW) ~ m^2	1.11	0.86	0.68
(in^2)	(1726)	(1330)	(1050)
Matrix Frontal Area, (WxL) ~ m^2	5.83	3.85	3.38
(in^2)	(9035)	(5970)	(5244)
Matrix Axial approach ~ Mn	0.125	0.16	0.205
Matrix Thickness, t ~ m	0.066	0.147	0.176
(in)	(2.6)	(5.77)	(6.92)
Pressure Loss ~ %	13.7	18.2	25.9
Total Heat Exchanger Weight ~ kg	933	1125	1447
(lbm)	(2056)	(2480)	(3190)

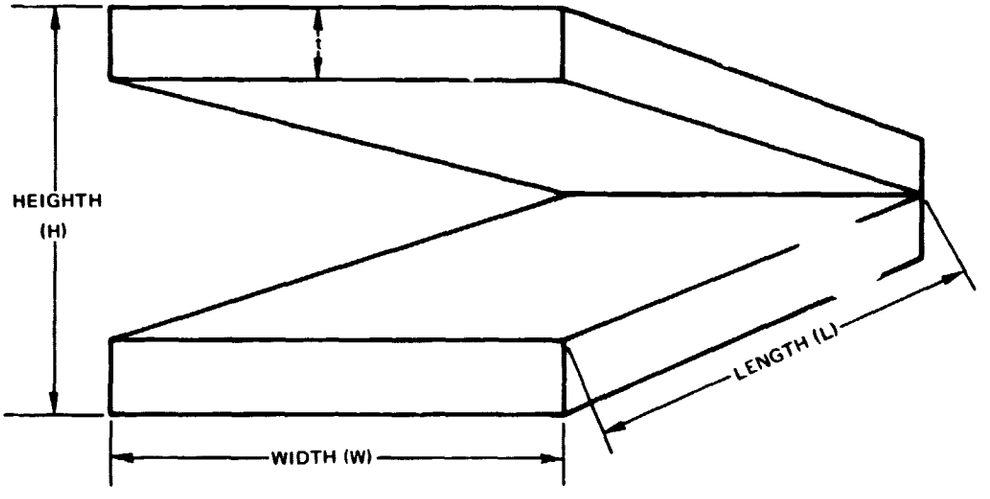

Note: All dimensions and weights based on engine size described in Table 4.3.3-I.

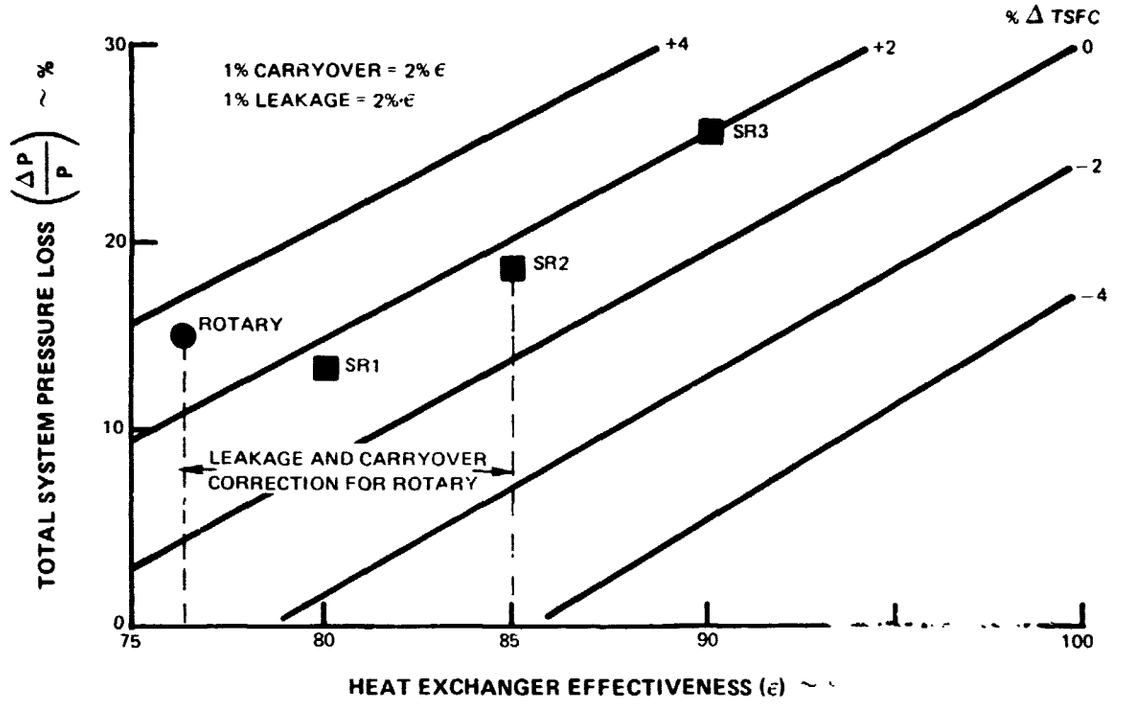

Figure 4.3.3.2-6 Sensitivity of Regenerative Engine TSFC to Changes in Heat Exchanger Effectiveness and System Pressure Loss

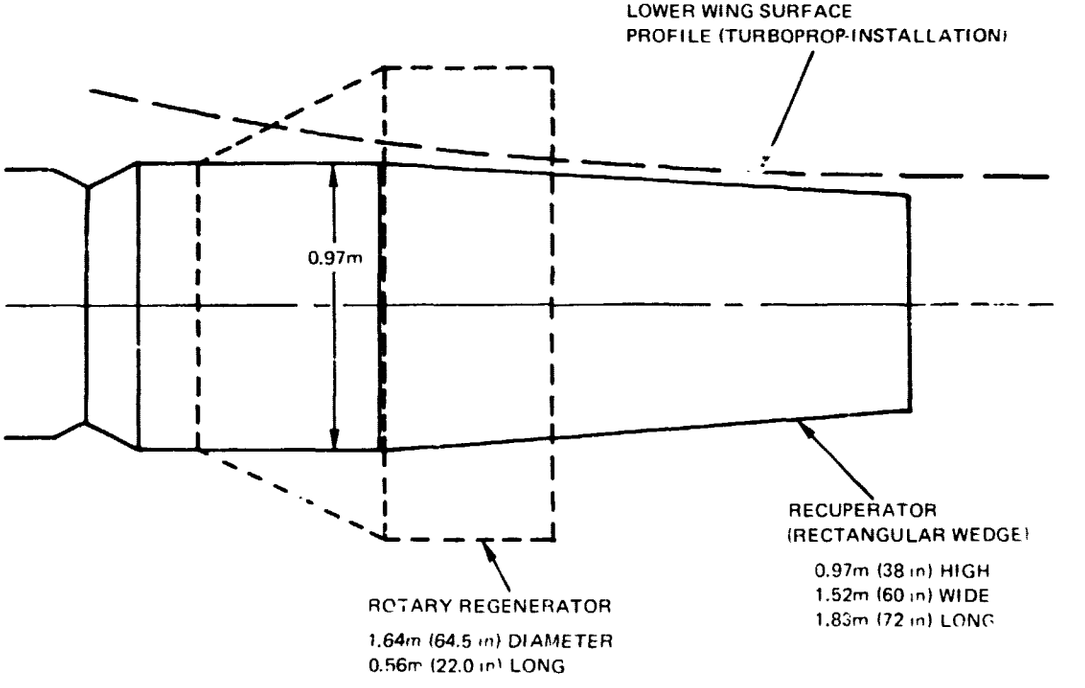

Figure 4.3.3.2-7 Heat Exchanger Packaging Requirements

TABLE 4.3.3.2-III

ROTARY/STATIONARY PACKAGING COMPARISON

	Stationary Recuperator	Rotary Regenerator
Nacelle Requirement ~ m (in)	0.96 X 1.52 (38 X 60)	1.64 Dia. (64.5)
Effectiveness (ϵ) ~ %	90	85
Total Pressure Loss $\frac{\Delta P}{P}$ ~ %	25.9	15.3
Matrix Weight ~ kg (lbm)	676 (1490)	163 (360)
Total Weight ~ kg (lbm)	1447 (3190)	1334 (2940)
Leakage and Carryover ~ %	0.3	5.1
Δ TSFC $_{Equivalent}$ (Excluding Nacelle Drag)	Base	+0.95%

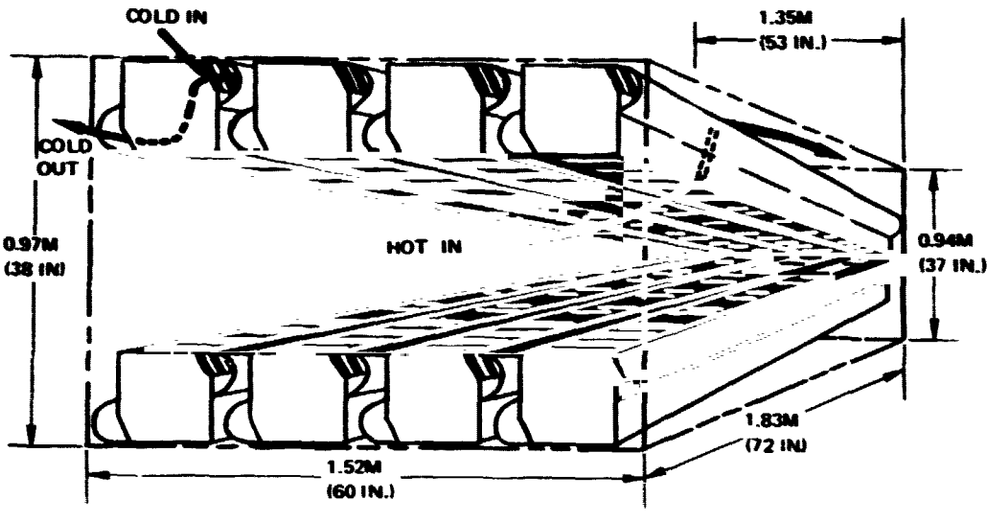

- Cold side fins – 14.5 per cm (37 per inch), 0.178 cm (0.070 inch) high
- Hot side fins – 6.3 per cm (16 per inch), 0.389 cm (0.153 inch) high
- 0.010 cm (4 mil) fin thickness
- 0.015 cm (6 mil) plate thickness
- 90% effectiveness
- 19.5% pressure loss (manifold and matrix only)

Figure 4.3.3.2-8 Details of the Plate-Fin Recuperator Heat Exchanger Selected for the STS 488

4.3.3.4 Propeller

Because the base size engine power output at the propeller sizing flight condition (9144 m (30,000 ft) ISA, 0.8 Mn. maximum cruise power setting) is essentially the same for both turboprop concepts, the propellers are identical. However, the two engines sized for the 200 passenger aircraft application would have different thrust requirements and therefore would require different size propellers. The discussion of design parameter selection and performance contained in Section 4.3.2.4 is also applicable to the STS-488 propeller.

4.3.4 Advanced Technology Considerations

The component characteristics of the STS-487 turboprop were based on advanced technology projected for 1985. The impact of this advanced technology in terms of potential component improvements were compared with those of a synthesized 1975 technology turbofan and the STF-477 turbofan. This comparison is presented in Table 4.3.4-I. As indicated in the table, many of the technology areas that require development work are common to both of the 1985 engines. These areas must be developed to substantiate the projected fuel consumption reduction.

TABLE 4.3.4-I

COMPARISON OF COMPONENT CHARACTERISTICS OF 1975 AND 1985 TECHNOLOGY FUEL CONSERVATIVE ENGINES AT CRUISE DESIGN POINT

	Major Changes (1975 to 1985) Turbofan/Turboprop	Potential Benefits Turbofan	Turboprop
Cruise Design Cycle Parameters	1) Increase cycle pressure ratio from 25:1 to 45:1/40:1 2) Increase bypass ratio from 6:1 to 8:1/ N.A. 3) Increase maximum combustor exit temperature by 111°C (200°F)/ 111 to 222°C (200 to 400°F)	a) Improved TSFC	a) Improved TSFC
Fan	1) Eliminate part span shrouds 2) Improve airfoil shapes 3) Reduce endwall losses 4) 61 m/sec (200 ft/sec) higher tip speed	a) +1.8 percentage points efficiency	N.A.
Propeller	1) Improve blading shapes 2) Reduce spinner and hub losses	N.A.	a) +20.0 percentage points propeller efficiency
Compressor	1) Increase pressure ratio per stage by 7 percent 2) Increase inlet corrected tip speed by 152 m/sec (500 ft/sec) 3) Improve blading 4) Reduce tip clearance	a) +3.3 percentage points polytropic efficiency	a) +3.3 percentage points polytropic efficiency
Diffuser/Burner	1) Improve diffuser design 2) Reduce burner exit temperature profile 3) Reduce emissions	a) −1.0 percent pressure loss	a) −1.0 percent pressure loss
Burner/Turbine Gaspath Materials	1) Improve burner liner 2) Use monocrystal/eutectic airfoils 3) Use high temperature protective coatings 4) Improve turbine seals	a) Increased cycle pressure ratio capability b) −3.6 percent chargeable cooling air	a) Increased cycle pressure ratio capability b) −3.6 percent chargeable cooling air

TABLE 4.3.4-1 (Cont'd)

	Major Changes (1975 to 1985) Turbofan/Turboprop	Potential Benefits	
		Turbofan	Turboprop
High-Pressure Turbine	1) Reduce load factor 2) Increase speed 3) Reduce endwall losses 4) Reduce cooling air penalty 5) Reduce tip clearance	a) +2.9 percentage points efficiency	a) +2.5 percentage points efficiency
Low-Pressure Turbine	1) Increase load factor/Reduce load factor 2) Improve aerodynamics 3) Reduce tip clearance	a) Reduced weight and cost b) + 1.1 percentage points efficiency	a) +2.1 percentage points efficiency
Free Turbine	1) High rpm through gearing 2) Improve aerodynamics 3) Reduce tip clearance	N.A.	a) Reduced weight and cost b) +1.5 percentage points efficiency

4.4 EVALUATION OF ENGINE/AIRCRAFT SYSTEMS

A domestic three-engine turbofan airplane, a domestic four-engine turboprop, and : n international airplane were used in the evaluation of the selected propulsion systems. B oth turbofan and turboprop international airplanes were four-engine configurations. All e:aluations assumed a Mach 0.8 cruise speed capability.

4.4.1 Study Groundrules

General domestic and international study aircraft parameters are listed in Table 4.4.1-1. Aircraft characteristics in both cases include high aspect ratio wings, supercritical aerodynamics, and advanced lightweight composite structure technology. The wing geometry was selected to minimize fuel use. The selected aircraft configurations and characteristics utilized are the results of data interchanges among NASA Lewis, Langley, and Ames Research Centers.

TABLE 4.4.1-1

STUDY AIRCRAFT PARAMETERS FOR ADVANCED ENGINE EVALUATION

	Domestic Aircraft	International Aircraft
Design Cruise Mach No.	0.8	0.8
Design Range, km (n. mi)	5560 (3000)	10200 (5500)
Nominal Mission Range, km (n. mi.)	1300 (700)	3700 (2000)
Number of Passenger Seats	200	200
Number of Engines, Turbofan	3	4
Number of Engines, Turboprop	4	4
Maximum Take-Off Field Length, m (ft)	2440 (8000)	3200 (10500)
Max. Approach Speed at Max. Landing Weight, m/sec (knots)	69.5 (135)	72.0 (140)
Seat Pitch, First Class, m (in.)	0.965 (38)	0.965 (38)
Seat Pitch, Tourist, m (in.)	0.864 (34)	0.864 (34)
Take-off Wing Loading, N/m^2 (lbf/ft^2)	5583 (116.6)	6607 (138)
Wing Quarter Chord Sweep, radian (degrees)	0.44 (25)	0.44 (25)
Wing Aspect Ratio	12	12

Appendix A presents the airplane aerodynamics, weight, and pricing calculations (including the engine nacelles) used to evaluate the advanced engines. Also included are the study economic groundrules.

The fuel consumption characteristics of the various combinations of powerplants and aircraft were calculated for both the design range and nominal mission ranges. The fuel calculations include fuel used in flight plus ground maneuver fuel. Direct operating cost and return on investment were selected as economic figures of merit. DOC and ROI computations were based on nominal mission performance and revenue characteristics. The noise and emission characteristics of the engines were assessed and compared against proposed or projected rules. A noise goal of 10 EPNdB below current FAR regulations and projected 1981 EPA emission rules were assumed as design goals.

4.4.2 Fuel Consumption Characteristics

Fuel use by the advanced technology turbofan (STF 477), turboprop (STS 487), and regenerative turboprop (STS 488) was estimated by utilizing a computer simulation of the entire airplane systems. The engine factors considered in evaluating the fuel consumption included installed TSFC (Section 4.2.3), propulsion system weight (Section 4.2.4), and propulsion system thrust characteristics.

Fuel consumption as a function of flight distance for average missions is plotted in Figures 4.4.2-1 and -2. The turboprop system fuel requirements were calculated to be at least 15 percent lower than that of the turbofan engine. Improved cruise TSFC accounted for the major portion of the fuel savings. The higher take-off and climb thrust capability of the turboprop resulted in higher climb gradients, which also contributed significantly to fuel savings potential. For example, the domestic turboprop thrust to average mission take-off gross weight ratio at sea level, 51.4 m/sec (100 knots) exceeded the turbofan system by 38 percent. The shorter cruise range, domestic aircraft flight emphasized the benefits of the improved climb performance of the turboprops to account for an additional 2 to 3 percent fuel savings relative to the international flight.

The substantial weight difference between the simple and regenerative turboprop installations accounted for a 5 percent difference in fuel burned by the two powerplants.

The aircraft system weight breakdowns and fuel loads are compared for each engine configuration in Tables 4.4.2-I and -II. A 6 to 9 percent average mission take-off gross weight reduction was estimated for the simple turboprop relative to the turbofan systems, generally reflecting the lower fuel load requirement. The average mission take-off gross weight of the regenerative turboprop domestic airplane was only 0.5 percent lighter than the turbofan-powered airplane; the international aircraft average mission gross weight increased by 3 percent for the regenerative turboprop relative to the turbofan system.

4.4.3 Economic Evaluation

The economic evaluation of the unconventional engines required engine price and maintenance cost estimates in addition to the engine and airplane information obtained from the fuel-burned analysis. The acquisition and maintenance cost data were combined with airframe costs, fuel costs, and crew costs to determine the direct operating costs of the total aircraft systems. Revenue assumptions, DOC, and indirect operating cost (IOC) estimates were all combined in order to estimate the airline ROI for the various engine concepts. All of the economic comparisons were based on the aircraft typical missions and other groundrules discussed in Appendix A.

4.4.3.1 Engine Price Estimates

Price estimates were made for the turbofan, turboprop, and regenerative turboprop engine subsystems (Table 4.4.3.1-I). All values were made relative to the turbofan engine subsystem as a baseline. The constant thrust cases shown in the table were scaled as required to

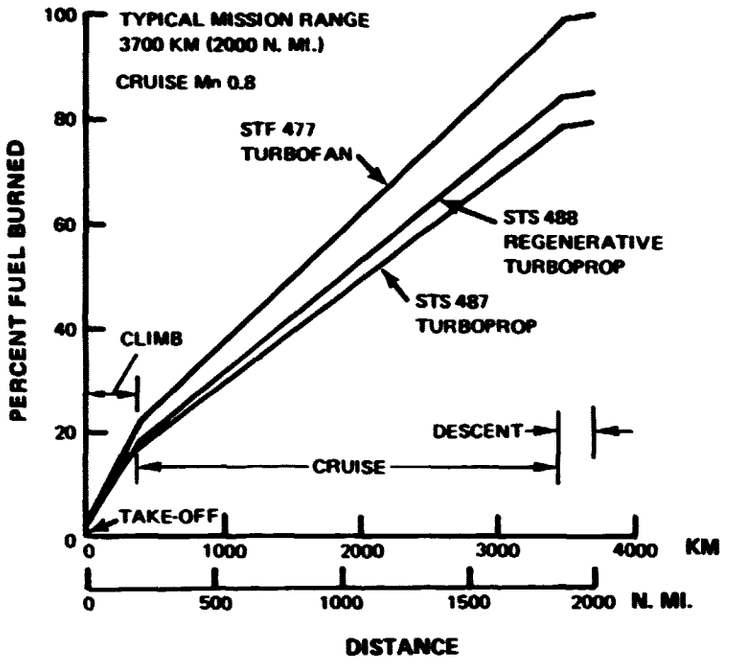

Figure 4.4.2-1 *Mission Fuel Consumption for the Three Study Propulsion Systems on the International Aircraft Configuration*

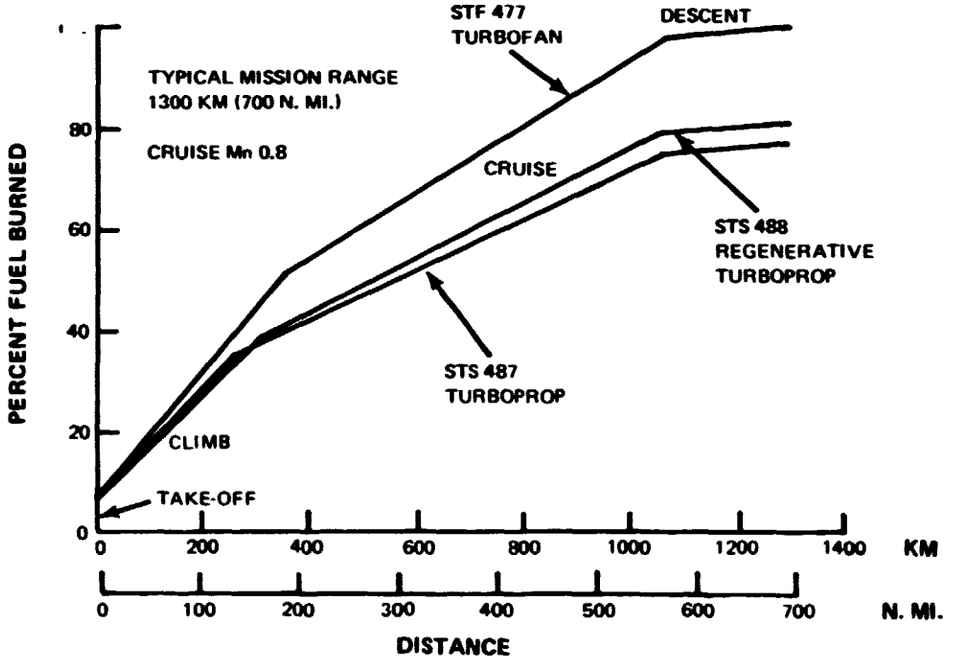

Figure 4.4.2-2 *Mission Fuel Consumption for the Three Study Propulsion Systems on the Domestic Aircraft Configuration*

TABLE 4.4.2-I

WEIGHT COMPARISONS OF ADVANCED TECHNOLOGY ENGINES IN DOMESTIC AIRCRAFT AT MACH 0.8

	STF 477[1]		STS 487[2]		STS 488[2]	
	kg	lbm	kg	lbm	kg	lbm
Design Range, 5,560 km (3,000 n. mi.)						
Take-Off Gross Weight	101,827	224,490	91,850	202,492	100,126	220,737
Payload, 200 Passengers	18,597	41,000	18,597	41,000	18,597	41,000
Fuel						
Used	21,656	47,742	16,480	36,331	17,732	39,092
Reserve	4,466	9,846	3,386	7,464	3,629	8,000
TOTAL	26,122	57,588	19,866	43,795	21,361	47,092
Average Stage Length, 1,300 km (700 n. mi.)						
Take-Off Gross Weight	76,325	168,268	68,891	151,876	75,977	167,496
Payload, 110 Passengers	10,229	22,550	10,229	22,550	10,229	22,550
Fuel						
Used	4,988	10,996	3,840	8,465	4,053	8,935
Reserve	4,000	8,820	1,435	3,164	1,527	3,366
TOTAL	8,988	19,816	5,275	11,629	5,580	12,301
Operating Empty Weight						
Propulsion	7,046	15,534	6,755	14,893	11,884	26,199
Structure	29,052	64,049	26,421	58,248	27,841	61,378
Systems	6,589	14,526	6,098	13,444	6,340	13,976
Furnishings and Equipment	8,972	19,781	8,796	19,391	8,789	19,376
Operating Items	5,449	12,012	5,317	11,721	5,314	11,716
TOTAL	57,108	125,902	53,387	117,697	60,168	132,645

1. Three engines
2. Four engines

TABLE 4.4.2-II

WEIGHT COMPARISONS OF ADVANCED TECHNOLOGY ENGINES IN INTERNATIONAL AIRCRAFT AT MACH 0.8

	STF 477		STS 487		STS 488	
	kg	lbm	kg	lbm	kg	lbm
Design Range, 10,200 km (5,500 n. mi.)						
Take-Off Gross Weight	132,026	291,065	118,689	261,660	128,788	283,926
Payload, 200 Passengers	19,278	42,500	19,278	42,500	19,278	42,500
Fuel						
Used	44,533	98,177	35,102	77,386	37,444	82,549
Reserve	6,668	14,701	5,078	11,194	5,369	11,837
TOTAL	51,201	112,878	40,180	88,580	42,813	94,386
Average Stage Length, 3,700 km (2,000 n. mi.)						
Take-Off Gross Weight	89,915	198,226	83,776	184,693	92,032	202,894
Payload, 110 Passengers	10,614	23,400	10,614	23,400	10,614	23,400
Fuel						
Used	13,589	29,958	10,757	23,715	11,518	25,392
Reserve	4,165	9,181	3,174	6,998	3,203	7,062
TOTAL	17,754	39,139	13,931	30,713	14,721	32,454
Operating Empty Weight						
Propulsion (4 Engines)	7,390	16,293	7,553	16,652	13,147	28,984
Structure	31,548	69,551	29,496	65,026	31,079	68,517
Systems	7,294	16,080	6,910	15,234	7,202	15,877
Furnishings and Equipment	9,066	19,987	9,075	20,007	9,068	19,992
Operating Items	6,249	13,776	6,197	13,661	6,201	13,670
TOTAL	61,547	135,687	59,231	130,580	66,697	147,040

meet the thrust needed by the aircraft systems. The engine prices were estimated by Pratt & Whitney Aircraft. Hamilton Standard provided the propeller and gearbox prices, and AiResearch Manufacturing of California estimated the recuperator price.

TABLE 4.4.3.1-1

RELATIVE ENGINE PRICE

Constant Maximum Cruise Thrust at Mach 0.8, 9.14 km (30,000 ft) Altitude

Subsystem	Turbofan (STF 477)	Turboprop (STS 487)	Regenerative Turboprop (STS 488)
Turbotan Engine	1.00	---	---
Turboshaft Engine	---	0.83	0.98
Propeller and Gearbox	---	0.17	0.16
Recuperator	---	---	0.20
SUBTOTAL	1.00	1.00	1.34
Nacelle	0.33*	0.17	0.25
TOTAL	1.33	1.17	1.59

*Includes reverser

Identical price estimates were obtained for the total base turbofan (gas generator, fan, and engine control) and the turboprop (turboshaft engine, gearbox, propeller, pitch control, and engine control). The lower turboshaft engine price relative to the turbofan reflects the elimination of the fan rotor and fan case and the smaller gas generator flow size. The regenerative engine includes a fully cooled free turbine and heat exchanger plumbing, resulting in a turboshaft engine price 2 percent lower than that of the turbofan.

The nacelle prices of the turboprops are substantially less than the turbofan nacelle price because of the elimination of the pylon and the thrust reverser and reduced nacelle size. The increased nacelle interior volume required to package the recuperator resulted in a wetted area 41 percent larger for the STS 488 than for the STS 487 turboprop. The total turboprop propulsion system installation price is 12 percent lower than the turbofan and the total regenerative turboprop propulsion system price is 19 percent higher than the turbofan.

4.4.3.2 Engine Maintenance Cost Estimates

Comparative shop maintenance costs were estimated for the turbofan and turboshaft engines as shown in Table 4.4.3.2.-I. The engine values were estimated by Pratt & Whitney Aircraft. The turboshaft gas generator cost reflects the elimination of the fan component maintenance requirements and one less turbine stage than the baseline turbofan. The high regenerative turboshaft cost level results from the added maintenance requirements of the cooled free turbine and the complex burner section needed in conjunction with the recuperator.

The propeller and gearbox range of values were determined from data provided by Hamilton Standard with an uncertainty band added to account for the unknowns in the reliability and maintainability of these components.

TABLE 4.4.3.2-I

RELATIVE ENGINE MAINTENANCE COSTS

Constant Maximum Cruise Thrust at Mach 0.8, 9.14 km (30,000 ft) Altitude

Subsystem	Turbofan (STF 477)	Turboprop (STS 487)	Regenerative Turboprop (STS 488)
Turbofan Engine	1.00	- - -	- - -
Turboshaft Engine	- - -	0.90	1.15
Propeller and Gearbox	- - -	0.06 to 0.18	0.06 to 0.18
Recuperator	- - -	- - -	0.17
TOTAL	1.00	0.96 to 1.08	1.38 to 1.50

Recuperator maintenance was found to represent a substantial percentage of the total cost based on an assumed scrap life of 30,000 hours, which is three times the design life of present regenerators. As improved materials become available, this increase in life could be achieved. Even with this increased life, however, the regenerative turboprop maintenance cost could be as much as 50 percent greater than that of the turbofan or turboprop engines.

4.4.3.3 Direct Operating Cost Comparison

Direct operating costs were evaluated for the various unconventional engines in domestic and international aircraft based on the cost information discussed in Sections 4.4.3.1 and 4.4.3.2. Results of the analysis are shown in Table 4.4.3.3-I. Relative to the baseline turbofan, the turboprop system had a substantially improved DOC, while the regenerative turboprop DOC was substantially greater.

TABLE 4.4.3.3-I

DIRECT OPERATING COST COMPARISON

	Percent ΔDOC Relative to Conventional Turbofan			
	Domestic Airplane		International Airplane	
Cost Element	Turboprop	Regenerative Turboprop	Turboprop	Regenerative Turboprop
Fuel* and Oil	−5	−4	−6	−5
Engine Maintenance	+2 to +4	+12 to +14	−1 to +1	+6 to +8
Airframe Maintenance, Equipment Depreciation, Crew, Insurance	−2	+3	−2	+2
TOTAL	−3 to −5	+11 to +13	−7 to −9	+3 to +5

*Fuel price 8¢ /liter (30¢ /gal.) domestic airplane, 12¢ /liter (45¢ /gal.) international airplane.

In the domestic airplane case, the assumption of a four-engine turboprop in comparison with the baseline trijet resulted in a higher turboprop engine maintenance cost (Table 4.4.3.3-I), even though the cost per turboprop engine was lower. The smaller, lower cost turboprop airplane incurred lower depreciation losses. This counterbalanced the greater engine maintenance cost of this airplane, with the result that DOC improvement potential directly reflected the fuel cost reduction. The regenerative turboprop, because of very high engine procurement and maintenance costs, suffered a very substantial DOC penalty of over 10 percent.

The long range international airplane case, where fuel costs represent a larger portion of the DOC, responded less drastically to the maintenance cost trends. The overall result was a more favorable DOC trend for the turboprop engines relative to the domestic airplane. Regenerative turboprops remained at higher DOC levels than the turbofan in the international airplane. The simple turboprop is clearly superior to the alternate regenerative cycle in reducing both fuel consumption and DOC.

4.4.4 Benefits Relative to JT9D-70 Technology

In reference 1 the 1985 technology STF 477 turbofan fuel consumption and direct operating cost benefits were determined relative to the 1975 turbofan technology. Assuming full utilization of fuel conservative technology in the advanced engine, a fuel savings of 10 to 17 percent was estimated. The attendant DOC ranged from a 3 percent decrement to a 5 percent improvement. These benefits are considered to be the highest achievable with turbofan advances and are possible only with an all-out effort aimed at reducing fuel consumption. Unless adequate funding is available to proceed with the required technology programs, these advances and benefits will be reduced.

These relationships were superimposed on the turbofan to turboprop comparisons taken from this study and used in determining the potential of the three advanced engine cycles relative to the 1975 turbofan. The results of this evaluation are summarized in Figures 4.4.4-1 and -2. A high efficiency advanced propeller in combination with an advanced turboshaft engine could reduce the fuel consumption in future advanced transports by 28 to 35 percent compared with similar aircraft powered by present technology turbofans. Regeneration results in a reduction in fuel savings potential relative to the high pressure ratio simple turboprop cycle.

With the higher costs associated with energy conservative concepts, small improvements in DOC are possible with advanced turbofans. Advanced turboprops were estimated to offer a 6 to 14 percent DOC reduction from current engine technology for long range, fuel conscious applications. The regenerative turboprop offered no economic incentives for further concept exploration.

The simple cycle turboprop shows sufficient promise to continue concept evaluation as a possible companion to future turbofan engines.

4.4.5 Noise and Emission Benefits

4.4.5.1 Acoustical Benefits

With projected technology improvements for the 1990 operational time period in both noise source and attenuation characteristics, the STF 477 turbofan and the STF 487 turboprop far field noise characteristics are similar at take-off, while the turboprop is somewhat quieter during approach. Noise estimates were made at take-off, approach, and sideline for a 120,000 kg (265,000 lbm) take-off gross weight Mn 0.8 international quadjet with turboprops and then compared to a 132,000 kg (290,000 lbm) take-off gross weight Mn 0.8 international quadjet with advanced technology turbofans. The turboprop engines were scaled to 67,600 N (15,200 lbf) take-off thrust at 51.4 m/sec (100 knots) rotation speed, and the turbofan was scaled to 54,900 N (12,350 lbf) take-off thrust at a similar take-off speed. Results of the international quadjet analysis are summarized in Figures 4.4.5.1-1 and 4.4.5.1-2. Comparisons are made only for the international aircraft because the domestic turboprop has four engines while the domestic turbofan had previously been defined with three engines. For this reason a meaningful noise comparison of the domestic airplanes is more difficult to make.

Technology improvements in both noise source and attenuation characteristics are required to achieve the FAR 36 minus 10 EPNdB noise level for both the turboprop and the turbofan. Figures 4.4.5.1-1 and 4.4.5.1-2 show the required improvements for the international aircraft. Propeller source noise reductions of 2 to 3 EPNdB through improved airfoil design to reduce tones and broadband noise are required. Additional noise reductions may be attainable by reducing propeller speed during approach. Improvements in the burner design are required to reduce core noise and total noise should the propeller reductions not be achieved. Additional reductions of generated noise will be possible through optimization of turbine blade and vane numbers and spacing. The application of advanced acoustic treatment concepts, such as tailoring to the modal structure of the noise and the use of segmented liners to provide attenuation of turbine and core noise, is also possible. These gas generator noise reduction

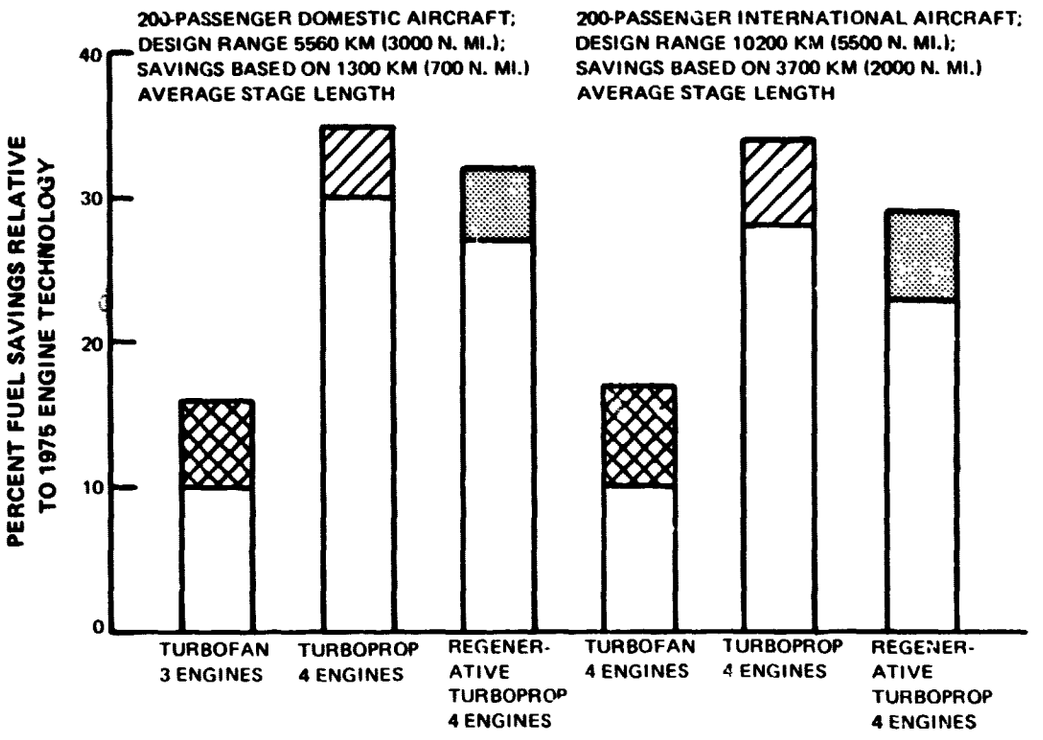

Figure 4.4.4-1 Projected Fuel Savings With Future Energy-Efficient Propulsion Systems

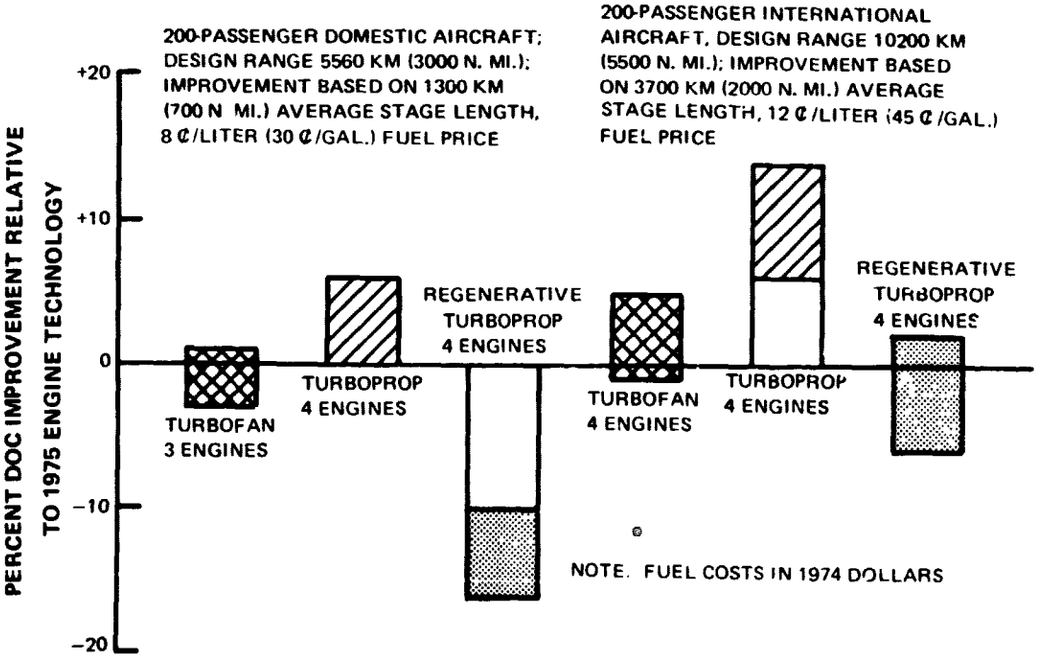

Figure 4.4.4-2 Projected Direct Operating Cost Improvement With Future Energy-Efficient Propulsion Systems

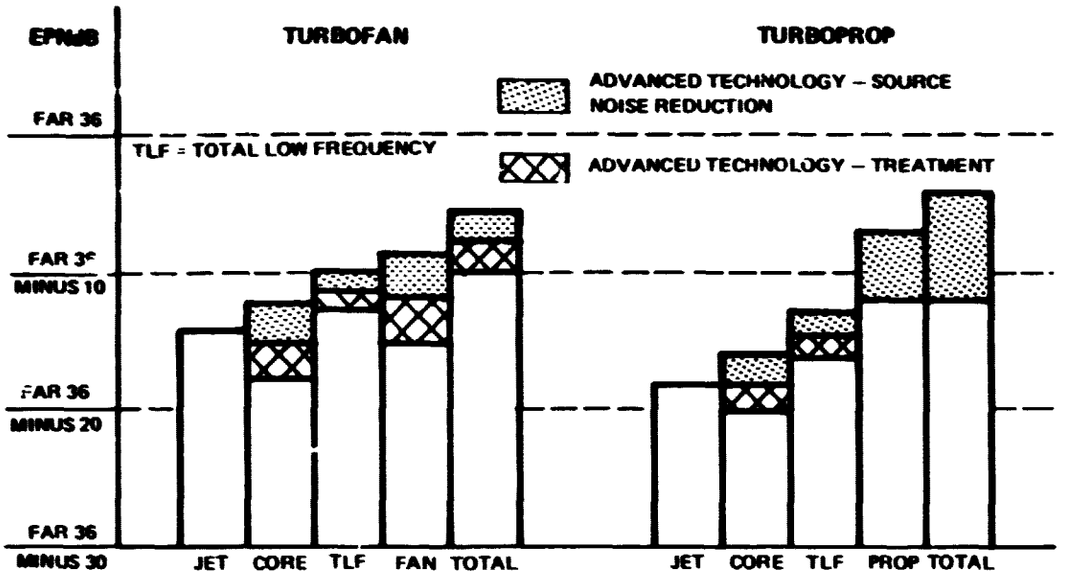

Figure 4.4.5.1-1 *Advanced Technology Propulsion System Take-Off Noise Levels on the International Quadjet Aircraft*

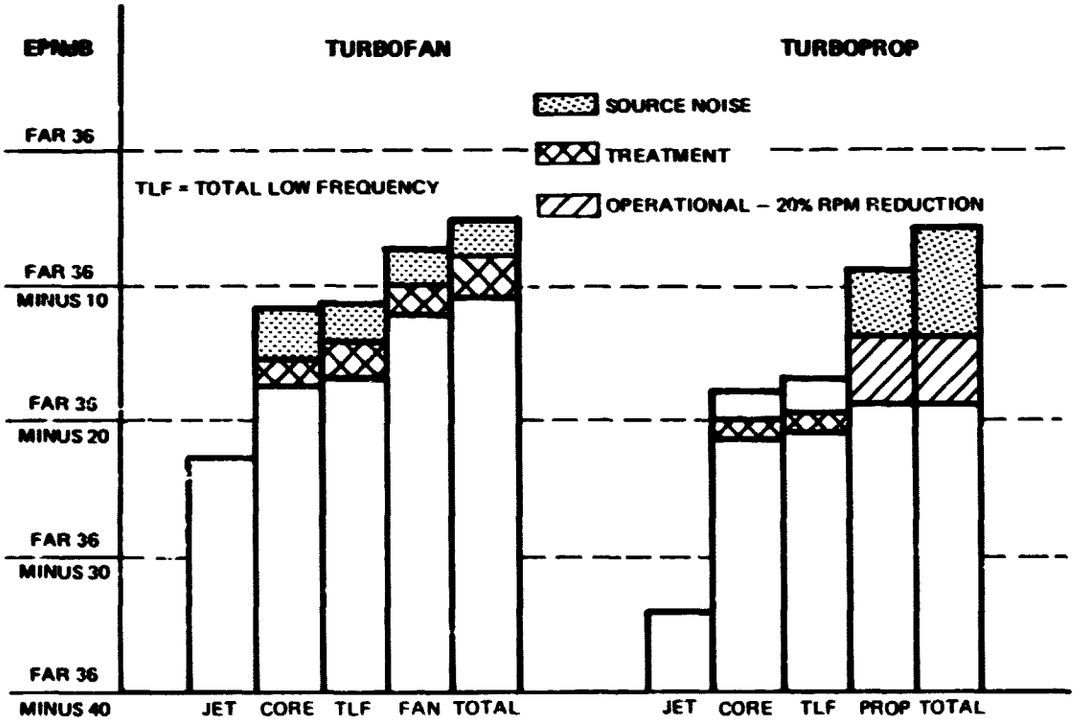

Figure 4.4.5.1-2 *Advanced Technology Propulsion System Approach Noise Levels on the International Quadjet Aircraft*

concepts, while required to meet the FAR 36 minus 10 EPNdB noise level for the turbofan engines, may not be required on the turboprop engines. The lower noise level from the turboprop gas generator is attributable to the smaller size gas generator for the very high bypass ratio turboprops and at the take-off noise measuring station the much higher airplane altitude. During approach, in addition to the size effect, there is a reduced combustor exit temperature requirement relative to the turbofan engines.

Near field or interior cabin noise levels were estimated for the turboprop-powered airplane by Hamilton Standard. The projected cabin noise level for the advanced technology propeller is shown in Figure 4.4.5.1-3 as a function of the ratio of attenuation material added to the fuselage. To obtain cabin noise levels comparable to the typical turbofan-powered aircraft indicated in Figure 4.4 5.1-3, a turboprop airplane with current technology propellers would require a much larger ratio of attenuating material weight to fuselage weight.

4.4.5.2 Emissions Benefits

Emissions estimates were made for the selected cycle of the advanced technolcgy turboprop and the turbofan. These estimates were based on the current on-going emissions reduction programs for the JT8D and JT9D engines in addition to the NASA Experimental Clean Combustor Program (ECCP). The selected burner concept consisted of a swirl burner called a vortex burning and mixing (Vorbix) burner based on the ECCP design in combination with a modified pilot to improve low power emissions. This selection was based on the observed low emission levels of the Vorbix burner at intermediate and high engine power settings and the low carbon monoxide (CO) and total hydrocarbons (THC) emission characteristics of the aerating nozzles at low power settings.

The calculated emission levels of the turboprop are compared to the turbofan levels and proposed EPA standards in Figure 4.4.5.2-1. The emissions levels for the turboprop are lower than the turbofan because of its lower TSFC level. The high pressure ratio of the fuel conservative turboprop and turbofan aggravates the oxides of nitrogen (NO_x) generation at high power levels so that, even with emission advances, it is estimated that the EPA standards will be exceeded. Further advances in emissions technology is therefore required to meet the needs of the fuel conservative engines.

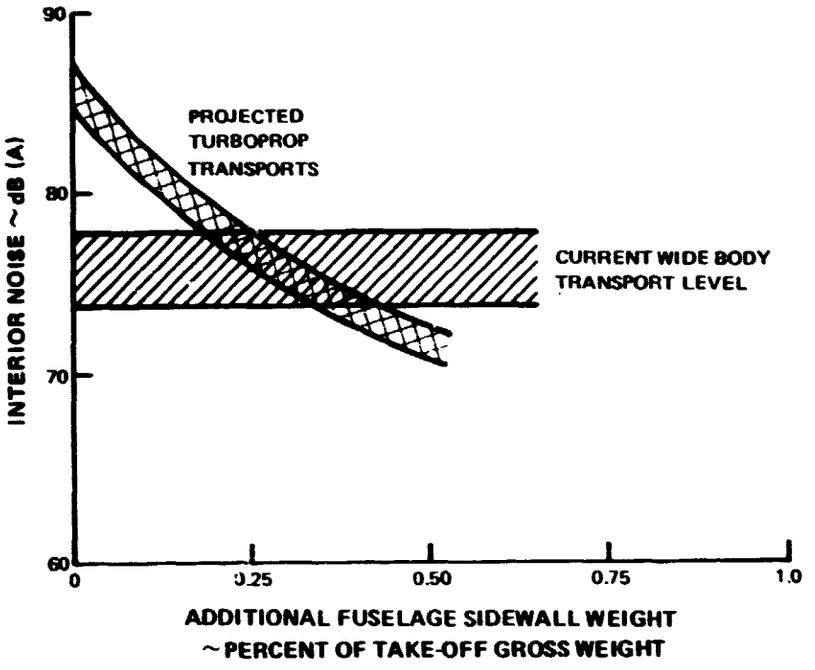

Figure 4.4.5.1-3 *Interior Cabin Noise Levels for Advanced Technology Propulsion Systems As a Function of Attenuating Material Weight Increase*

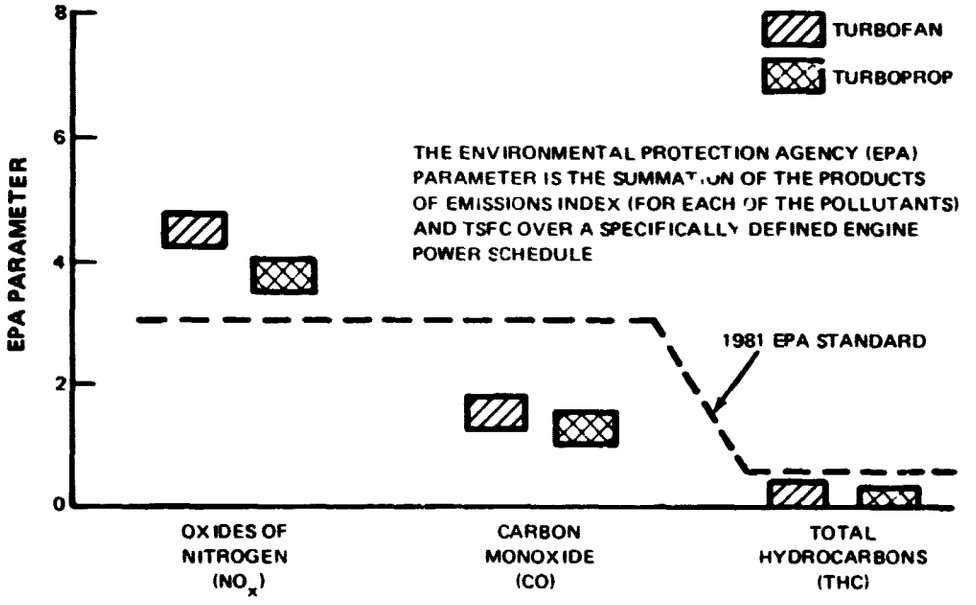

Figure 4.4.5.2-1 *Comparison of Calculated Exhaust Emission Levels for the Advanced Technology Turbofan and Turboprop*

4.5 RECOMMENDED TECHNOLOGY PROGRAMS

This section describes the technology programs that are recommended to achieve the potential fuel savings for the engines described in Section 4.4. The programs divide between the primary cycle subsystem (gas generator) and the propulsor subsystem with potential fuel savings as presented in Table 4.5-I. Benefits are based on the full achievement of the goal propeller efficiency. An additional small gain in fuel savings is projected through the use of advanced materials.

TABLE 4.5-I

1985 TURBOPROP TECHNOLOGY REQUIREMENTS AND POTENTIAL BENEFITS

	Fuel Savings Relative to 1975 Technology Turbofan
• Advanced Primary Cycle Subsystem (Gas Generator)	10% to 14%
■ High Temperature Combustor and Turbine Airfoil Materials and Coatings	
■ Efficient, High-Speed High Spool System	
■ Improved Passive and Active Clearance Control Seals	
• Advanced Propulsor Subsystem	18% to 20%
■ Moderate Load Factor Power Turbine	
■ High Efficiency, Composite Propeller	
■ Efficient, Lightweight Gear	
• High Strength-to-Density Ratio Engine Materials	0 to 1%
■ Titanium Base Alloys	
■ Nickel Alloy Disk	

4.5.1 Gas Generator Programs

The gas generator technology requirements of the turboshaft engine are the same as those for the advanced turbofan gas generator (ref. 1). A detailed description of the recommended programs for developing the gas generator and high strength-to-weight materials was presented in ref. 1. The following sections contain a brief description of those programs.

4.5.1.1 High Temperature Combustor and Turbine Airfoil Materials and Coatings

The projected fuel savings for future turbine engines reflect an increase in combustor liner and turbine blade metal temperatures of 83°C to 111°C (150°F to 200°F). An advanced high temperature combustor liner material and a monocrystal (or directionally solidified eutectic) turbine blade alloy show promise for such high temperature applications. Oxidation and erosion resistant and/or insulative coatings will also be needed for the turbine blades, vane platforms, and outer air seals. Developing this technology would require intensive metallurgical investigations and rig test efforts. Investigations would also be necessary to address the areas of fabrication and repair of high temperature materials and coatings.

4.5.1.2 Efficient, High-Speed High-Pressure Spool System

The combination of technological advances in the aerodynamics of the compressor, combustor, and high-pressure turbine has shown significant potential for reducing fuel consumption in future aircraft engines. Research and technology programs are required in each of these areas if the potential improvements are to be realized. An advanced high-pressure spool system would also serve as a vehicle for demonstrating new materials, advanced cooling techniques, active clearance control, and high-speed bearings and seals.

Additional analytical and test programs are recommended to reduce airfoil and endwall aerodynamic losses for maximum compressor efficiency. This effort would include testing the compressor both as an individual component and as part of a high-pressure spool system.

The recommended program for developing an advanced combustor would concentrate on reduced emissions, in conjunction with high temperature and high pressure operation. A selected low-emissions combustor concept would be evaluated in a rig and also as part of the high-pressure spool. A portion of this program would also address optimizing a diffuser aerodynamic design for integration into the high-pressure spool.

The desire for higher turbine efficiency with increased rotational speed and reduced load factor increases operating stress levels and other aerodynamic losses. Thus, the suggested turbine development program would focus on resolving these limitations, while improving performance efficiency. Component performance verification would be required by operating the turbine in a high-pressure spool engine simulating both gaspath and non-gaspath engine temperatures and pressure conditions.

High rotational speeds, coupled with increased pressure levels of the gas generator, require significant advances in the engine main bearings and bearing compartment seals. The technology programs recommended for these components would develop new design concepts to achieve a high speed level, while emphasizing durability.

4.5.1.3 Improved Passive and Active Clearance Control Seals

A program is recommended to develop the technology and systems to actively and passively modulate turbine and compressor blade tip clearances throughout the flight envelope. This effort would encompass assessing mechanical, pneumatic, and thermal-responsive schemes for reducing tip clearances to near zero at the cruise operating point.

4.5.1.4 High Strength-to-Density Ratio Materials

Utilization of high strength-to-density ratio materials in future aircraft engines lies in the fuel savings resulting from the reduction in propulsor system weight. Because high-temperature titanium alloys represent a lightweight alternative to steel and nickel base alloys, a program would be planned to test the component fabricated with this material both on an individual basis and incorporated into an engine. Similarly, the use of advanced nickel alloy high-pressure turbine disks offers an appreciable weight savings. The materials development program for this alloy would concentrate on determining the feasibility of various approaches to meet the strength requirements for advanced turbine disks.

4.5.2 Advanced Propulsor Subsystem

The advanced propulsor system is tied to the capabilities of the drive turbine and the advanced propeller/gearbox system. No unique technology program is required for the power turbine, because the reduction gear permits operating the turbine at higher speeds and reduced load factor levels conducive to high efficiency. Technology programs for the propeller/gearbox system must address objectives of reduced noise and cabin vibration, increased reliability, lower weight and improved efficiency. These programs are discussed in the following sections.

4.5.2.1 Moderate Load Factor Turbine

A major portion of the potential improvement in the power turbine is contingent upon aerodynamic advances. The use of a speed reduction gear permits high rotational speeds and reduced load factor in the turbine for increased efficiency. Since the load factor and, therefore, the aerodynamics of any power turbine that drives a reduction gear would be about midway between a high load factor, direct-drive low-pressure turbine and a low load factor, high-pressure turbine, no unique technology program is required. The power turbine would benefit from the recommended technology programs already outlined in Section 4.5.1.

4.5.2.2 Advanced Propeller/Gearbox System

A multitiered technology program is required for the advanced propeller/gearbox system before it can be introduced into commercial service. The technology plan presented in Figure 4.5.2.2-1 presents a comprehensive program culminating in flight tests of an advanced technology turboprop within ten years from the start of the program. The engine testing would combine an available (possibly modified) current technology turboshaft engine and an advanced propeller/gearbox system during the latter stages of the engine program.

The main objective of the plan provides for acquiring basic information to prove the concept of the propeller/gearbox system in order to give a high degree of confidence to successful completion of an engine test program. In order to begin the initial engine test program at the end of the fifth contract year into the program, specific tasks in four propeller technology areas must be accomplished:

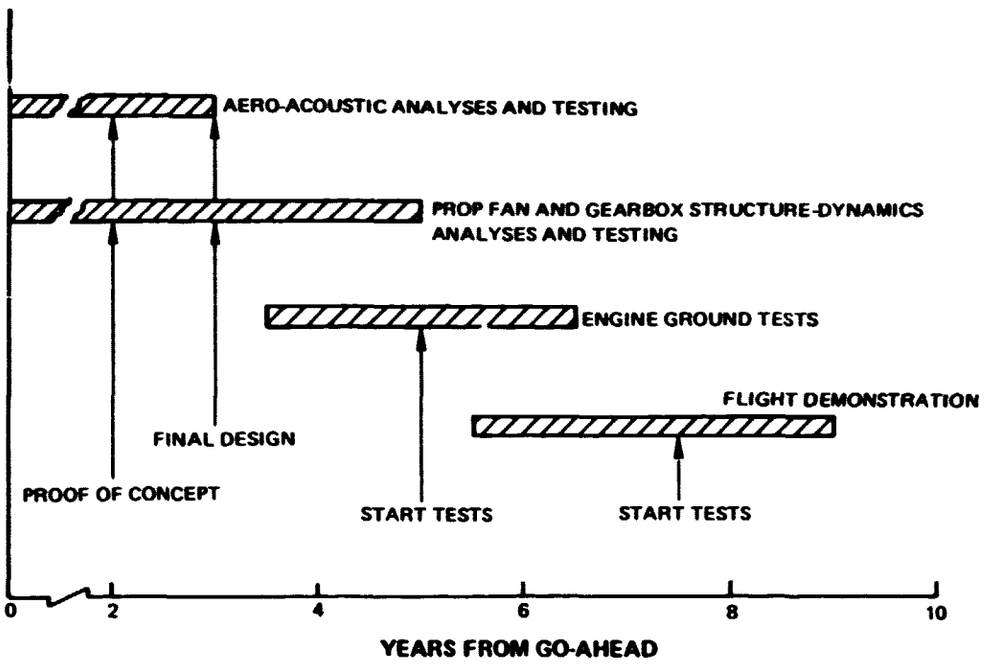

Figure 4.5.2.2-1 Recommended Turboprop Propulsion System Technology Program

- Aerodynamics and Acoustics
- Structures and Dynamics
- Mechanical Design
- Component Technology

Two general elements make up the initial years of the propeller/gearbox program: 1) a proof of concept program and 2) an experimental aerodynamic and acoustic program. Applicable data and methodology which now exist in the literature and at Hamilton Standard are being utilized as the basis for effort currently in process to develop the methodology for the aerodynamic and the acoustic design of the system. The planned effort will utilize the results from the recommended experimental program to refine this methodology. In considering the Aerodynamic and Acoustic Technology Program it should be noted that the experimental programs have been overlapped to establish the technology base for a full scale engine demonstration test program scheduled to start at the end of the fifth contract year.

To evaluate performance of the advanced state-of-the-art propeller airfoils, technology programs are required to determine the effects of varying sweep, Reynolds number, cascade, and Mach number. A prop-fan rig would be used to evaluate the effects of the number of airfoils, blade root solidity, tip sweep, airfoil thickness distribution, reverse thrust performance, and the interacting effect of the prop-fan aftbody.

Additional technology programs are recommended to determine nacelle, spinner, and inlet shape effects on the prop-fan flow field, pressure recovery, body drag, and body critical Mach number. The technology programs would also include the interacting effects of nacelle and wing at different wing locations and wing shapes, thicknesses, and sweeps.

Technology programs are recommended to establish the near and far field, high and low speed noise characteristics required for designing advanced propellers to meet the probable stringent FAR noise regulations. In addition, the influence of the wing on noise produced would be defined.

A research program is required to design, fabricate, and test gearing that will step down the speed of the power turbine to match the speed requirements of the propeller. The general design criteria include high-ratio, high-torque, high-power gear which is suitable for use on a commercial aircraft. The design objective is to provide a gearing concept which will meet the requirements of safety, weight, and maintainability for a turboprop.

4.5.3 Other Technology Programs

Low fuel consumption over the entire flight cycle and over the life of the engine will require advances in control and reductions in both short term and long term engine performance deterioration. Stringent noise requirements are likely, and methods of achieving noise levels well below FAR 36 will be necessary without incurring a significant fuel consumption penalty. The economic results of this study suggest that effort must be undertaken on specific

means to make fuel-conservative engines more economically attractive to purchase and maintain. Programs for these technologies are summarized in this section.

4.5.3.1 Advanced Acoustical Technology

The compliance with stringent noise requirements such as FAR 36 minus 10 EPNdB, will require advances in propeller, combustor, and turbine noise technology. For the combustor, the recommended program is directed toward developing analytical models of noise sources, as well as testing combustors consistent with the requirements of low emissions. Since the noise characteristics of the turbine are not well defined, a noise prediction system would be developed under the defined program. In addition, cascade tests would be recommended to define wake characteristics of high-to-moderate stage loading blades.

In addition to noise source reductions, improved attenuation of core and turbine source noise is required. A recommended program is directed toward increasing attenuation levels in each of these areas by at least 2 EPNdB without increasing the treated area.

4.5.3.2 Full Authority, Electronic Digital Control

A digital electronic propulsion control presents possibilities for significant fuel savings when coupled with aircraft control systems. Although Pratt & Whitney Aircraft is conducting extensive research and development in the area of digital electronic controls, an additional study program is recommended. The scope of the effort would include the definition and evaluation of the benefits of an integrated aircraft/engine control system using digital electronic engine controls and digital aircraft controls. This integrated control system, as a minimum, would consider TSFC, noise, and dynamic response characteristics, provide satisfactory safety characteristics for any system malfunction, and incorporate diagnostic capabilities to reduce maintenance effort. This study program would be expanded to include demonstration testing in a suitably modified aircraft.

4.5.3.3 Reduced Maintenance Costs

The impact of designs to improve specific fuel consumption have a tendency to increase engine price and maintenance cost, thereby reducing the potential cost benefits of low TSFC. The area of maintenance costs requires equal effort and can produce substantial impact. A study program directed at determining the causes for engine part scrappage and necessity for repair would provide the definitive design guidance needed to reduce the projected increases in engine maintenance cost. Such a study would also suggest technology programs which would explore and identify means of achieving higher parts durability and life and thus improve the operating costs of low-TSFC engines.

SECTION 5.0 CONCLUSIONS AND RECOMMENDATIONS

This report summarizes the results of the study of Unconventional Aircraft Engine Designed for Low Energy Consumption. A survey and analysis of possible alternates to the conventional turbofan was conducted with the object of assessing further fuel consumption reduction for subsonic transports of the 1990's. This section presents the conclusions and recommendations that were drawn from the results of this study program.

- Projected advances in gas turbine component technology can produce a 10 to 15 percent energy savings potential relative to present turbofan technology without resorting to complex cycle features such as heat exchangers or intermittent combustion processes. The benefits of these technological advancements apply equally to turbofan or turboprop propulsion systems.

- The advanced turboprop system presently shows the greatest potential for fuel conservation. This potential is tied to the capabilities of an advanced propeller at contemporary flight speeds. Aerodynamic, acoustic, and structural verification are critical to the further pursuance of the advanced propeller system.

- Numerous assumptions were made in the turboprop system integration evaluation which require additional substantiation. Propulsion system integration studies by airplane manufacturers are recommended together with a propeller technology development program to establish a firm technical base on which to further assess the concept. The technology program should include the propeller/nacelle/wing aerodynamic interference testing necessary to establish the installed characteristics up to Mach 0.8.

- An orderly experimental program which ultimately leads to turboprop flight demonstration is recommended in order to verify the performance, reliability, and passenger comfort aspects to enhance potential customer acceptance.

APPENDIX A

AIRCRAFT CHARACTERISTICS AND CALCULATIONS USED IN ADVANCED TECHNOLOGY TURBOFAN AND UNCONVENTIONAL ENGINE EVALUATION

This appendix presents the airplane aerodynamics, weight, and pricing calculations, including the engine nacelle, used to evaluate the advanced technology turbofan and unconventional engines.

Aircraft Aerodynamics for New Engine Evaluation

Profile drag predictions were made by the component buildup method, in which the drag coefficient C_D is:

$$C_D = C_{DP\,min} + \Delta C_{DP} + C_{DI} + \Delta C_{DWD}$$

where $C_{DP\,min}$ is the minimum profile drag coefficient, ΔC_{DP} is the incremental variation of profile drag coefficient due to lift, C_{DI} is the ideal induced drag coefficient, and ΔC_{DWD} is the subsonic wave drag coefficient. The ideal induced drag coefficient was computed by the standard formula for an elliptically loaded wing, $C_{DI} = C_L{}^2/\pi\overline{AR}$, where C_L is the lift coefficient and $\overline{AR}$ is the wing aspect ratio. Figure A-1 illustrates schematically this drag buildup procedure. Drag coefficients are referenced to wing planform area.

Skin-friction drag coefficients, based on the Prandtl-Schlichting equation for turbulent boundary layer over a flat plate, were computed for the wing, tail, and fuselage. These coefficients were modified by the effects of wing and tail thickness ratios (thickness to chord, t/c), fineness ratio, and compressibility effects to estimate $C_{DP\,min}$. A typical profile drag variation with flight speed is shown in Figure A-2. The additional variation in profile drag (ΔC_{DP}) with changes in the lift coefficient is based on correlations with wing sweep, thickness, and camber. The subsonic wave drag coefficient C_{DWD} is a function of the flight Mach number relative to the critical Mach number and lift coefficient. The high speed drag characteristics are shown quantitatively in Figure A-3.

Trends of critical Mach number assumed with quarter chord wing sweep angle ($\Lambda_{C/4}$) and thickness ratio of the supercritical airfoils are shown in Figure A-4. The level of supercritical technology used was consistent with that used for the Advanced Technology Transport (ATT) studies under NASA contract NAS3-15550. The drag rise characteristics assumed for these wings are shown in Figure A-5 as a function of lift coefficient and Mach number relative to critical Mach number.

Wing geometry trends are depicted in Figures A-6, A-7, and A-8. Wing designs were selected on the basis of minimizing fuel consumption. Results of Pratt & Whitney Aircraft studies have indicated that for minimization of typical mission fuel, cruise Mach number should be 0.06 to 0.04 below the wing critical Mach number. Therefore, for any cruise Mach number, a quarter-chord wing sweep and thickness ratio combination could be determined (with use of Figure A-4) based on this criterion.

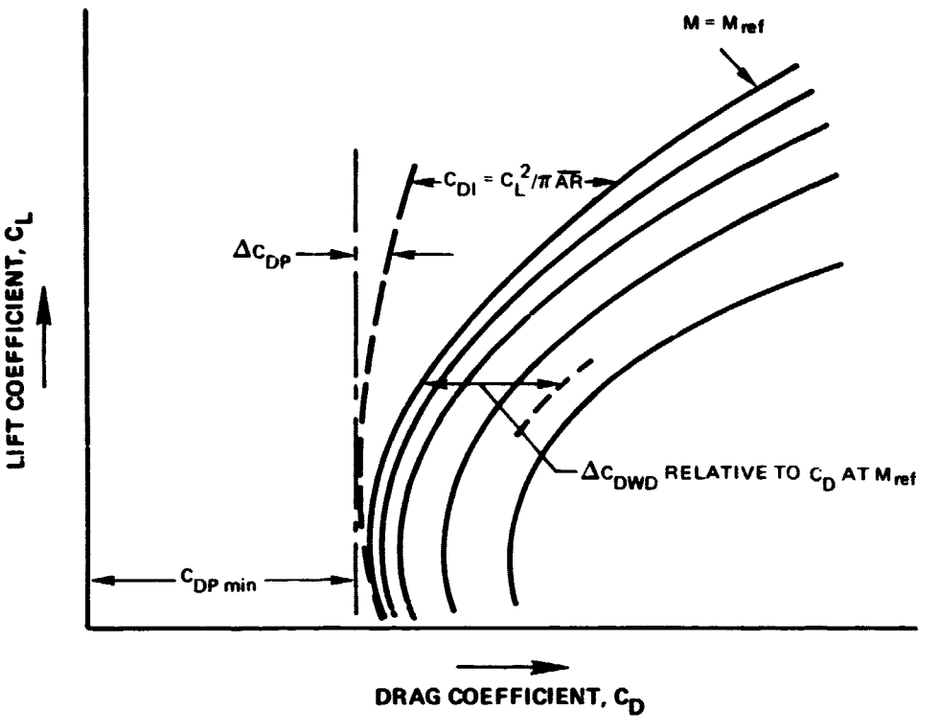

Figure A-1 Drag Polar Construction Procedure

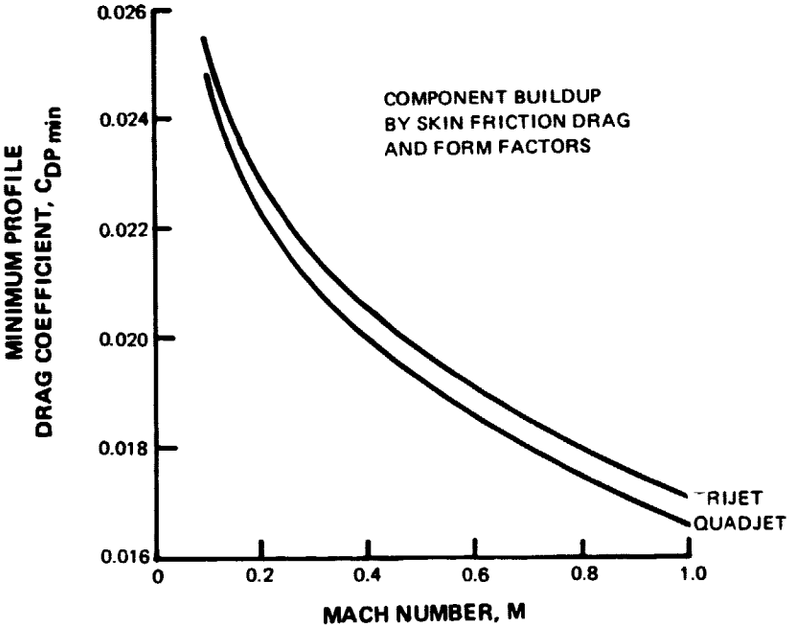

Figure A-2 Typical Minimum Profile Drag Coefficient for Altitude of 9,144 m (30,000 ft)

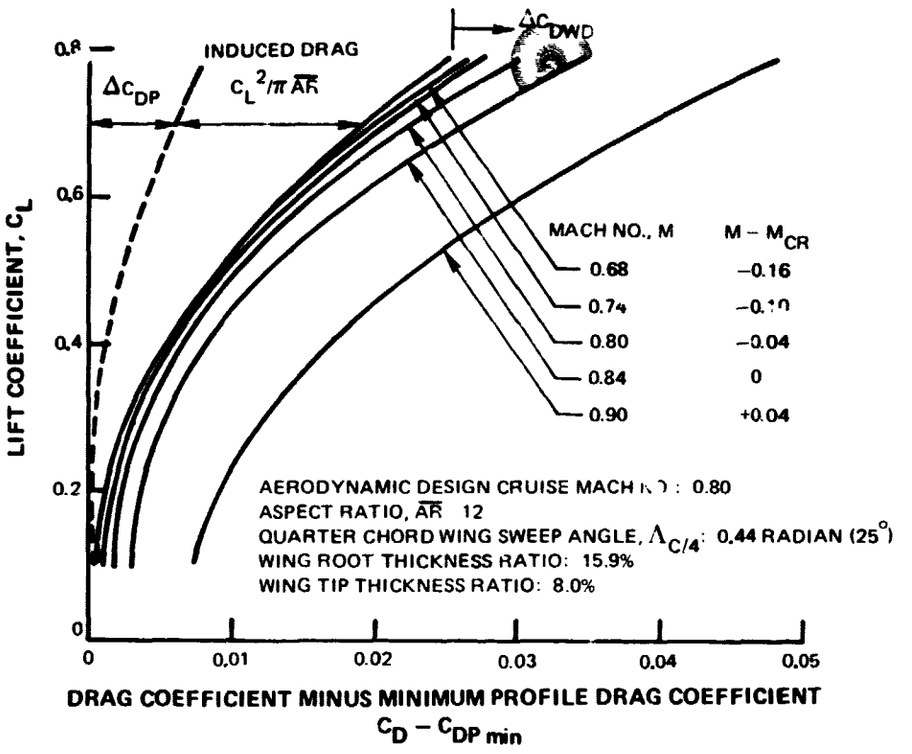

Figure A-3 High Speed Drag Characteristics

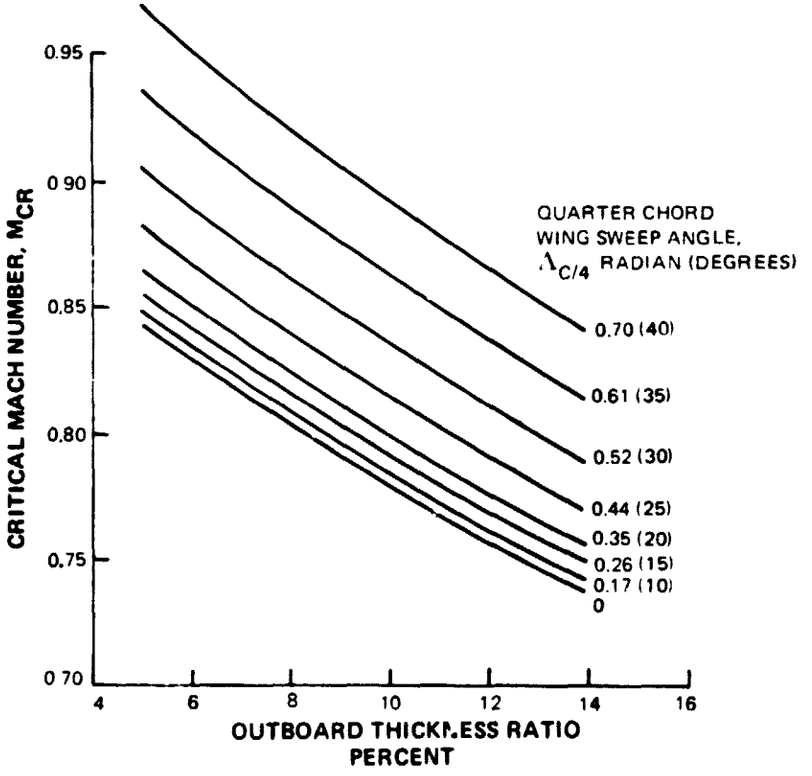

Figure A-4 Supercritical Airfoil Technology, Lift Coefficient C_L = 0.40

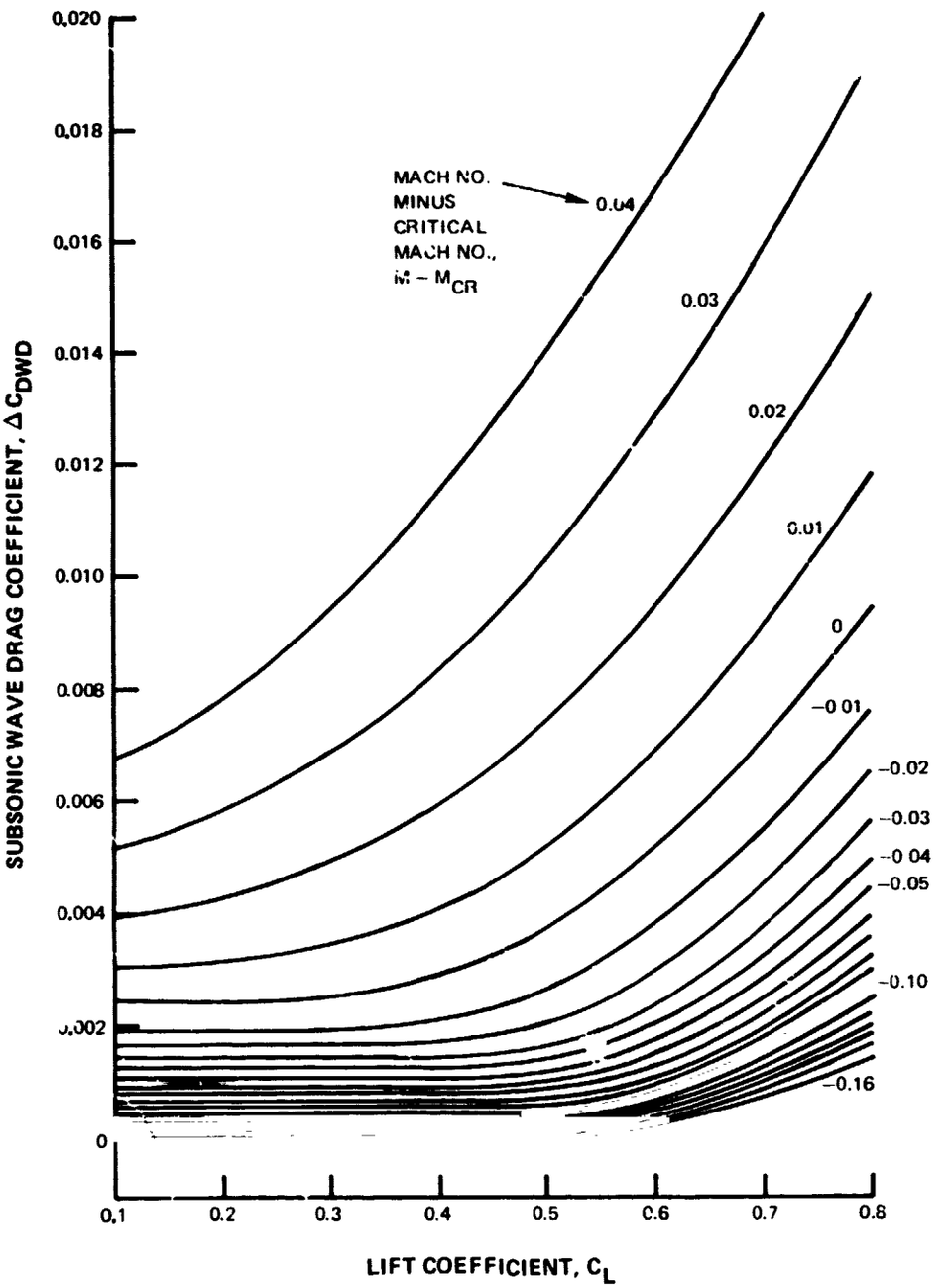

Figure A-5 Drag Rise Characteristics of Wings

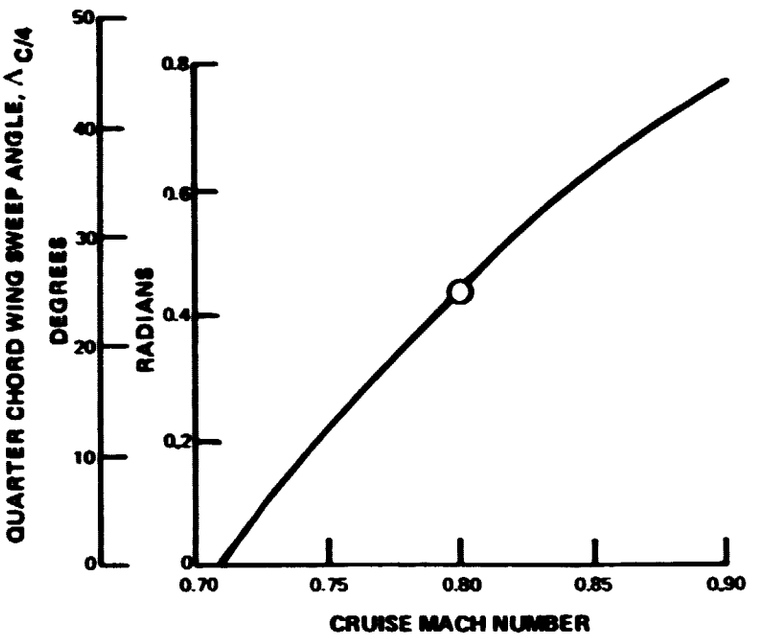

Figure A-6 Wing Quarter Chord Sweep Trends

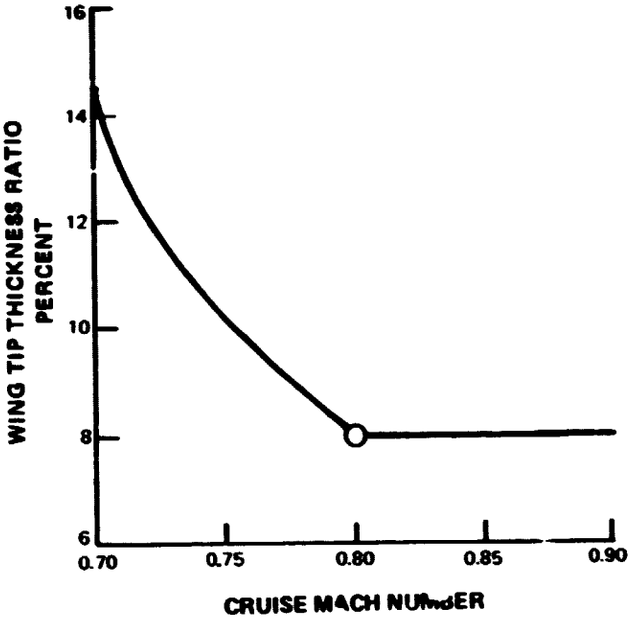

Figure A-7 Wing Thickness Ratio Trends

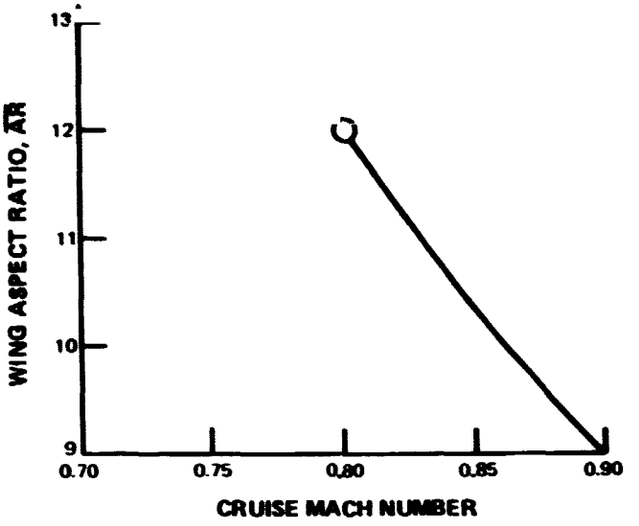

Figure A-8 Wing Aspect Ratio Trends

Wing aspect ratio and weight were based on an equation which related these variables with the wing parameters of sweep and thickness ratio as follows:

$$\text{Wing Weight} = K_1 \left(\frac{\overline{AR}^{0.8}}{(t/c)^{0.4} \cos \Lambda_{C/4}} \right)^{K_2}$$

The term in parentheses is called the wing weight parameter, and K_1 and K_2 are empirical constants. The fact that this parameter is approximately the same for all current aircraft led to the method for determining aspect ratio of advanced aircraft. A wing weight parameter of 2.9, reflecting the high aspect ratio wing, was used to determine aspect ratio up to a limiting value of 13.0 for the study aircraft (ref. 10).

Available industry information indicated a practical lower limit to wing outboard thickness ratio of 8 percent. This lower limit was assumed at Mach numbers of 0.8 and higher. Wing loadings were selected for the study aircraft to minimize fuel consumption within take-off distance and approach speed limits. The wing geometry, specified in Table A-I, was selected based o these analyses.

Aircraft Weights for New Engine Evaluation

A component buildup method was used to estimate aircraft weight. Correlations of aircraft component weights, as related to component geometric and physical characteristics, were used for predicting the weight of all of the aircraft structural items and systems (electronic, aircraft, and fuel).

TABLE A-I

MACH 0.8 AIRCRAFT CHARACTERISTICS

Wing Characteristics

Take-off Wing Loading, 3-Engine Aircraft, N/m^2 (lbf/ft^2)	5583 (116.6)
Take-off Wing Loading, 4-Engine Aircraft, N/m^2 (lbf/ft^2)	6607 (138)
Quarter Chord Sweep, radian (degrees)	0.44 (25)
Aspect Ratio	12
Taper Ratio	0.33
Root Thickness Ratio, %	15.9
Tip Thickness Ratio, %	8

Horizontal Tail Characteristics

Quarter Chord Sweep, radian (degrees)	0.52 (30)
Aspect Ratio	4.03
Taper Ratio	0.35
Average Thickness Ratio, %	9.5
Ratio of Horizontal Tail Area to Wing Area, 3-Engine Aircraft	0.175
Ratio of Horizontal Tail Area to Wing Area, 4-Engine Aircraft	0.246

Vertical Tail Characteristics

Quarter Chord Sweep, radian (degrees)	0.52 (30)
Aspect Ratio	1.0
Taper Ratio, 3-Engine Aircraft	0.7
Taper Ratio, 4-Engine Aircraft	0.35
Average Thickness Ratio, %	10.5
Ratio of Vertical Tail Area to Wing Area, 3-Engine Aircraft	0.183
Ratio of Vertical Tail Area to Wing Area, 4-Engine Aircraft	0.186

Nominal Fuselage Characteristics

Length, 3-Engine Aircraft, m (ft)	48.2 (158)
Length, 4-Engine Aircraft, m (ft)	45.7 (150)
Height, m (ft)	5.24 (17.2)
Width, m (ft)	5.03 (16.5)
Number of Aisles	2
Seat Pitch, First Class, m (in.)	0.97 (38)
Seat Pitch, Tourist, m (in.)	0.86 (34)
Number of Passengers, First Class	30
Number of Passengers, Tourist	170

The equations used for structural weight estimates are based on regressions of current, aluminum structure aircraft data. These equations were adjusted to predict composite structure weights. Table A-II shows the precentage reduction in weight of the airframe structural components assumed by composite substitution (ref. 11, 12).

TABLE A-II

DIRECT SUBSTITUTION OF COMPOSITE STRUCTURAL COMPONENTS FOR ALUMINUM STRUCTURE

Component	Weight Reduction–percent
Fuselage	15.5
Tail	12.7
Wing	24.6

Weights of furnishings and equipment, and operating items are primarily functions of the number of passengers, the number of crew personnel, cargo volume, fuel capacity, and range.

Nacelle Geometries and Engine Installations for New Engine Evaluation

Sketches of the engine installations are shown in Figure A-9. Factors describing the nacelle geometries are listed in Table A-III along with installation assumptions.

The turboprop installations are based on Hamilton Standard guidelines for prop-fan installations (ref. 13). Another criterion specified by Hamilton Standard, and adhered to in the study airplanes, was a minimum propeller tip-to-ground clearance of 6 feet. An under-the-wing engine location was chosen for both prop-fan engines. This mounting configuration provides, relative to an over-the-wing arrangement, better engine and gearbox accessibility, easier engine-gearbox-propeller removal, and, with an offset gearbox, a less tortuous engine inlet gaspath shape. Also, the offset gearbox presents fewer design problems for the propeller pitch control mechanism.

The gas generator is located such that the low pressure turbine or free turbine has an aft placement limit at the wing quarter chord. This location reduces the possibility of wing structural damage or fuel tank rupture due to turbine blade/disk discharge.

The STF 477 nacelle design incorporated features developed in an ongoing P&WA nacelle study. Two features of this nacelle, relative to those of current, modern nacelles, are an extended afterbody length and increased fan cowl boattail angle. These features provide sufficient closure to meet the primary stream exit area requirements without resorting to an external plug. The STF 477 inlet design was based on considerations of low drag and low noise. The inlet contours provide a good compromise between the opposing requirements of low spillage drag and low inlet weight/surface area. Inlet length was established to allow adequate noise suppression treatment to meet a total noise requirement of FAR 36 minus 10 EPNdB.

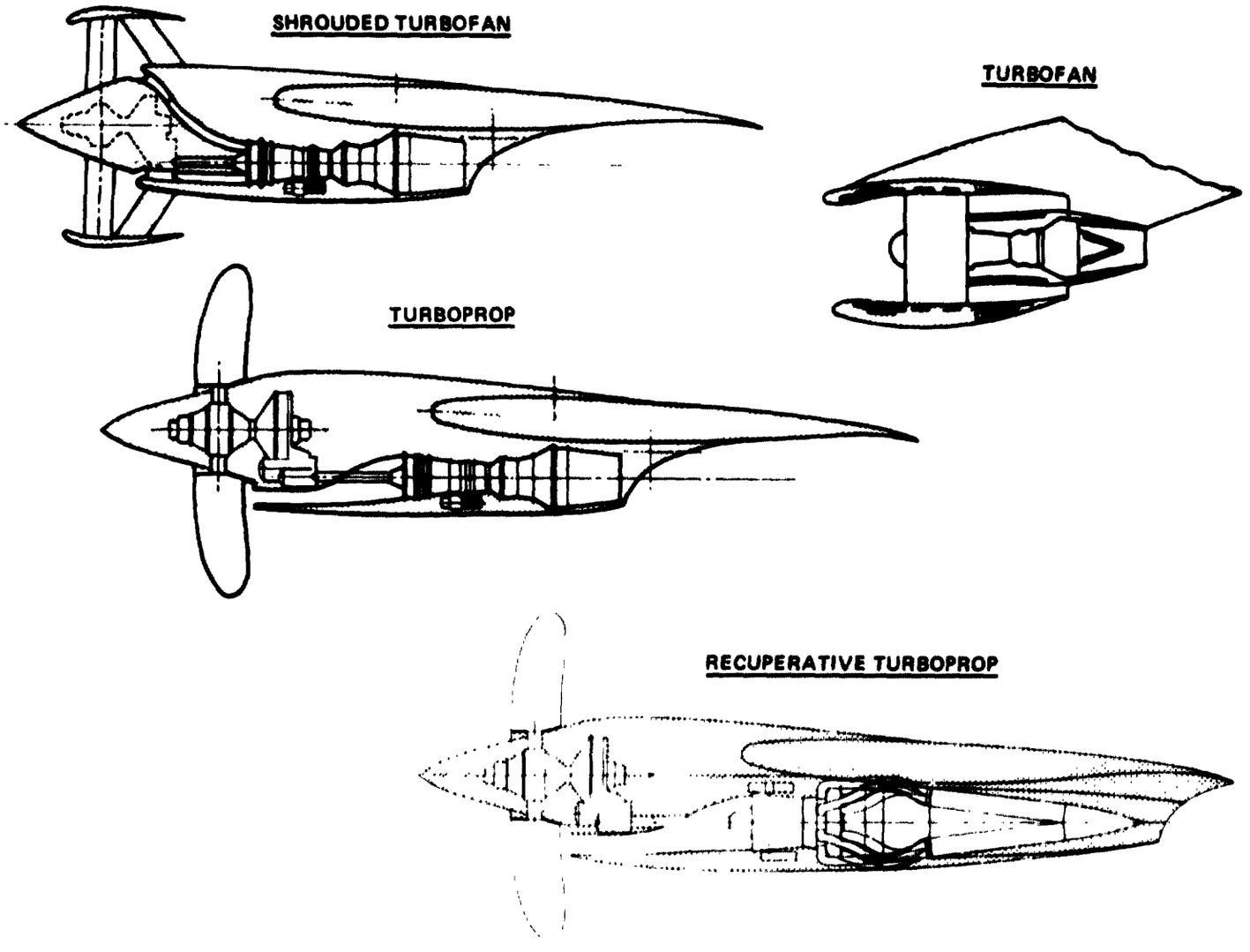

Figure A-9 Sketches of Unconventional Engine Installations and an Advanced Turbofan Nacelle

TABLE A-III

NACELLE GEOMETRY AND ENGINE INSTALLATION

	Turboprop	Regenerative Turboprop	Variable Pitch Shrouded Fan	Conventional Turbofan
Ratio of Fan Cowl Length to Maximum Nacelle Diameter	— —	— —	0.492	1.86
Ratio of Highlight Diameter to Maximum Nacelle Diameter	— —	— —	0.90	0.84
Ratio of Inlet Length to Maximum Nacelle Diameter	— —	— —	0.123	0.55
Ratio of Highlight Area to Throat Area	— —	— —	1.05	1.25
Ratio of Throat Area to Fan Face Area	— —	— —	0.92	0.94
Engine Corrected Airflow/Fan Face Area, Design Cruise, kg/sec/m^2 (lbm/sec/ft^2)	— —	— —	203 (41.5)	203 (41.5)
Fan Face Mach Number, Design Cruise	— —	— —	0.6	0.6
Throat Mach Number, Design Cruise	—	— —	0.70	0.67
Fan Maximum Boattail Angle, radian (degrees)	— —	— —	0.14 (8)	0.201 (11.5)
Engine Primary Corrected Airflow/Compressor Face Area, Design Cruise, kg/sec/m^2 (lbm/sec/ft^2)	181 (37)	181 (37)	181 (37)	181 (37)
Compressor Face Mach Number, Design Cruise	0.5	0.5	0.6	0.6
Afterbody Boattail Angle, radian (degrees)	— —	—	— —	0.454 (25)
Ratio of Maximum Nacelle Diameter to Propeller Diameter	0.35	0.35	— —	— —
Ratio of Distance Between Propeller Plane and Wing Quarter Chord to Propeller Diameter	1.00	1.00	— —	— —
Propeller Tip Side-of-Body Clearance, percent of propeller diameter	80	80	— —	— —
Propeller Tip Separation, percent of propeller diameter	33	33	— —	— —
Engine Spanwise Location, percent of wing semispan:				
International Aircraft, Inboard Engines	31	31	31	34
International Aircraft, Outboard Engines	52	52	52	60
Domestic Aircraft, Inboard Engines	30	30	36	28
Domestic Aircraft, Outboard Engines	50	50	50	— —

Installation Weight

For the advanced technology turbofan, nacelle weight estimates were based on correlations of data of current aircraft and engines. Cowl (inlet, fan, boattail, side, and afterbody) weights were estimated by multiplying a correlated area density (kg/m^2, lbm/ft^2) of the cowl component by its associated surface area. The weights were reduced by 10 percent for composites. Thrust reverser weights were made proportional to fan stream airflow. Engine accessories weights were made proportional to the primary stream airflow. Engine mount weights were assumed to be proportional to the bare engine weight. Wall treatment weights for noise reduction were a function of the treated areas. Pylon weights were correlated against thrust, nacelle diameter, and the distance between the engine and the wing.

Installed weight penalties for the prop-fan configurations were based on information received from Hamilton Standard and correlations of data from existing turboprop-powered aircraft such as the Lockheed Electra and Canadair CL-44. Also, design data on early 1950's proposed turboprop-powered aircraft, such as the DC-6B and Douglas 1224-A, were used to estimate installation weights.

Completely installed prop-fan engine weight was assumed to be 130 percent of the uninstalled prop-fan weight. The 30 percent weight penalty, assumed to account for the nacelle structure and all associated engine system requirements, was provided by Hamilton Standard.

A review of data compiled on the existing and early 1950's proposed turboprops indicated that the installed weight of a turboprop propulsion system could be defined as follows:

- Installed weight is the sum of the uninstalled turboprop weight and the installation weight.

- Uninstalled turboprop weight is the sum of the bare engine weight, propeller weight (propeller blades, spinner, and pitch change system), and gearbox weight.

- Installation weight is the sum of the weights of the nacelle (cowling and fairings, structure, inlet) and the starting, exhaust, gearbox cooling, fire control, hydraulic, and electrical systems.

The nacelle weights were found to be strongly dependent on nacelle wetted area and maximum diameter, D_{max}. The formulation,

- Nacelle weight is the product of nacelle area density ρ_A and nacelle wetted area,

was found to represent the historical nacelle weight trends of turboprop-powered aircraft. The area density ρ_A appeared to be a function of the maximum nacelle diameter (Figure A-10). Available data on the associated engine systems showed that these weights were approximately 40 percent of the bare engine or gas generator weight.

Application of the above formulation for nacelle weight and the associated engine systems weight percentage to the STS 487 prop-fan configuration resulted in an installation weight equal to 30 percent of the sum of the bare engine, gearbox, and propeller weights.

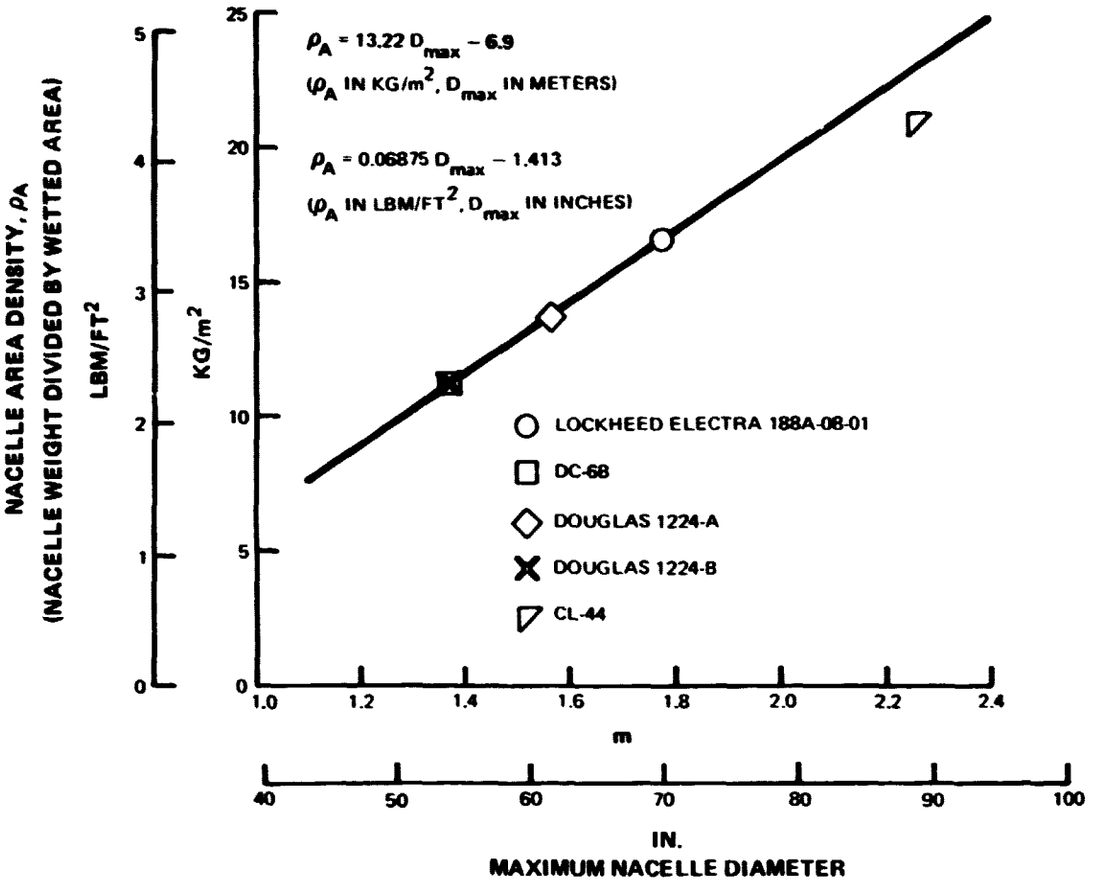

Figure A-10 Turboprop Nacelle Weight Trends

The installation weight for the STS 488 regenerative turboprop was estimated by multiplying an effective weight per unit area by the nacelle wetted area. This effective weight per unit area was determined as the quotient of the installation weight of the STS 487 turboprop and its wetted area and was equal to 34.2 kg/m^2 (7 lbm/ft^2). The resulting installation weight of the regenerative turboprop was 27 percent of the uninstalled (bare engine, propeller, gearbox, recuperator) STS 488 weight.

The installation weight for the variable pitch shrouded fan was estimated by using methods applicable to conventional turbofans for the fan cowl and by using the previously described turboprop installation weight methods for the nacelle and associated engine systems weight.

The resulting fan cowl weight was 9 percent of the uninstalled engine (bare engine, gearbox, and propeller) weight, and the nacelle and associated engine systems weight was 21 percent of the uninstalled engine weight.

Pod Drag for New Engine Evaluation

The total pod drag for the STF 477 turbofan was the sum of the isolated fan cowl drag, pylon drag, wing-nacelle interference drag, and scrubbed afterbody cowl and pylon drags. Isolated cowl drag accounted for the profile plus spillage drag of the fan cowl (inlet, fan case covering, and fan cowl boattail).

The external drag of the afterbody and scrubbed portion of the pylon was based on estimates of the profile drag penalties of these components when washed by the fan exhaust stream. These drag penalties were accounted for in the nozzle performance data that were used in the engine performance matching decks.

Pylon drag was estimated by the component buildup method for wing profile drag (described at the beginning of this appendix). Interference drag was computed as a function of the fan exit diameter and the distance between the wing and the engine.

At the Mach 0.8, 9.144 km (30,000 ft), maximum cruise rated power condition, about 38 percent of the total pod drag was fan cowl drag. Pylon drag accounted for approximately 29 percent, interference about 19 percent, and the scrubbed afterbody and pylon surfaces contributed 14 percent of the pod drag.

The propulsion system drags for the unconventional engines were computed as the sum of the nacelle drag, nacelle-wing interference drag, incremental wing drag due to scrubbing by the propeller slipstream, and, for the variable pitch shrouded fan, isolated fan cowl drag.

The entire nacelle surfaces of the STS 487 turboprop and STS 488 regenerative turboprop were assumed to be scrubbed by the propeller slipstream. The gearbox, gas generator, and primary nozzle wrap was assumed scrubbed by the fan exhaust stream for the variable pitch shrouded fan. Skin friction drag estimates based on the slipstream or exhaust stream flow conditions were increased by 20 percent (for pressure drag penalties) to give the profile drag of the scrubbed nacelle surfaces.

The fan cowl drag of the variable pitch shrouded fan was computed as the isolated skin friction drag of a body of revolution. Freestream conditions were used.

Increments in wing drag due to the higher Mach number flow over the wing behind the propeller or fan were estimated for the unconventional engine applications. The resultant drag change was assumed to be due to the incremental profile drag caused by scrubbing, a drag rise increase resulting from an increase in the flow Mach number relative to the wing critical Mach number, and a possible reduction in drag resulting from the reduced angle of attack. The incremental wing profile drag due to scrubbing was computed as the product of the wing profile drag coefficient (freestream conditions), the scrubbed wing area, and the incremental dynamic pressure of the higher Mach number flow.

Drag rise increases due to the higher speed flow of the slipstreams were estimated to cause substantial drag increases. Alleviation of these drag rise increases by higher wing sweep (or lower section thickness ratios) is possible. Although the higher wing sweep causes increased

wing weight, and a resultant drag increase, preliminary analysis indicated the resultant drag increases would be about 50 percent of those of the turboprops and 14 percent of those of the variable pitch shrouded fan if no steps were taken to alleviate the drag rise increase.

The increased dynamic pressures in the slipstreams of the unconventional engines allow aircraft with these engines to fly at reduced cruise angles of attack for the same total lift. The results of a preliminary analysis investigating the effect of reduced angles of attack only on drag due to lift indicated that for the STS 487 turboprop-powered airplane, approximately a 3 percent reduction in airplane drag is possible. Additional drag reductions might occur in subsonic wave drag (drag rise) because of the lower possible angles of attack.

The estimated magnitude of the drag increase due to the higher wing weight if sweep were increased to reduce slipstream-caused drag rise was about equal to the reduction in airplane drag due to slipstream-induced lower angles of attack for the STS 487. Because of these offsetting tendencies, no drag penalties were applied to the unconventional engines for these slipstream effects.

Wing nacelle interference drag was assumed to be equal to the profile drag of an area equivalent to the wing area covered by the nacelle. This assumption was based on Hoerner (ref. 14).

The percentage contributions of each of these drag components to the total pod drag for the unconventional engines is summarized in Table A-IV.

TABLE A-IV

POD DRAG BREAKDOWN

	STS 487 Turboprop (Percent)	STS 488 Regenerative Turboprop (Percent)	Variable Pitch Shrouded Fan (Percent)
Fan Cowl	--	--	45.8
Scrubbed Nacelle Surfaces	70.2	76.7	26.5
Wing Scrubbing	12.3	8.2	14.5
Wing-Nacelle Interference	17.5	15.1	13.2
TOTAL	100.0	100.0	100.0

Nacelle and Aircraft Pricing Method

Nacelle prices of both the unconventional engines and the STF 477 turbofan were based on regressions of current aircraft data. Engine cowl and fan cowl prices, engine mount prices, and pylon prices were assumed to have the same cost per kilogram as the airframe, i.e., approximately $242.50/kg ($110/lbm). Thrust reversers were priced at $362.50/kg ($164.50/lbm), and accessories were priced at $319.50/kg ($145/lbm).

Economic Groundrules

Direct operating cost (DOC) and return on investment (ROI) are used as measures of economic attractiveness. The methods used for predicting DOC are based on ATA formulae, reports of airframe and airline companies, cost estimating relationships (such as those developed by the Rand Corporation), and Pratt & Whitney Aircraft estimates of engine-related DOC components. These methods are consistent with those of NASA CR-134645 (ref. 15). Table A-V shows the components of DOC and values of some of the factors used to compute them.

The economic model used to compute ROI required estimates of indirect operating costs (IOC), as well as DOC. Indirect operating cost calculations were based on the method described on page 271 of reference 15 and on the 1970 Lockheed method. The formulae used to calculate the various IOC components are shown in Table A-VI. The method of calculating ROI is shown in Table A-VII.

TABLE A-V

FACTORS USED IN CALCULATION OF DIRECT OPERATING COST

- Crew cost: Dollars per block hour are a function of take-off gross weight (TOGW) and cruise speed.
- Fuel: Block fuel per block hour times 8 ¢/liter (30 ¢/gal.), domestic, and 12 ¢/liter (45 ¢/gal.), international.
- Oil: Block fuel per block hour times 0.16 ¢/liter (0.6 ¢/gal.), domestic, and 0.24 ¢/liter (0.9 ¢/gal.), international (2% of block fuel cost).
- Insurance: 1% of flyaway price, per year.
- Airframe maintenance labor: $7.30 per manhour; manhours per block hour a function of airframe weight and average flight time.
- Airframe maintenance materials: Function of airframe weight and average flight time.
- Engine maintenance labor: $7.30 per manhour, manhours per block hour a function of average flight time and engine design.
- Engine maintenance materials: Function of engine design, size, and average flight time.
- Maintenance burden: Equal to sum of airframe and engine maintenance material and labor costs.
- Depreciation: 15 years to 0 residual value, includes 6% airframe spares and 30% engine spares.

- Airframe price, millions of mid-1974 dollars

$$= 0.207W_A^{0.7}(Q/250)^{-0.42} + (8.6/Q)W_A^{0.89} + 0.003S + 0.600$$

- W_A is the AMPR* airframe weight in kilograms divided by 453.6 (or AMPR weight in lbm divided by 1000).
- Q = quantity of airplanes = 300
- S = number of seats per airplane = 200
- ATA formula for utilization: Block hours per year = 4275 (BT + 0.3)/(BT + 1.3) + 475
- BT = block time = flight time + 0.25 hours
- Revenue load factor: 55 percent
- Typical domestic aircraft mission stage length: 1300 km (700 n. mi.)
- Typical international aircraft mission stage length: 3700 km (2000 n. mi.)

*AMPR (referring to the Aeronautical Manufacturers' Planning Report) is an aircraft weight concept. Essentially, AMPR weight is the take-off gross weight less payload, engines, furnishings, fuel, instruments, electrical and other accessory equipment, and parts and fluids replaced at regular maintenance intervals. This concept is defined more completely in reference 16.

TABLE A-VI

FACTORS USED IN CALCULATION OF INDIRECT OPERATING COST

Mid-1974 Dollars

	Domestic Aircraft	International Aircraft
Cabin Attendant, dollars per block hour		
Standard body aircraft	20.2S/27	23.6S/27
Wide body aircraft	20.2S/27 + 20.2	23.6S/27 + 23.6
Aircraft Servicing, dollars per flight		
Fueling and cleaning	0.78 W_L	1.91 W_L
Landing fee	0.43 W_L	1.05 W_L
Aircraft control	71	174
Ground Equipment and Facilities, dollars per flight		
Maintenance and burden	0.44 W_L	0.84 W_L
Depreciation and amortization	0.47 W_L	0.90 W_L

General and Administrative

For both the domestic and international aircraft, general and administrative costs were assumed to be 6 percent of the total of DOC, cabin attendant, aircraft servicing, and ground equipment and facilities costs.

Definition of Symbols

S is the number of seats per aircraft (200).

W_L is the maximum landing weight in kilograms divided by 453.6 (or max. landing weight in lbm divided by 1000).

TABLE A-VII

FACTORS USED IN CALCULATION OF RETURN ON INVESTMENT

- Basic ROI formula, mid-1974 dollars:

$$\frac{\text{ROI}}{1-(1+\text{ROI})^{-15}} = \frac{\text{Annual Cash Flow}}{\text{Initial Investment}}$$

- Annual Cash Flow = Revenue + Depreciation – DOC – IOC – Taxes
- Initial Investment, domestic aircraft = (1.06 X airplane cost) + (3.9 X engine price)
- Initial Investment, international aircraft = (1.06 X airframe cost) + (5.2 X engine price)
- Initial Investment terms: 100 percent purchase at delivery
- Revenue: Dollars per passenger-kilometer (mile) based on Airline Operators' Guide data
- Taxes: Income and other taxes equal to 50 percent of net earnings, with no investment tax credit

APPENDIX B

LIST OF SYMBOLS AND ABBREVIATIONS

A_F	Fan Face Annular Flow Area
AMPR	Aeronautical Manufacturers' Planning Report (see Table A-IV)
A_N	Fan Nozzle Throat Area
AR	Aspect Ratio
ATA	Air Transport Association
ATT	Advanced Technology Transport
Avg.	Average
BT	Block Time, Hours
C_D	Drag Coefficient
C_{DI}	Ideal Induced Drag Coefficient
ΔC_{DP}	Incremental Variation of Profile Drag Coefficient Due to Lift
$C_{DP\ min}$	Minimum Profile Drag Coefficient
ΔC_{DWD}	Subsonic Wave Drag Coefficient
CET	Combustor Exit Temperature
C_L	Lift Coefficient
C_{Li}	Integrated Propeller Lift Coefficient
CO	Carbon Monoxide
Compr.	Compressor
CV	Exhaust Nozzle Velocity Coefficient
Diam.	Diameter
DOC	Direct Operating Cost
ΔDOC	Change in Direct Operating Cost
DN	Bearing Bore Diameter Times Speed, mm-rev/min
D_P	Propeller Diameter
dB(A)	Interior Cabin Noise in Decibels
D_{MAX}	Maximum Nacelle Diameter
ECCP	Experimental Clean Combustor Program
EGT	Exhaust Gas Temperature, °C(°F)
E_o	Cycle Energy Output
EPAP	Environmental Protection Agency Parameter
EPNdB	Equivalent Perceived Noise Decibels
EPR	Engine Pressure Ratio
FAA	Federal Aviation Administration
FAR 36	Federal Aviation Regulations Part 36
F-L-H	Fan/Low-Pressure Compressor/-High-Pressure Compressor
FOD	Foreign Object Damage
FPR	Fan Pressure Ratio
FT, ft	Feet
gal.	Gallon
Geom.	Geometry
HR, hr	Hour
HP, hp	Horsepower
HPA	High Pressure Air
HPC	High Pressure Compressor
HPG	High Pressure Gas
HPX	Horsepower Extraction
HPT	High Pressure Turbine
IN, in	Inches
IOC	Indirect Operating Cost
ISA	International Standard Atmosphere
K_1, K_2	Wing Weight Empirical Constants
KG, kg	Kilogram
KM, km	Kilometer
KW, kw	Kilowatt
LB, lb	Pound
lbm	Pounds Mass
lbf	Pounds Force
L/D	Lift-to-Drag Ratio
LEC	Low Energy Consumption
LFC	Laminar Flow Control
LPT	Low Pressure Turbine
LPA	Low Pressure Air
LPC	Low Pressure Compressor
LPG	Low Pressure Gas
M	Mach Number
M_{ref}	Reference Mach Number
M_{CR}	Critical Mach Number
m	Meter
mm	Millimeter
Max.	Maximum
Min.	Minute
Mn	Mach Number
N	Newton
N.MI.,n.mi	Nautical Mile
NO_x	Oxides of Nitrogen
OPR	Overall or Cycle Pressure Ratio
Q	Quantity of Airplanes
Q_A	Available Heat Energy Input
Q_R	Heat Energy Rejection
REGEN	Regeneration
rev	Revolution

APPENDIX B (Cont'd)

LIST OF SYMBOLS AND ABBREVIATIONS (Cont'd)

ROI	Return on Investment
RPM	Revolutions Per Minute
s	Entropy
S	Number of Seats Per Airplane
SEC, sec	Seconds
SHP	Shaft Horsepower
st. mi.	Statute Mile
T	Temperature
t/c	Thickness-to-Chord Ratio
THC	Total Hydrocarbons
$T_{A\ avg.}$	Average Temperature of Heat Addition
$T_{R\ avg.}$	Average Temperature of Heat Rejection
TLF	Total Low Frequency Ratio
TSFC	Thrust Specific Fuel Consumption
TOGW	Take-Off Gross Weight
Turb.	Turbine
Vorbix	Vortex Burning and Mixing
W_A	AMPR Weight in Kilograms Divided By 453.6 (AMPR Weight in lbm Divided By 1000)
W_L	Maximum Landing Weight in Kilograms Divided by 453.6 (Maximum Landing Weight in lbm Divided By 1000)
Wgt.	Weight
Δ	Incremental
η_{th}	Thermal Efficiency
$\Delta_{\eta T}$	Turbine Ffficiency Penalty
$\Lambda_{C/4}$	Quarter Chord Wing Sweep Angle
$\in$	Heat Exchanger Effectiveness
ρ_A	Nacelle Weight Per Unit Wetted Area
λ	Influence Coefficient
η_{ideal}	Ideal Propulsive Efficiency

REFERENCES

1. Gray, D.E.: Study of Turbofan Engines Designed for Low Energy Consumption. NASA CR-135002, April 1976. Pratt & Whitney Aircraft. Contract NAS3-19132.

2. Boenig, F.H.: Feasibility Investigation of Constant Volume Combustion. Report PWA-2887, July 1966. Pratt & Whitney Aircraft. Contract AF33(615)-2992.

3. Swithenbank, J., Brown, D.J., and Saunders, R.J.: Some Implications of the Use of Pulsating Combustion for Power Generation Using Gas Turbines. Journal of the Institute of Fuel, September 1974, pp. 181-189.

4. Anon.: Comprex® – The Best Pressure-Changing System for Vehicle Engines. (Descriptive Pamphlet.) Brown, Boveri & Company, Ltd., 5401 Baden, Switzerland.

5. Chatterton, E.E.: Compound Diesel Engines for Aircraft. Journal of the Royal Aeronautical Society, September 1954, pp. 613-627.

6. Anon.: Compound Diesel Engine Design Analyzed. Aviation Week, May 17, 1954, pp. 30-33.

7. Kraft, J. and Civinskas, K.C.: Preliminary Evaluation of a Turbine/Rotary Combustion Compound Engine for a Subsonic Transport. TMX 71906. NASA Lewis Research Center. March 1976.

8. Hancock, J. P. and Hinson, B. L.: Inlet Development for the L-500. AIAA-69-448, American Institute of Aeronautics and Astronautics Fifth Propulsion Joint Specialist Conference, June 9-13, 1969.

9. Anon.: Prop-Fan Advanced Technology Weight Estimation for the Eight-Blade Prop-Fan Configuration. United Technologies Corp., Hamilton Standard Div. report SP 05A76, February 27, 1976.

10. Anon.: Fuel Conservation Possibilities for Terminal Area Compatible Aircraft. NASA CR-132608, March 1975. Boeing Commercial Airplane Co. Contract NAS1-12018.

11. Anon.: Advanced Transport Technology Program. General Dynamics, Convair Aerospace Div. report FZM-5779, 27 August 1971. Contract NAS1-10702.

12. Anon.: Study of the Application of Advanced Technologies to Long-Range Transport Aircraft. Interim Oral Status Report. 1 September 1971. Lockheed-Georgia Co.

13. Anon.: Guidelines for Prop-Fan Installations. United Technologies Corp., Hamilton Standard Div. report SP 08A76, February 27, 1976.

14. Hoerner, S. F., Fluid Dynamics Drag. Hoerner Fluid Dynamics, Brick Town, New Jersey, 1965.

15. Sallee, G. P.: Economic Effects of Propulsion System Technology on Existing and Future Transport Aircraft. NASA CR-134645, 1974. American Airlines, Inc.

16. Levenson, G. S. and Barro, S. M.: Cost Estimating Relationships for Aircraft Airframes. The Rand Corporation, report No. RM-4845-PR, May 1966.